2022

# Complex Quantum Contagion: A Quantum-Like Approach for The Analysis of Co-Evolutionary Dynamics of Social Contagion

Ece Mutlu
*University of Central Florida*

# COMPLEX QUANTUM CONTAGION: A QUANTUM-LIKE APPROACH FOR THE ANALYSIS OF CO-EVOLUTIONARY DYNAMICS OF SOCIAL CONTAGION

by

ECE ÇİĞDEM MUTLU
B.S. Boğaziçi University, 2015
M.Sc. Boğaziçi University, 2017

A dissertation submitted in partial fulfilment of the requirements
for the degree of Doctor of Philosophy
in the Department of Industrial Engineering and Management Systems
in the College of College of Engineering and Computer Science
at the University of Central Florida
Orlando, Florida

Summer Term
2022

Major Professor: Ozlem Ozmen Garibay

# ABSTRACT

Modeling the dynamics of social contagion processes has recently attracted a substantial amount of interest from researchers due to its wide applicability in network science, multi-agent systems, information science, and marketing. Unlike in biological spreading, the existence of a reinforcement effect in social contagion necessitates considering the complexity of individuals in the systems. Although many studies acknowledged the heterogeneity of the individuals in their adoption of information (or behavior), there are no studies that take into account the individuals' uncertainty during their decision-making despite its theoretical and experimental evidence in behavioral economics, decision science, cognitive science, or multi-agent systems. This resulted in less than optimal modeling of social contagion dynamics in the existence of phase transition in the final adoption size versus transmission probability. We believe that it is mainly because traditional approaches do not consider the uncertainty stemming from agent interactions through an information exchange that can influence individuals' emotions, change subconscious feelings, and trigger subjective biases. To address this problem, we propose quantum-like generalization of social contagion analysis for the analysis of co-evolutionary dynamics of social contagion. For this purpose, we employed Inverse Born Problem (IBP) to represent probabilistic entities as complex probability amplitudes in edge-based compartmental theory and demonstrated that our novel approach performs better in the prediction of social contagion dynamics through extensive simulations on random regular networks.

*I dedicate this thesis to my mom, dad and lovely sister. Without their patience, understanding support, and most of all love, the completion of this work would not been possible.*

# ACKNOWLEDGMENTS

In completing this thesis, I owe a debt of thanks to many persons, who have supported me throughout this emotionally tough yet intellectually fruitful experience. While being grateful to all of them, I would like to emphasize some of them particularly because of their best guidance and support.

First and foremost, I am much thankful to my advisor, Dr. Ozlem Ozmen Garibay, for her endless patience for motivating me and her colossal support. One simply could not wish for a better and friendlier supervisor. I also would like to thank my mentor Dr. Ivan Garibay for inspiring me to venture into this research area. I am grateful to both of them for granting me the freedom to think outside the box and be creative. Their guidance is the foundation of this thesis in all the time of research.

In addition to my advisor, I would like to thank my thesis committee: Dr. Vladimir Boginski, Dr. Luis Rabelo, and Dr. Mary Jean Amon for their insightful comments, constructive criticism and challenging questions.

I would also like to thank my friends, and specically to my lab-mates Amirarsalan Rajabi, Aida Tayebi and Toktam Oghaz, who have always been there for me, and for providing me valuable support and for boosting my moral whenever I lost my encouragement.

My sincere thanks go to my family, particularly to my husband Ege Tütüncüler and my sister Tugce Mutlu, who have been the greatest contributors to my success, and who have been supporting me throughout my life. My thanks cannot compensate their contribution. I will forever be in their debt for preparing me for whatever life throws at me.

# TABLE OF CONTENTS

# LIST OF FIGURES

# LIST OF TABLES

# CHAPTER 1: INTRODUCTION

Contagion, in the simplest sense, is the spreading of an entity from one source to another through direct or indirect contact. Although this term is primarily used in epidemiology to define the spreading of a disease from one person to another, it recently has a more broad meaning since ideas, emotions and behaviors can also be contagious. Researchers have mainly classified these spreading dynamics in different disciplines into two main categories: Biological and social contagion. Despite the analogy between these spreading mechanisms, social contagion has been found to have a distinct inherent characteristic, which is called social reinforcement effect [2, 3, 4], compared to biological spreading. In the reinforcement effect in social contagion, the simple contagion mechanism in epidemic spreading, which assumes that even one single activated source might be sufficient for the transmission, is transformed into a more complex contagion mechanism.

American Psychological Association (APA) Dictionary defines social contagion as "the spread of behaviors, attitudes, and affect through crowds and other types of social aggregates from one member to another[1]". Interaction among people in their daily lives and its consequences has been an intuitive concept for years; however, the scientific explanation of social contagion and its relevance was first emphasized by Gustave Le Bon in his well-known book "The crowd: A study of popular mind" (1895). Le Bon's social contagion theory focus on the impacts of social influence on people's perceptions, attitudes, and behaviors in a concept of diffusion and tries to understand the causal factors behind their adoption. Although the terms "diffusion" and "adoption" are interchangeably used in the related studies, we refer to diffusion as a process in which behavior spreads among entities through certain channels; whereas, adoption is used as a decision and posterior implementation of acceptance or rejection for a modification through a series of stages [5].

[1] https://dictionary.apa.org/social-contagion

The pioneering study of Granovetter [6], in which a mathematical approach for social contagion is firstly introduced, proposed a linear threshold model based on the assumption that individuals' behavior in a network can be affected by their neighbors' actions. In this receiver-centric model, individuals adopt a behavior only if a certain fraction of neighbors have already adopted the behavior. Later, Goldenberg's pioneering study [7] of diffusion in marketing became another well-known technique in social contagion studies. In this sender-centric model called the independent cascade model, each adopted node has a single chance to influence one of its susceptible neighbors. Recently, inspired by epidemic models, one of the most commonly used methods in the literature of social contagion studies is the message passing approach [8], in which individuals within the target population (or network) are divided into mutually exclusive compartments based on their current status and their future status at any time can be predicted based on the predefined rate of contact between compartments and their certain transition rates. As opposed to the conventional compartmental models, the reinforcement effect is also included with the existence of a threshold value for individuals to adopt the behavior. Therefore, the message passing approach is considered a non-Markovian process, which makes it more realistic in the application of real-world diffusion.

The most challenging task in employing any of these approaches in social contagion analyses is to model the complexity of individuals. This complexity arises due to either the heterogeneity of the individuals in their adoption threshold or the uncertainty in their decision-making process during adoption. Although earlier studies employed a simplistic threshold model, i.e., uniform threshold distribution in social contagion studies, to address the former challenge, recent studies utilized more complex threshold distributions such as binary [4], tent-like function [9], truncated normal distribution function [10] or sigmoid function [11]. To the best of our knowledge, the uncertainty in their decision-making process has not been addressed yet in social contagion analyses despite its theoretical and experimental evidence in behavioral economics, decision science, cognitive science, or multi-agent systems. Although the whole process in social contagion studies is based on

the assumption that individuals are perfectly rational and do follow the rules of classical probability theory and logic while taking an action during the process, it is well-known that only bounded rationality can exist [12] and individuals do not obey the classical probability rules [13, 14, 15, 16]. It is mainly due to agent interactions through an information exchange that can influence individuals' emotions, change subconscious feelings, and trigger subjective biases [12, 17]. Furthermore, the impacts of such behavioral effects become more significant when individuals make their decision under uncertainty [15]. To address this complexity in human decision-making and explain the corresponding irrationality and existing paradoxes and fallacies, researchers developed numerous quantum-like approaches [18, 19, 15, 20, 21, 22]. Although classical approaches argue that human inference deterministically jumps between definite states across time, the main assumption behind quantum-like approaches is that competitive beliefs exist in the human mind at the same time. They form a composite entangled prospect for the decision-maker. Because behavior spreading in a social contagion is fueled with the successful transmission of behavior (or information) among two entangled binary prospects (adopting/not adopting) of decision-makers in a network, the utilization of these approaches in social contagion analyses may provide more realistic insights.

Since social contagion theory relates spreading of information such as rumors, fads; popularity of new products via word-of-mouth marketing, and also helps to understand the structure and dynamics of collective behavior, this phenomenon has gained researchers' interests from different disciplines like epidemiology, biology, and different social science fields. Therefore, it is highly studied in the existence of restricted contact [23], heterogeneous adoption threshold [4], local trend imitation [9], heterogeneous credibility [24] and with memory of non-redundant information [25]. All of these studies showed that these models are very effective in predicting social contagion dynamics within defined scenarios. Understanding and better modeling contagion dynamics in complex networks play a crucial role in shedding light on the spreading mechanisms of viral diseases, microfinance activities, false information, harmful emotions, and destructive technology adoptions.

Understanding the dynamics of social contagion not only gives us an opportunity to design more efficient anti-pathogen strategies during infectious disease outbreaks but also grants theoretical foundations to predict collective behaviors, and even mitigate the propagation of false information in social systems. We believe that the application of a quantum-like approach to extant social contagion models may improve their performance by better simulating human decision-making in the adoption process.

## Motivation: Violations to Normative Theories of Rational Choice

Humans are complex creatures. What makes them so complex is the difficulty in understanding and predicting their behavior. Pioneering neoclassical economic thought assumed that individuals act with perfect rationality, and their decision-making process can be represented by utility functions. Although the well-known Expected Utility (EU) theory of von Neumann and Morgenstern [26] is accepted as one of the most significant axioms in explaining human decision-making, Allais' paradox [27] showed the complexity of human behavior under uncertainty; since the notion of perfect rationality of individuals is an over-simplification of more complex phenomena. EU theorem, therefore, is improved to become the Subjective Expected Utility (SEU) theorem by pairing utility and probability functions to represent agents' desires and beliefs, respectively, by Leonard Savage and Richard Jeffrey [13].

Savage's Sure Thing Principle [13] states that if one prefers action A over B under the state of the world X and again prefers action A over B under the complementary state of world X (X'), then he/she prefers action A over B when you do not know the state of the world. Although classical decision-making analysis used to rely on this well-known principle, previous experiments showed that the human mind does not follow the rule of probability theory while making a decision, and this phenomenon is highly observed in the case of uncertainty. The well-known experiment of

Tversky and Shafir demonstrated this as follows: Participants are asked two consecutive gambles in which they have an equal chance of winning $200 or losing $100. The experiment includes three conditions;

(i) The students were informed that they won the first gamble.

(ii) The students were informed that they lost the first gamble.

(iii) The students were not informed about the outcome of the first experiment.

The results showed that if they knew that they won or lost the first gamble, %69 and % 59 of participants second gamble, respectively. Since the majority is more likely to choose to play under both winning (the world X) and losing (the complementary state of world X (X')), it is expected them to choose to play the second game when they were not informed about the outcome of the first game according to the Sure-Thing Principle. However, the majority did not choose to play the second gamble (only %36 wanted to play again). This is called as disjunction effect.

In another experiment of Twersky & Kahneman in 1983, participants are very briefly informed about a woman Linda who used to be a philosophy student at a liberal university. It is also told that Linda used to be very active in an anti-nuclear movement. After this brief introduction about Linda, participants are asked to rank the likelihood of the following cases that can be Linda's present situation:

(a) Active in the feminist movement

(b) A bank teller

(c) Active in the feminist movement and a bank teller

(d) Active in the feminist movement and not a bank teller

(e) Active in the feminist movement or a bank teller

Although b refers to a marginal probability and c is the joint probability of b with another event, and therefore it is expected from participants to assign more likelihood to b than c, more participants decided the likelihood relation will be as follows $c > b$. This example of a violation of normative theories is called a conjunction fallacy.

Nevertheless, these experiments demonstrated the insufficiency of the SEU theorem either in explaining the complexity of human decision-making. All these open questions regarding the complexity of decision-making remained relevant for years, and the work of Aerts & Aerts pioneered the field of Quantum Cognition by showing the necessity of a form of quantum statistics [28]. Quantum cognition is a research area in which quantum mechanics foundations are integrated into the mathematical principles used in cognitive science. For years, unobserved cognitive biases which are known to have strong effects on individuals' decisions and actions, are represented by probabilistic models using latent variables; however, these models are highly complex, and latent variables are not sufficient in explaining the causality relations of observed / unobserved effects and the behavior. Recent research shows that quantum probabilistic models yield better results in explaining complex behavior which cannot be easily explained by the pure classical models. The superiority of these models are shown in many studies from human decision-making [29, 30, 31, 19, 32, 15] to Prisoner's Dilemma [33], or even in biological interactions of cells [34].

## Quantum Theory in The Concept of Decision-Making

Following the mid-century invention of the computer and subsequent cognitive revolution in psychology, human minds are increasingly being regarded as linear, deterministic, computer-like machines in the social sciences in recent decades. Although this theory brought significant contributions to the cognitive science and psychology bodies of literature, the assumption that the human brain makes computations according to the rules of classical computer science theories has been

challenged with the quantum brain theory which assumes the human mind works as a non-linear dynamical complex system [35]. Assuming that the brain makes computations as a quantum computer does, yield remarkable alteration in our understanding of the mind. The differences between classical and quantum brains might be better understood with a closer look at the difference between classical and quantum computers. Classical computers make computations by using a binary digit (0 or 1) system, called bits, and serial binary operations help to transform inputs to outputs. In quantum computing, on the other hand, not only binary states but also their superpositions, called a qubit, can create serial interactions for the operation from input to output. In this regard, "Quantum brain theory hypothesizes that quantum processes at the elementary level are amplified and kept in superposition at the level of the organism, and then, through downward causation constrain what is going on deep within the brain [36]." Accordingly, macro-level external information is transferred into the micro-level internal quantum state, and the decoherence-free subspace of the brain carries out the quantum computation. By considering this principle of the quantum brain, Busemeyer and Bruza [19] explained six reasons for the application of quantum theory to the fields of cognition and decision as follows:

- *Judgments are based on indefinite states:* According to the classical models, the decision-making process is assumed to be stochastic since its definite time-dependent state (trajectory) is not known. However, it is argued that in the case of a known trajectory (.g., seed selection in a Monte-Carlo simulation), it is possible to predict the outcome with classical probability rules since the human inference deterministically jumps from one state to another.

  To exemplify, suppose that you are exposed to social media content in which two opponent groups think positive and negative about the topic, and you are supposed to believe one of them by weighing evidence. In such a case, the classical probability theory denotes that at each time step you are in a definite state concerning positive or negative opinion - say $p \geq 0.5$ and $p < 0.5$ means you have a positive and negative opinion, respectively. Here,

classical decision science models cognitive systems as if they were particles with definite sample paths through state space. Whereas, there are indefinite states, called superposition states, in quantum decision models to identify the undefined state of the cognitive system at a specific time before a decision is made. Thus, the positive or negative opinion cannot be identified with $p$, but with complex amplitudes, to consider the potential of both options.

- *Judgments create rather than record:* Although classical theory argues that the outcome of the decision-making process is simply a reflection of the current state that has a strong connection and correlation with past states, the quantum theory assumes that the decision is made through an interaction between a current indefinite state and a concept that the person tries to decide.

  To exemplify, a person's opinion or current mental state can show differences concerning a specific question that is asked. Bohr states that the answer we obtain from a quantum system is formed by the interaction of the indefinite state and the specific question that is asked. This interaction constructs the definite state out of an indefinite state.

- *Judgments disturb each other, introducing uncertainty:* As aforementioned above, the quantum theory dictates that a person's state will change from an indefinite to a more definite one after a question is asked. Since the state of mind changes after a person answers the first question, this causes one to respond differently to subsequent questions, making the order of questioning crucial. Since the probability of consecutive events is computed with a joint probability of individual events in the classical decision-making theory, the quantum decision-making theory argues that consecutive events are non-commutative and order effect is undeniable. This effect is also known as the source of uncertainty in people's judgments. An answer to the former question creates a definite state by itself but an indefinite state with respect to a different question.

- *Judgments do not always obey classic logic:* The classical probability theory, which is based on Kolmogorov axioms, assigns the probability values for events as a set value. Then the Boolean logic in the decision-making mechanism is used to compute the probability of events in given scenarios. The most important property in classical probability theory is the existence of the distribution axiom. If we define $\{G, A, P\}$ as the concepts that an individual is a good person, an anti-vaxxer, and a pro-vaxxer, respectively, the distributive axiom proposes that $G \cap (A \cup P) = (G \cap A) \cup (G \cap P)$. That can be also identified as follows: If one tries to decide if an individual is a good person or not without knowing he is a pro or anti-vaxxer, this event can happen in two mutually exclusive ways: either $G \cap A$ or $G \cap P$. By using the distributive axiom, one can derive the probability of event $G$ as:

$$\begin{aligned} p(G) &= p((G \cap A) \cup (G \cap P)) = p(G \cap A) + p(G \cap P) \\ &= p(G)p(G|A) + p(G)p(G|P) \end{aligned}$$

  Bayesian statistics rules and their inferences are made based on this foundation of total probability law. However, the law of total probability is violated as in seen in two-slit experiments in physics and in disjunction effect in decision-making, which we described previously.

  In quantum probability theory, which is based on von Neumann axioms, the probability values for events are assigned as subspaces of a vector space. An indefinite or superposition state can be a point anywhere within the vector space, whereas definite states are the basis for vector space. The most important distinction with the classical theory here is not obeying the distributive axiom of Boolean logic. Thus, in addition to truthful or false attributes, another ambiguous thought may be represented by a superposition.

- *Judgments do not obey the principle of unicity:* As the basis of cognitive and decision models today, the classic (Kolmogorov) probability theory relies on the principle of unicity. An exhaustive and complete description of all possible events occurs in a single sample space.

Therefore, if $A$ and $B$ represent two possible events in an experiment, then $A \cap B$ denotes an event too, which is a very constrictive phenomenon. On the other hand, quantum probability theory does not obey the principle of unicity. The assumption is broken as soon as we introduce incompatible questions into the theory causing measurements to become non-commutative.

- *Cognitive phenomena may not be decomposable:* For any given experimental condition in cognitive science, researchers often propose a large collection of random variables to model a cognitive process, but the actual findings are only a small subset of these variables. The assumption is then made that there is a complete joint distribution, or a joint probability distribution to account for all the variables, which allows for the determination of the observed marginalized distribution for any subset of variables. On the other hand, real-world experiments show that some cases may not be decomposable and cannot be identified as a single joint distribution. In quantum entanglement, two seemingly separate and distinct systems behave like one. When this occurs, these systems are referred to as "quantum correlated."

## Purpose of the Study

The main purpose of this study is to better model the social contagion dynamics to shed light on the control of viral disease, microfinance activities, false information, harmful emotions, and technology adoptions. For this purpose, we aim to develop a novel methodology for social contagion analyses by engaging knowledge and skills from multiple disciplines including network science, cognitive science, quantum information theory, and artificial intelligence -called quantum social contagion.

Since quantum social contagion is a complex phenomenon, we also aim to address the following issues that can be considered as subsidiary purposes of this study: i) creating a comprehensive

approach for social contagion analysis that considers the heterogeneity of individuals and the uncertainty in their decision-making in a social contagion process, ii) developing a general overview of quantum social dynamics regardless of the changing network properties, iii) proposing a heuristic approach that can ease the complexity of quantum approach in a social contagion analysis, iv) generalizing the quantum social contagion by not only considering the diffusion of a single event but focusing on the simultaneous existence of multiple events in a given network. All these items will help us to better understand the social contagion dynamics by considering various behaviors of individuals, numerous network structures, and diverse behavior characteristics.

## Research Questions

- To better model the complexity of human decision-making and explain existing paradoxes and fallacies, researchers developed numerous quantum-like approaches [18, 19, 15, 20, 21, 22]. Does the quantum-like approach model the dynamics of social contagion better?
- The most challenging task in employing social contagion analyses is to model heterogeneity of the individuals in their adoption threshold. Current studies that use the classical approach demonstrated the existence of discontinuous phase transitions in the final spreading size versus transmission probability. What type of phase transitions are observed when agents are modeled as quantum decision-makers?
- The variability of the social contagion dynamics with changing network properties (assortativity, density, clustering, degree distribution, etc.) is highly studied among researchers [37, 38]. Does the superiority/incapacity of quantum-based probabilistic models in social contagion analyses over classical models vary with changing network properties?
- Quantum-like probabilistic models yield extra interference terms compared to classical approaches. Some studies that utilized quantum-like approaches in decision-making systems

tunes these parameters manually [30], [39]; while others do automatically by using a static heuristic [32] and/or dynamic heuristic [21]. Can a heuristics based on entropy measures be an alternative to the extant heuristics in the literature?

- Despite the great interest in modeling a contagion of single behavior, there might be competing or cooperating contagions in the complex network in real case scenarios. Does quantum contagion is applicable for these complex contagions, or is it too complex to handle?

## Statement of Contributions

In this study, we aim to better model social contagion dynamics by utilizing quantum-like approach in its mathematical modeling. During the ideation, development, and generation of this thesis, I have conducted several studies on social contagion with the main focus of information diffusion by using an interdisciplinary point of view. Following you can find several contributions to the scientific community:

- **Mutlu, E.**, & Garibay, O. O. (2022). "An Entropy-Based Heuristic Approach For The Quantum-Like Generalization of Social Contagion". Submitted to 7th International Workshop on Social Sensing Special Edition on Information Operation on Social Media. An ICWSM 2022 Workshop.

In this paper, we propose a belief-entropy-based heuristic approach to predict interference effect in quantum-like generalization of social contagion. Based on simulations of uncorrelated random regular networks (RRNs) using the proposed approach, we concluded that belief entropy is useful for detecting interference in quantum-like generalizations of social contagion models. These results should lead to increased use of quantum social contagion models in any application area without having to deal with calibration issues or time constraints.

- **Mutlu, E.**, & Garibay, O. O. (2021, July). "A Quantum Leap for Fairness: Quantum Bayesian Approach for Fair Decision Making". In International Conference on Human-Computer Interaction (pp. 489-499). Springer, Cham.

Here, we aim to introduce quantum Bayesian approach as a candidate for fair decision-making in causal learning, motivated by the human decision-making literature in cognitive science. We demonstrated that quantum Bayesian perspective creates well-performing fair decision rules under high uncertainty on the well-known COMPAS (Correctional Offender Management Profiling for Alternative Sanctions) data set.

- **Mutlu, E.C.** & Garibay, O.O. (2021). "Quantum Contagion: A Quantum-Like Approach for the Analysis of Social Contagion Dynamics with Heterogeneous Adoption Thresholds". Entropy, 23(5), 538.
  https://doi.org/10.3390/e23050538

In this study, we employed the Inverse Born Problem (IBP) to represent probabilistic entities as complex probability amplitudes in edge-based compartmental theory, and demonstrated that our novel approach performs better in the prediction of social contagion dynamics through extensive simulations on random regular networks.

- **Mutlu, E.C.** (2020). "Quantum Probabilistic Models using Feynman Diagram Rules in Human Decision-Making". In proceedings of the Twenty-Fifth AAAI/SIGAI Doctoral Consortium collocated with the Thirty-Fourth Conference on Artificial Intelligence.
  https://doi.org/10.1609/aaai.v34i10.7137

The project, mainly, aims to expand the use of current quantum probabilistic models in human decision-making from two agents to multi-agent systems. First, I cultivate the classical Bayesian

networks which are used to understand information diffusion through human interaction on online social networks (OSNs) by taking into account the relevance of multitude of social, psychological, behavioral and cognitive factors influencing the process of information transmission. Since quantum like models require quantum probability amplitudes, the complexity will be exponentially increased with increasing uncertainty in the complex system. Therefore, the research will be followed by a study on optimization of heuristics. Here, I suggest to use an belief entropy based heuristic approach. This research is an interdisciplinary research which is related with the branches of complex systems, quantum physics, network science, information theory, cognitive science and mathematics. Therefore, findings can contribute significantly to the areas related mainly with social learning behavior of people, and also to the aforementioned branches of complex systems. In addition, understanding the interactions in complex systems might be more viable via the findings of this research since probabilistic approaches are not only used for predictive purposes but also for explanatory aims.

- **Mutlu, E.C.**, Garibay, I. (2020). "CD-SEIZ: Cognition-Driven SEIZ Compartmental Model for the Prediction of Information Cascades on Twitter". In proceedings of the 11th The Computational Social Science Society of the Americans (CSS2020) - Springer Collection (in press).

We tackle the problem of predicting information cascades by presenting a novel variant of SEIZ (Susceptible/ Exposed/ Infected/ Skeptics) model that outperforms the original version by taking into account the cognitive processing depth of users. We define an information cascade as the set of social media users' reactions to the original content which requires at least minimal physical and cognitive effort; therefore, we considered retweet/ reply/ quote (mention) activities and tested our framework on the Syrian White Helmets Twitter data set from April 1st, 2018 to April 30th, 2019. In the prediction of cascade pattern via traditional compartmental models, all the activities

are grouped, and their summation is taken into account; however, transition rates between compartments should vary according to the activity type since their requirements of physical and cognitive efforts are not same. Based on this assumption, we design a cognition-driven SEIZ (CD-SEIZ) model in the prediction of information cascades on Twitter. We tested SIS, SEIZ, and CD-SEIZ models on 1000 Twitter cascades and found that CD-SEIZ has a significantly low fitting error and provides a statistically more accurate estimation.

- **Mutlu, E.C.**, Garibay, I. (2020). "Effects of Assortativity on Consensus Formation with Heterogeneous Agents". Accepted by 6th International Conference on Computational Social Science (IC2S2 2020).

Despite the widespread use of Barabasi's scale-free networks and Erdos-Renyi networks of which degree correlation (assortativity) is neutral, numerous studies demonstrated that online social networks tend to show assortative mixing (positive degree correlation), while non-social networks show a disassortative mixing (negative degree correlation). First, we analyzed the variability in the assortativity coefficients of different groups of the same platform by using three different subreddits in Reddit. Our data analysis results showed that Reddit is disassortative, and assortativity coefficients of the aforementioned subreddits are computed as -0.0384, -0.0588 and -0.1107, respectively. Motivated by the variability in the results even in the same platform, we decided to investigate the sensitivity of dynamics of consensus formation to the assortativity of the network. We concluded that the system is more likely to reach a consensus when the network is disassortatively mixed or neutral; however, the likelihood of the consensus significantly decreases when the network is assortatively mixed. Surprisingly, the time elapsed until all nodes fix their opinions is slightly lower when the network is neutral compared to either assortative or disassortative networks. These results are more pronounced when the thresholds of agents are more heterogeneously distributed.

- **Mutlu, E.C.**, Garibay, I. (2019). "The Degree-Dependent Threshold Model: Towards a Better Understanding of Information Diffusion Dynamics on Online Social Networks". In proceedings of the 10th The Computational Social Science Society of the Americans (CSS2019) - Springer Collection (in press).

In this study, we use Twitter data of size 30,704,025 tweets to mimic the adoption of a new opinion. Our results show that the threshold is not only correlated with out-degree of nodes, which contradicts other studies, but also correlated with nodes' in-degree. Therefore, we simulated two cases in which thresholds are out-degree and in-degree dependent, separately. We concluded that the system is more likely to reach a consensus when thresholds are in-degree dependent; however, the time elapsed until all nodes fix their opinions is significantly higher in this case. Additionally, we did not observe a notable effect of mean-degree on either the average opinion or the fixation time of opinions for both cases, and increasing seed size has a negative effect on reaching a consensus. Although threshold heterogeneity has a slight influence on the average opinion, the positive effect of heterogeneity on reaching a consensus is more pronounced when thresholds are in-degree dependent.

- Garibay, I., Oghaz, T., Yousefi, N., **Mutlu, E.C.**, ... (2019). "Deep Agent: Studying the Dynamics of Information Spread and Evolution in Social Networks". In proceedings of the 10th The Computational Social Science Society of the Americans (CSS2019) - Springer Collection (in press)

This paper explains the design of a social network analysis framework, developed under DARPA's SocialSim program, with novel architecture that models human emotional, cognitive and social factors. Our framework is both theory and data-driven, and utilizes domain expertise. Our simulation effort helps understand- ing how information flows and evolves in social media platforms.

We focused on modeling three information domains: cryptocurrencies, cyber threats, and software vulnerabilities for the three interrelated social environments: GitHub, Reddit, and Twitter. We participated in the SocialSim DARPA Challenge in December 2018, in which our models were subjected to an extensive performance evaluation for accu- racy, generalizability, explainability, and experimental power. This paper reports the main concepts and models, utilized in our social media modeling effort in devel- oping a multi-resolution simulation at the user, community, population, and content levels.

## Statement of Originality

I certify that the intellectual content of this thesis is the product of my own work to the best of my knowledge. Some parts of this dissertation include published contents from my own studies and all the assistance received in preparing this thesis and sources have been acknowledged. Please see Appendix B for the permission to reuse published article content. This thesis has not been submitted for any degree or other purposes.

# CHAPTER 2: CLASSICAL SOCIAL CONTAGION ANALYSIS

Cambridge Dictionary defines diffusion as "the action of spreading in many directions". Information spread through a set of intermediate users in a network is called information diffusion. With social media being the platform used by many individuals, users are able to communicate with each other and share their ideas, opinions, and emotions freely. This fast-paced alteration in individuals' communication style triggered researchers to analyze the formation, evaluation, and dissemination of information.

## Mathematical Models of Social Contagion

Information spread through a set of intermediate users in a network is called information diffusion. The pioneering study of Granovetter [6], in which a mathematical approach for information diffusion is firstly introduced, has been developed by researchers from different disciplines. Nowadays, there are numerous approaches to model information diffusion in networks. We can classify those approaches into two main categories according to their purpose [40]: i) Explanatory, ii) Predictive models. Explanatory models aim to examine the information diffusion process by elucidating each individual factor's effects and their interactions. Predictive models, on the other hand, focuses on the prediction capability based on certain factors. These methods are generally investigated under two main classes: i) Graph-based models, ii) Non-graph-based methods. Graph-based models include well-known threshold and cascading methods and assume that information spread is driven through interactions in a static network. Non-graph-based methods compromise epidemic models like SI, SIR, SIRS, SEIZ models, and partial differential equation models that we will not cover due to their rare use in information diffusion studies [41].

*Bass Model*

Diffusion is a process in which innovation or information spreads among entities through certain channels. At the same time, adoption can be defined as a decision and posterior implementation of acceptance or rejection for a modification. Although these two terms are interchangeably used in the studies related to the diffusion of information and adoption of innovation, the distinction between these two phenomena and their applications is explained in [5] in detail. To sum up, adoption is an individual-focused process in which a series of stages is undergone, and a state is finalized with either adopting or not adopting. Diffusion signifies a process behavior in which innovation/information travels within a population. Although collective behavior in the original models of information diffusion models, i.e. Independent cascade model [7], linear threshold model [6] and that of innovation adoption models, i.e. Bass model [42], differ in some respects. As aforementioned in Section 1, the independent cascade model is sender-centric, and each active node has a probability of influencing at least one of each neighbor with the given probability. The linear threshold model is receiver-centric, and it is based on the following assumption: A node can be activated only if a substantial fraction of its neighbor is already active.

The Bass model, which defines customers' purchases with a set of differential equations by considering the aggregate first-purchase growth of a category of a durable good, on the other hand, is a well-known approach to predict new product/innovation adoption in marketing. The model assumes external and internal influences for new customers to adopt (purchasing the product). Exogenous influences are stem from the advertisement or external communications initiated by a firm, while the interactions among the adopters in the network (word-of-mouth) are considered endogenous influences. The Bass model expresses the linear relationship between innovation adoption and the number of adopters in the previous time step [43]. Its capability of predicting a new product adoption in a single market [44] and finding the optimal pricing [45] and advertising decisions

[46] caught the attention of researchers for years. To integrate different factors, e.g., uncertainty on sales, customer risk aversion [47], interpersonal communication, tie strength [48] etc., various modifications to the original Bass model have been done. Granovetter's original version of the threshold model, on the other hand, focuses only on endogenous influence due to interactions between individuals. However, information can be diffused either internally through neighbors in a network or through external sources such as news channels, Internet articles, or advertisements. Therefore we can argue that the main advantage of Bass type of models compared to threshold models is the existence of a parameter to model exogenous influence.

The Bass model is criticized for two reasons: i) It assumes a perfectly mixed network, i.e., every individual in a network can communicate with each other, which is generally violated in real-world applications, ii) another disadvantage of the Bass model is that the individuals' purchase behaviors are approximated; however, real-world applications show that people may exhibit different purchase behavior (heterogeneous adoption). This over-simplification triggered new approaches that try to focus on the heterogeneous population. Thus, Chatterjee and Eliashberg [49] proposed a micro-modeling approach to incorporate adoption heterogeneity in Bass models; however, its necessity of strong assumptions made this approach less popular.

### *Epidemic Models*

Motivated by the mathematical approach of Daniel Bernoulli in 1760 to model the spread of smallpox, Kermack and McKendrick introduced the foundation of the compartmental models, i.e., SIS (Susceptible-Infected-Susceptible) and SIR (Susceptible-Infected-Susceptible) for the analysis of disease spread. The common feature of these epidemic methods is that individuals (or agents) within the target population (or network) are divided into mutually exclusive compartments based on their current status and their future status at any time can be predicted based on the predefined

rate of contact between compartments and their certain transition rates. These statuses may define different compartments in the transmission of a disease, an innovation, a change in cultural belief, or a specific rumor. In this research, we mainly focus on these methods in the modeling of the spread of information.

Pioneering studies [50, 51, 52, 53] introduced the application of compartmental models outside of the epidemiology and new variations are proposed to model information diffusion on complex networks over the years. The interpretation of compartmental models in a social context exhibits significant differences since i) individuals have a driving force in acquiring new ideas or innovations, while that is the opposite for getting a disease. ii) dynamics are different, e.g. An individual may recover after being infected, but recovered status is not easy to transfer in information diffusion concept [54]. These differences triggered researchers to identify qualitative and quantitative differences in the application of compartmental models for information diffusion studies. In one of the simplest compartmental models, i.e. SIS model, the whole population is divided into two main compartments: Susceptible and Infected. Individuals can transition back and forth with respect to the specified transition probabilities. Although this model is commonly used in the modeling of repeatable diseases, e.g., flu, cold, or allergy, it is the most simplistic view of these approaches and the modeling of information spread may require more complex models [55]. If we define $\beta$ and $\lambda$ as the rate of contact from susceptible to infected, and from infected to susceptible, again, the time-dependent model can be defined by the following set of ordinary differential equations (ODEs):

$$\frac{d[S]}{dt} = -\beta \frac{SI}{N} + \lambda \frac{I}{N} \tag{2.1a}$$

$$\frac{d[I]}{dt} = \beta \frac{SI}{N} - \lambda \frac{I}{N} \tag{2.1b}$$

where $N(t)$ denotes the number of individuals in the population which equals to $S(t) + I(t)$. A

more complex epidemic model, i.e. SIR model, additionally defines recovered compartment for the individuals that recover the disease after they become infected. Despite its common use and good performance in epidemiology, its applications on information diffusion models are quite rare since recovered status is not easy to transfer in these concepts [54]. If we define $\beta$ and $\lambda$ as the rate of contact from susceptible to infected, and from infected to recovered statuses, the system can be defined with the following set of ODEs:

$$\frac{d[S]}{dt} = -\beta \frac{SI}{N} \tag{2.2a}$$
$$\frac{d[I]}{dt} = \beta \frac{SI}{N} - \lambda \frac{I}{N} \tag{2.2b}$$
$$\frac{d[R]}{dt} = \lambda \frac{I}{N} \tag{2.2c}$$

Bettencourt et al. [56] proposed the SEIZ compartmental model in which time delay between interaction and adoption is introduced. Many studies demonstrated its superior performance in modeling information diffusion compared to aforementioned methods [57, 54, 58]. The system can be analyzed by the following set of ordinary differential equations:

$$\frac{d[S]}{dt} = -\beta \frac{SI}{N} - b\frac{SZ}{N} \tag{2.3a}$$
$$\frac{d[E]}{dt} = -(1-p)\beta \frac{SI}{N} + (1-l) - \beta \frac{SZ}{N} - \rho \frac{EI}{N} - \varepsilon E \tag{2.3b}$$
$$\frac{d[I]}{dt} = p\beta \frac{SI}{N} + \rho \frac{EI}{N} + \varepsilon E \tag{2.3c}$$
$$\frac{d[Z]}{dt} = lb\frac{SZ}{N} \tag{2.3d}$$

Here, $\beta$, $b$, and $\rho$ represent the rate of contact between S and I, S and Z, and E and I; while $p$ and $l$ denote transition rate from S to I, and from S to Z, respectively. In addition to these compartmental models used in epidemiology, new variants of these models are suggested to consider the different

tie strengths, social factors, and network structures. Wang et al. [59] developed the SEIR model, in which Exposed status is added to the traditional SIR model, to consider the effect of user login frequency on information diffusion. In the following years, the value of information on individuals' behavior is considered in S-SEIR model [60]. The effect of fans is in the SCIR model [61] by adding one more compartment for the contacted individuals. An infection recovery kinetic process is added in the analysis of information diffusion dynamics in the irSIR model [62]. In contrast, the fSIR model [63] focuses on the effect of neighbors fractionally. Recently, we have proposed the CD-SEIZ model in which transition rates vary for different types of diffusion activities since their requirements of physical and cognitive efforts are not the same [55].

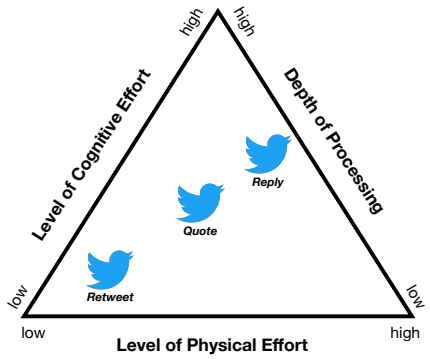


Figure 2.1: Depth of processing of different twitter activities based on level of cognitive and physical efforts [1]

In the context of Twitter, for example, SEIZ model demonstrated superior performances in the modeling the information cascades on online social networks; however, researchers employed this model to predict only retweet behaviour based on the assumption that information propagation can be described with the activity of re-sharing (retweet in Twitter) of the specific user-generated content. On the other hand, information can diffuse in a variety of ways on Twitter. *Retweet* is one of the most common diffusion tools in which users have shared the content as is. Furthermore, users

can *Reply* the original content and share their comment on it, which may trigger the exposition of the original and reply content of other users at the same time. *Quote* is also considered as a type of *Retweet*, which enables the re-share of the original content by adding your own comment on it. Despite the accepted definition of the Twitter cascade, that is the summation of *Retweet*, *Reply*, and *Quote* activities on a user-generated content, the studies employed the compartmental model to model information propagation on Twitter considered *Retweet* counts only. On the other hand, we proposed a new compartmental model (CD-SEIZ) based on the fact that different type of actions on Twitter require cognitive and physical efforts and processing depths.

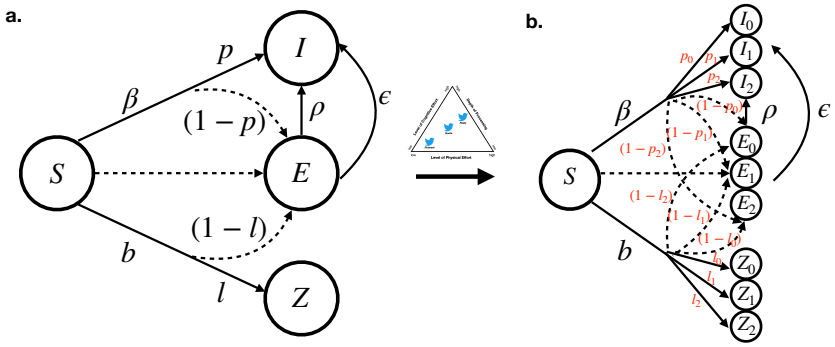


Figure 2.2: a. Original SEIZ and b. our proposed cognition-driven SEIZ (CD-SEIZ) model. Subscripts 0,1 and 2 refers retweet, quote and reply in a sorted order.

Inspired by the current findings in [1], we argue that different actions in Twitter require different physical and cognitive efforts along with varying processing depth. Levens et al. demonstrated that *Retweet* action requires the least cognitive and physical efforts since it requires an online audience to read the content and push a single button without adding any new content. It is followed by *Quote* action which requires more physical and cognitive effort since users need to process the information and think about writing an original content additionally. *Reply*, on the other hand, has more processing depth than *Quote* because users communicate directly one or more other users in this action. This significant change in level of physical and cognitive efforts, and depth of

processing of the different actions on Twitter (Figure 2.1) motivated us to diversify the transition rate between compartments in the SEIZ model for different types of activities. Since the rate of contact of users between compartments depends on the user's engagement on the Twitter platform, we kept all these parameters as constant for each type of activity. The proposed framework of the cognition-driven SEIZ (CD-SEIZ) model and definitions of its parameters can be seen in Figure 2.2 and Table 2.1 and 2.2, respectively. The ODE rules of the CD-SEIZ model can be written as:

$$\frac{d[S]}{dt} = \sum_{i=0}^{2} \left[ -\beta \frac{SI_i}{N} - b\frac{SZ_i}{N} \right] \tag{2.4a}$$

$$\frac{d[E_i]}{dt} = -(1-p_i)\beta \frac{SI_i}{N} + (1-l_i) - \beta \frac{SZ_i}{N} - \rho \frac{E_i I_i}{N} - \varepsilon E_i \tag{2.4b}$$

$$\frac{d[I_i]}{dt} = p_i \beta \frac{SI_i}{N} + \rho \frac{E_i I_i}{N} + \varepsilon E_i \tag{2.4c}$$

$$\frac{d[Z_i]}{dt} = l_i b \frac{SZ_i}{N} \quad \text{for } i = \{0,1,2\} \tag{2.4d}$$

Table 2.1: Definitions of The Parameters in SEIZ Model

| ***Parameter*** | ***Definition*** |
|---|---|
| $\beta$ | Rate of contact between $S$ and $I$ |
| $b$ | Rate of contact between $S$ and $Z$ |
| $\rho$ | Rate of contact between $E$ and $I$ |
| $p$ | Transition rate of $S \rightarrow I$, given contact with $I$ |
| $1-p$ | Transition rate of $S \rightarrow E$ , given contact with $I$ |
| $l$ | Transition rate of $S \rightarrow Z$, given contact with $Z$ |
| $1-l$ | Transition rate of $S \rightarrow E$ , given contact with $Z$ |
| $\varepsilon$ | Incubation rate |

Table 2.2: Definitions of The Parameters in CD-SEIZ Model

| ***Parameter*** | ***Definition*** |
|---|---|
| $\beta$ | Rate of contact between $S$ and $\sum_{i=0}^{2} I_i$ |
| $b$ | Rate of contact between $S$ and $\sum_{i=0}^{2} Z_i$ |
| $\rho$ | Rate of contact between $\sum_{i=0}^{2} E_i$ and $\sum_{i=0}^{2} I_i$ |
| $p_i$ | Transition rate of $S \rightarrow I_i$, given contact with $I_i$ |
| $1-p_i$ | Transition rate of $S \rightarrow E_i$ , given contact with $I_i$ |
| $l_i$ | Transition rate of $S \rightarrow Z_i$, given contact with $Z_i$ |
| $1-l_i$ | Transition rate of $S \rightarrow E_i$ |
| $\varepsilon$ | Incubation rate |

*Threshold Models*

A network (graph) $G$ is defined as a set of vertices (nodes) $V$, and the interactions between them called edges (links) $E$, i.e. $G = (V,E)$. According to the network characteristics, nodes may denote people, proteins, economic goods, words. At the same time, edges may represent the social interaction between people, the chemical connection of the proteins, the relation between different products, or the co-existence of the words in a sentence. Threshold models are based on the assumption that individuals' behavior in a network can be affected by their neighbors' actions. The *Linear Threshold Model (LTM)* was first proposed by Granovetter [6] to model collective behavior. In this model, there are $N$ agents in a network, who can be in one of the states of active or inactive, and each agent $v$ has a threshold value $\phi_v$ in changing its status. For each neighbor of $v$ ($u \in \Gamma(v)$), the edge between them has a non-negative weight $w_{u,v}$ such that $\sum_{u\in\Gamma(v)} w_{u,v} \leq 1$. An inactive agent $v$ becomes active in the next time step only if $\sum_{u\in\Gamma(v)} w_{u,v} \geq \phi_v$. This process continues until every agent in the network stabilizes their status. To exemplify, Figure 2.3 shows a schematic representation of LTM: Suppose that we focus on a given small network in which node $i$ and $j$ are inactive at $t = 1$. Since the average opinion of the neighbors of $i$ ($\bar{o}_i$) exceeds its threshold ($\phi_i$), the node $i$ will be active at $t = 2$ , while the node $j$ will remain inactive since $\phi_j > \bar{o}_j$. In the

next time step, since $\bar{o}_j$ will be increased due to being $i$ active, the node $j$ will be active at $t = 3$.

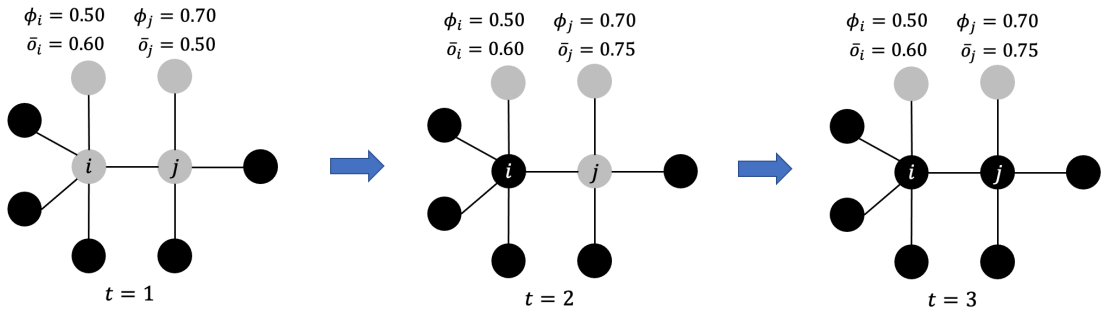


Figure 2.3: A graphical representation of LTM.

The most challenging task in applying the threshold model is the determination of threshold distributions of agents in the system. In many studies, the heterogeneity of the agents has been poorly defined or ignored, and threshold distribution is assumed to be either homogeneous (uniform) [64, 65, 66] or binary [4]. Although these studies provide very comprehensive details about the dynamics of the information diffusion process, some researchers criticized these processes' deterministic structure and argued that more randomness should be given by increasing heterogeneity in individual threshold values. These studies employed more complex threshold distributions such as tent-like function [9], truncated normal distribution function [10] or sigmoid function [11].

The dependency of the threshold in LTM to a linear constraint of edge weight has been extended, and numerous alternatives have been proposed [67]. One of the most well-studied variants of LTM is called the *Majority Threshold Model (MTM)*, in which a node becomes active if the majority of its neighbors are active. This intuitive method has mainly been applied in voting systems [68], distributing computing and influence maximization problems [69]. In the *Small Threshold Model (STM)*, whereas, threshold values are kept as minimal constant values to ease the optimization of influence maximization problems [69]. In the *Unanimous Threshold Model (UTM)*, the threshold

of each node is taken to be equal to its degree; however, its applications are limited with the studies related to complex network security and vulnerability [67]. All these methods still continue to be improved for specific application areas, but *Generalized Threshold Model (GTM)* which is the specialized version of the LTM, can be accepted as the most common method.

### *Cascading Models*

After Goldenberg's pioneering study of diffusion in marketing, this stochastic approach has become another well-known technique in information diffusion studies. Again, each node can be either in active or inactive states. According to Rogers [70], there are a small set of active nodes at the beginning, who are called early adopters and information disseminates in a network through cascades initiated by these early adopters. The main idea behind the *Independent Cascade Model (ICM)* is that an active node $i$ has a single chance to influence one of its inactive neighbors, i.e., the node $v$ with a probability $p_{u,v}$. Whether the influencing attempt is successful or not, the node $i$ will not make any further attempt in the next time steps. Sequential order is considered in the existence of attempts by multiple active nodes that try to influence one of their common neighbor nodes. As in threshold models, the process continues until there is no more possible attempt. Figure 2.4 shows a schematic representation of ICM: Suppose that only $i_1$ and $i_2$ are active nodes in the given small network; however, both of these nodes fail to influence $i_3$ in the next time step, while $i_2$ is successful in influencing $i_4$. Both nodes, i.e., $i_1$ and $i_2$, will be inactive at $t = 2$. If we suppose that the attempt of $i_4$ in influencing $i_6$ is successful, $i_4$ will be inactive while $i_6$ is active at $t = 3$. $i_5$ will also be inactive at $t = 3$ since it has no susceptible neighbor to influence.

Since ICM offers a probability of infection associated with each edge rather than using a single infection probability, it might be assumed as the generalized version of the SIR model mentioned in the previous section. As in LTM, different versions of ICM have been studied in information

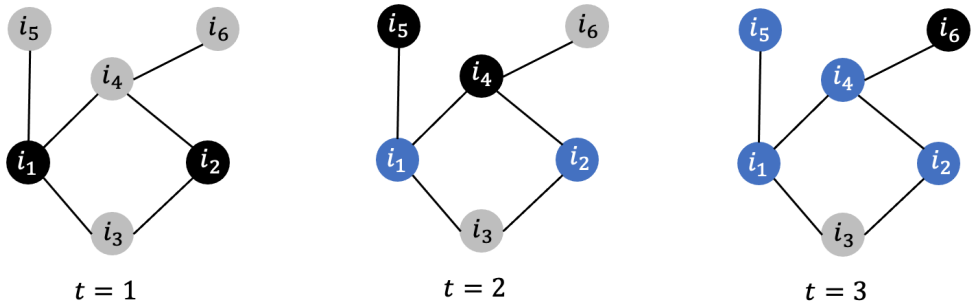


Figure 2.4: A graphical representation of ICM.

diffusion studies. In *Decreasing Cascade Model* [71], for example, the influence probability is obtained from a non-decreasing function. Therefore, the effect of attempts to activate an inactive node and its chance of being activated in the future will be no longer independent on the contrary of ICM. Since this modification's main purpose is to model "market-saturation", its application in information diffusion studies is rarely seen. Many studies proposed a topic-aware ICM by calibrating the different topics with different influence probability values [72, 73]. Wang et al. [74], for example, proposed an emotion-based ICM model information propagation on online networks by differentiating the information diffusion probabilities of the positive and negative sentiments. Leung and Chung [75] modified traditional ICM by adding the social persuasion parameter to show the effect of tie strength (user-to-user influence) on information propagation. They demonstrated their models' better prediction accuracy compared to traditional ICM with real-world OSN data. Myers et al.[76] proposed a model in which the effects of out-of-network factors are also considered in the ICM and showed that almost one-third of the information propagation in Twitter stems from the exogenous effects. On the other hand, some researchers modified the extant information diffusion models by considering the information's heterogeneity.

As we reviewed, there are numerous methods in simulating the information diffusion processes.

The efficiency and accuracy of these methods may show significant differences with changing network topology structures. In a recent study [77], three different network structures are generated, i.e., the preferential attachment, ER random, and small-world networks, to demonstrate the variability of information diffusion models with changing network characteristics. In the same study, the response variable of information diffusion efficiency is considered as the total number of adopted individuals at the steady state. They showed that the maximum information adoption size is observed in random networks (%90), and followed by the small-world network (%72) under the ICM model with a 0.4 probability of diffusion. The adoption's size is relatively small in the preferential attachment network (%4). This is not surprising because preferential attachment networks have power-law degree distribution, and the spread might be interrupted in the existence of unsuccessful influence attempts. Although these results show the differences between these models on different network structures, changing parameters might display different results.

## Online Applications of Social Contagion Models

Online social networks (OSNs) are the platforms in which users can freely communicate with each other easily, share their ideas and emotions freely, and participate in groups of people who have similar interests promptly. All aforementioned fast-paced activities caused the generation of an immense scale of data every day; thus, human-related studies have been gained more interest from researchers from different disciplines. One of the most appealing research areas related to OSNs is understanding the attributes and dynamics of information spread through intermediate users' set during this information exchange. The focal points in this process are users in a network structure and the information itself. The pioneering study of Granovetter [6], in which a receiver-centric linear threshold model (LTM) approach for information diffusion is firstly introduced, has been developed by researchers from different disciplines. As the sender-centric counterpart of LTM,

Goldenberg [7] proposed Independent Cascade Model (ICM) as an information diffusion modeling approach. Nowadays, there are numerous approaches to model information diffusion in networks, and we briefly surveyed these methods, i.e., threshold models, cascading models, epidemic models, game theory models, in Section 1. Here, we aim to give examples of real-world applications of information diffusion models on OSNs.

*First*, the general aim of applying information diffusion models on OSNs is to understand *what*, *how*, *why* and *how much* information disseminates. Researchers utilized information diffusion models in the investigation of trending (showing bursty behavior) topics detection and differentiation of true news and fake news (*what?*), and in the prediction of cascading pattern (*how?*), and understanding the self-organization in OSNs during information diffusion and effects of network structure on this process (*why?*), and in the estimation of the size of the information spread (*how much?*). Gruhl et al. demonstrated the effectiveness of the generative epidemic models for the analysis of the information spread on OSNs [78]. Leskovec et al. investigated the cascading behavior of rumors, viruses, and ideas in large blog graphs by using information diffusion models. Jin et al. [79] employed the SEIZ epidemic model to predict the sizes of different Twitter cascades. Additionally, he demonstrated the difference in the model parameters for true and false information to show these models' potential in rumor detection on OSNs. Wang et al. [59] developed the SEIR model, in which Exposed status is added to the traditional SIR model, to consider the effect of user login frequency on information diffusion. In the following years, the value of information on individuals' behavior is considered in S-SEIR model [60]. The effect of fans is in the SCIR model [61] by adding one more compartment for the contacted individuals. Fan et al. employed LTM and ICM models to understand network topology's effect on the information diffusion dynamics by considering different network structures obtained from the Sina Weibo microblogging platform. They demonstrated that cascade motifs display similar patterns when network structures and degree correlations are similar [80]. Weng et al. [81], on the other hand, argued that information

diffusion models could be used to investigate the evolution of the social network structure since they explain how new social links are constructed during the information propagation process. Due to these models' effectiveness in mimicking information diffusion over OSNs, some studies predicted the diffusion probabilities using real-world network data to calibrate their information diffusion models and simulate different cases to understand the effect of the different network topology [82, 83, 84].

Furthermore, some studies criticized the identicality of the information propagation or threshold probabilities in classical information diffusion models by arguing that these models generally underestimate the heterogeneity between messages or individuals. This poorly-defined heterogeneity for users triggered an extensive use of homogeneous (uniform) [64, 65, 66] and binary [4] threshold in many studies. To remedy this oversimplification and thereby provide a more holistic and accurate model, more complex threshold models such as tent-like function [9], truncated normal distribution function [10] or sigmoid function [11] are also used in the literature by looking the general information adoption behavior of users on OSNs. Leung and Chung [75] modified traditional ICM by adding the social persuasion parameter to show the effect of tie strength (user-to-user influence) on information propagation. They demonstrated their models' better prediction accuracy compared to traditional ICM with real-world OSN data. Myers et al.[76] proposed a model in which the effects of out-of-network factors are also considered in the ICM and showed that almost one-third of the information propagation in Twitter stems from the exogenous effects. On the other hand, some researchers modified the extant information diffusion models by considering the heterogeneity in the information itself. Many studies proposed a topic-aware ICM by calibrating the different topics with different influence probability values [72, 73]. Wang et al. [74], for example, proposed an emotion-based ICM to model information propagation on online networks by differentiating the information diffusion probabilities of the positive and negative sentiments.

*Second*, although these models are called information diffusion models, these methods and their

new variants are also used to model abstract values' contagiousness such as emotions or sentiments. Thus, we can list another common application of information diffusion models on online social networks as sentiment (emotion) spreading. Wang et al. [85] proposed an emotion-based ICM to model the process of sentiment spreading on Sina Weibo. In their novel method, the sentiment spreading process introduces the propagation probabilities for each possible message sentiment and executes a learning-based model that simultaneously considers user and tweet features. Wang et al. [86] introduced emotional transmissibility along with information transmissibility to describe the differences in the patterns of different emotions' contagion under the emotion-based SIR model. Xiong et al. demonstrated the effect of hub users in the evanescence of opposite emotions in a network by proving a better performance of emotional-based ICM and the spreader-ignorant-stifler model compared to traditional methods [87].

*Third*, another important application area of information diffusion models on OSNs is the influence maximization problem, which can be defined as "the problem of finding a small set of seed nodes in a social network that maximizes the spread of influence under certain influence cascade models" [88]. Numerous studies proposed models with simply tunable parameters to optimize the trade-off between running time and influence maximization accuracy and tested their algorithms on real networks. This specific problem has gained a lot of attention after Kempe et al.'s pioneering study in which LTM is employed to model diffusion of innovation under the concept of influence maximization of word-of-mouth marketing [89]. The literature recently has been enriched with the improvements of this research for either information diffusion and marketing approaches. Chen et al. [90] proposed a degree distribution-based node-degree heuristic approach to enhance the speed and the effectiveness of Kempe's original method. Liu et al. [91] addressed influence maximization problem under ICM in signed networks by introducing two opposite (constructive and destructive) influential types and showed the superiority of their algorithm in a more realistic scenario with the verification of their algorithm on a real-world, large-scale OSN. Recent research also showed

that state-of-art influence maximization models for a single network do not as well perform as on multi-layer networks in which spreading processes significantly differ on the same discussion in two different OSN platforms, i.e., Twitter and Facebook [92].

*Fourth*, these models are also utilized to identify segregated echo-chambers in the polarized discussions on OSNs. Xie et al. [93] investigated the polarization among the users in the climate-change discussion by using ICM and identified the different echo-chambers by defining activist and skeptic clusters. Lei et al. showed the difference in the message propagation activities of the users who clustered based on their previous tweeting activities to argue that information diffusion models as a community detection approach might be helpful for recommendation systems [94].

## Related Previous Works as a Motivational Source

### *Threshold Heterogeneity of Agents in Social Contagion Analysis*

While network study is not new, its focus has shifted from physical proximity and socio-economic networks to social media based networks. This change is arguably the product of the fast-paced information flow that is engendered by the technological advances of the 21st century, and the resulting impact on the needs and lifestyles of people. The need to address the newly emerged phenomenon of the creation and dissemination of information on social media has amplified interest in the field of network science. Indeed, network science applications have extended to the field of marketing [95, 96], sociology [97, 98], political science [99], physics [100], economics [101], machine learning [102] and biology [103], all attempting to reveal the interdependency between units of interest. Social media has allowed people's opinions to be voiced freely, with far reaching consequences; this phenomena has affected many things including the shift to online marketing and social media based political campaigning. The interplay between information from average

users and bigger entities is much larger than in the past due to social media. This reciprocity in information flow, the increase in the volume of information received and sent, and the ease of relaying information has made it imperative that researchers understand the dynamics of information and opinion formation, propagation, and exchange [104, 105, 106, 107].

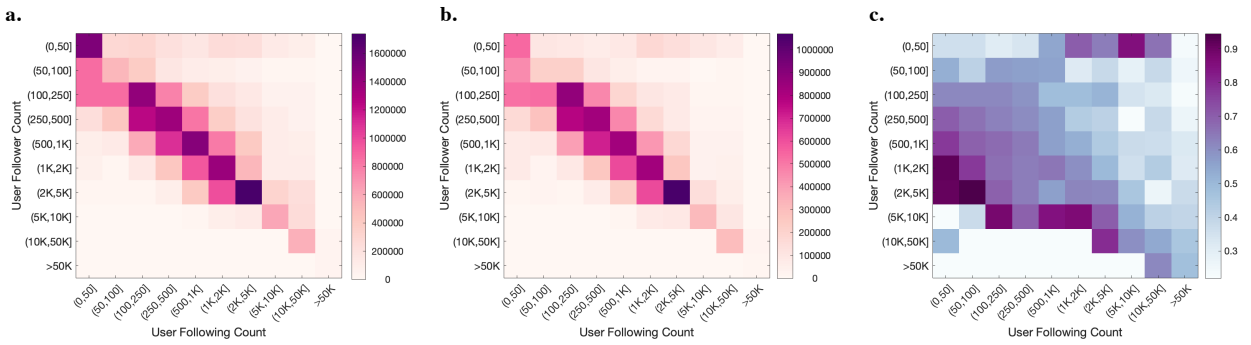


Figure 2.5: a. Number of users b. Number of retweeters c. The retweeting probability of users in each cluster -the element-wise ratio of number of retweeters in b to the number of users in a.

As aforementioned in previous subsections, in the mid-20th century, sociology pioneered the development of information and opinion diffusion as a subject of study. One of the early studies is the Markovian linear threshold model introduced by Granovetter [6]. According to the threshold model, individuals adopt a new opinion only if a critical fraction of their neighbors have already adopted the new opinion. Granovetter suggests that the threshold of individuals can be different, and are influenced by demographic and psychographic factors. However, this heterogeneity among researchers is poorly-defined, which leads to an extensive use of uniform [64, 65, 66] and binary [4] thresholds in many studies. Arguably, this assumption of homogeneous or binary thresholds is an oversimplification of reality and may produce misleading results. To remedy this oversimplification and thereby provide a more holistic and accurate model, more complex threshold models such as the tent-like function [9], the truncated normal distribution function [10] or the sigmoid function [11] are also used in the literature. In our study [82], we employ threshold model to understand the information diffusion behaviour of users in online social networks. Our Twitter data mining results

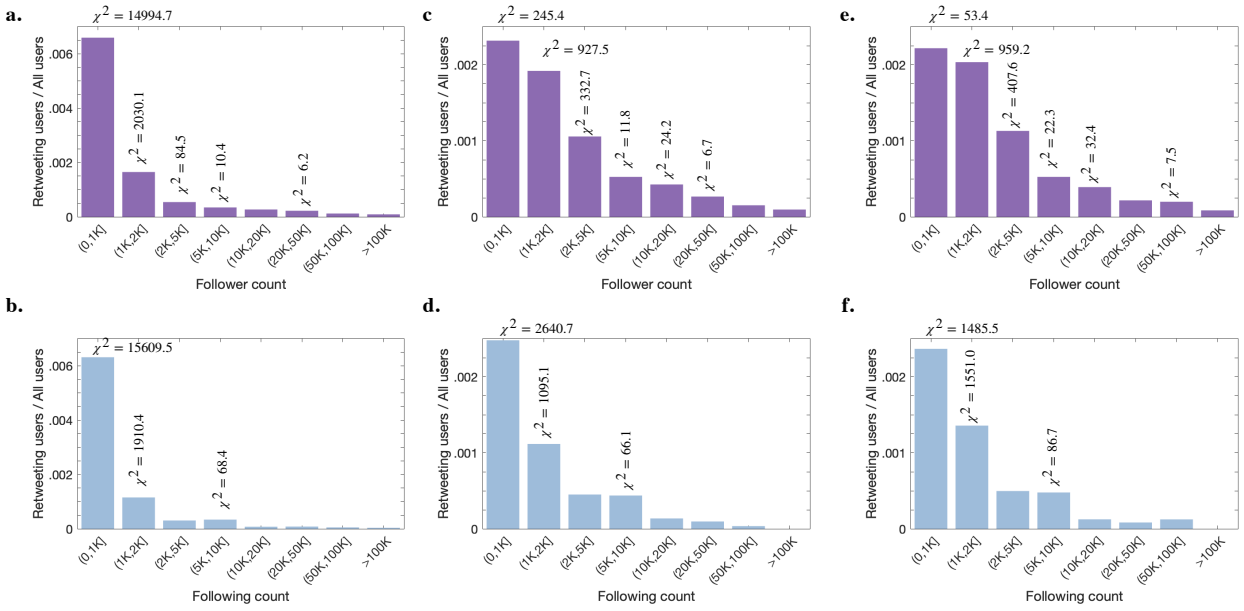


Figure 2.6: The ratio of retweeters of RT1, RT2 and RT3 to all users when we cluster users according to the their follower counts and following counts independently. Bar plots in a and b shows the results for RT1 users, c and d for RT2 users and e and f for RT3 users.

show that the threshold of an individual for sharing the information (retweeting) is affected either by their out-degree (number of followers) or in-degree (number followed). Some studies have already employed degree-dependent threshold models in explaining the dynamics of information diffusion [108, 109], however the degree dependency of an individual's threshold is associated only with their out-degree. Additionally, these studies have implemented threshold heterogeneity by using custom threshold functions, which renders the results less robust and less reliable. Therefore, we seek to analyze the sensitivity of information diffusion dynamics to in-degree and out-degree dependencies of thresholds.

The Twitter data set used for this study contains 30,704,025 tweets from the cybersecurity-related events from March 2016 to August 2017, of which 16,884,353 are retweets. We first collected follower and following counts of each user to relate the retweeting probability of users with the two

aforementioned counts. We then generated a matrix of rows representing follower count clusters, and columns representing following count clusters of all users in our data set (Figure 2.5a). We also filtered users who have retweets only and generated the same matrix (Figure 2.5b). Preliminary results showed that a majority of users are clustered around the areas where follower and following counts are not extreme, and the matrix of retweeted users show a similar pattern. Since retweeting probabilities of users in each cluster are not clear from these matrices only, we calculated the element-wise division of these two matrices to figure out the ratio of number of retweeters to the number of all users in each cluster. Results show that the retweeting probability of users who have a relatively low following count is higher, i.e., the threshold of a node seems to be positively correlated with its out-degree. On the other hand, the effect of varying follower count on the retweeting probability is unclear since the left-bottom of the matrix is empty (Figure 2.5c). To remedy this, we extracted the 3 most retweeted tweets (RT1, RT2, RT3) of retweet sizes 138,969, 58,546, and 57,280, respectively. We divided users into 8 clusters with respect to their follower (Figure 2.6a-2.6c) and following counts (Figure 2.6d-2.6f) independently rather than jointly. For each cluster, we calculated the ratio of the number of users who retweeted RT1, RT2, or RT3 to the number of all users, respectively, as in Figure 2.6c. The only difference is that instead of all retweeters, we focused on retweeters of RT1, RT2 and RT3. Thus, we could prevent the masking effect of non-active users in the whole data set. Results show that both follower and following counts have a negative effect on the retweeting probability of users. Furthermore, we applied a one-sided Chi-square test ($\alpha = 0.05$) to determine whether this decreasing pattern is statistically significant. We included relative $\chi^2$ values if the retweeting ratio in the cluster is significantly higher than that of next cluster (p-value is lower than 0.005). We observed that the retweeting probability decreases when follower count increases and this decreasing pattern is significant for almost all consecutive clusters. Nevertheless, the decrease between the consecutive clusters defined by following counts were significant only when following counts are not high. This is probably because clustering users according to their follower and following counts with the same limits has a notable effect

on the test statistics. Distributions of follower and following counts of users are not similar in the data set, i.e, the .8 and .9 quantiles and the maximum of the user following counts are 1916, 3860, and 3,136,215, while it is 2332, 5639, and 94,833,565 for user follower counts. When we decrease the number of clusters from 8 to 3 ($(0,1K],(1K,10K],(>10K]$), we observed that the retweeting probability decreases when following count increases, and this decreasing pattern is significant for all consecutive clusters ($\chi^2 = \{12602.8, 18087, 272.3\}$ for RT1, $\{2762.3, 1807.2, 52.0\}$ for RT2, and $\{1299.3, 987.1, 87.1\}$ for RT3). Thus, our data analysis shows that thresholds of individuals to disseminate information is positively correlated with their in-degree and out-degree.

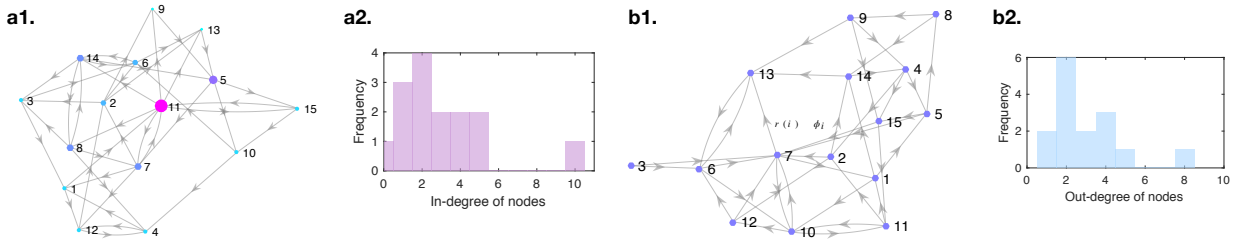


a3.

| | out-degree | in-degree | $r(i)$ | $\phi_i$ |
|---|---|---|---|---|
| 1 | 2 | 3 | 8 | 0.75 |
| 2 | 3 | 3 | 6 | 0.75 |
| 3 | 2 | 3 | 9 | 0.75 |
| 4 | 2 | 3 | 10 | 0.75 |
| 5 | 5 | 3 | 2 | 1 |
| 6 | 3 | 3 | 7 | 0.75 |
| 7 | 4 | 3 | 3 | 1 |
| 8 | 4 | 3 | 4 | 1 |
| 9 | 1 | 3 | 14 | 0.5 |
| 10 | 2 | 3 | 11 | 0.5 |
| 11 | 8 | 3 | 1 | 1 |
| 12 | 2 | 3 | 12 | 0.5 |
| 13 | 1 | 3 | 15 | 0.5 |
| 14 | 4 | 3 | 5 | 1 |
| 15 | 2 | 3 | 13 | 0.5 |

b3.

| | out-degree | in-degree | $r(i)$ | $\phi_i$ |
|---|---|---|---|---|
| 1 | 3 | 2 | 11 | 0.5 |
| 2 | 3 | 3 | 6 | 0.75 |
| 3 | 3 | 0 | 15 | 0.5 |
| 4 | 3 | 2 | 10 | 0.75 |
| 5 | 3 | 2 | 9 | 0.75 |
| 6 | 3 | 5 | 3 | 1 |
| 7 | 3 | 10 | 1 | 1 |
| 8 | 3 | 1 | 13 | 0.5 |
| 9 | 3 | 1 | 14 | 0.5 |
| 10 | 3 | 4 | 4 | 1 |
| 11 | 3 | 2 | 8 | 0.75 |
| 12 | 3 | 1 | 12 | 0.5 |
| 13 | 3 | 5 | 2 | 1 |
| 14 | 3 | 4 | 5 | 1 |
| 15 | 3 | 3 | 7 | 0.75 |

Figure 2.7: The representation of network when $N = 15$ and a1. out-degrees are power-law distributed and in-degrees are kept constant as $M_{in} = 3$, b1. in-degrees are power-law distributed and out-degrees are kept constant as $M_{out} = 3$. Histogram plots of a2. out-degrees in a1, b2. in-degrees in b1. In addition to out-degree and in-degree of nodes, their ranks $r(i)$ and thresholds $\phi_i$ are also given in the table for a3. the network in a1, b3. the network in b1.

The main aim of this study was to investigate the dynamics of information diffusion when thresholds are correlated with the degree-distribution of the nodes. For this purpose, we generated power-law distributed random numbers ($x_i$) to further assign them to the desired degree-distribution of the network. To understand the effect of out-degree dependent threshold and in-degree dependent threshold on the dynamics of opinion spreading separately, we created two independent networks:

1. **CASE I:** Out-degrees of the nodes ($k_{out}$) are power-law distributed and has the form $\sqrt{N}x^{\gamma}$ and in-degrees are kept constant ($M_{in}$).
2. **CASE II:** In-degrees of the nodes ($k_{in}$) are power-law distributed and has the form $\sqrt{N}x^{\gamma}$ and out-degrees are kept constant ($M_{out}$) .

Here, $N$ denotes number of nodes in the network (seed size) and $\gamma = 3$ for both cases for a fair comparison. Then, we added directed links between randomly selected node pairs $(i, j)$ by employing configuration model [110] if $i \neq j$ and $k_{out} < x_i$ for Case I, $k_{in} < x_i$ for Case II. In this network structure, self-edges are not allowed while multiple edges between same node pairs are possible. Since total in-degree in the network should be equal to the total out-degree in the network and total in-degree is equal to total out-degree, one can easily realize that the mean-degree of the network is equal to fixed in-degree ($M_{in}$) in Case I, and fixed out-degree ($M_{out}$) in Case II.

After generating networks, we employed the degree-dependent threshold model by assigning the threshold of node $i$ to share the information ($\phi_i$) as correlated with:

1. **CASE I:** its out-degree .
2. **CASE II:** its in-degree.

Since threshold heterogeneity is one of our main concerns in this study, we divided nodes into $N_{th}$ groups by their ranks which can be obtained by sorting their:

1. **CASE I:** out-degrees.

2. **CASE II:** in-degrees.

Then, we assigned thresholds as evenly spaced $N_{th}$ points between 0.5 and 1 to prevent the confounding effect of the mean-threshold, i.e. the average threshold is always constant as 0.75. Thus, increasing $N_{th}$ yields more heterogeneity among thresholds of individuals.

$$\phi_i = \begin{cases} 0.5 & \text{if } r(i) \leq \frac{N}{N_{th}} \\ 0.5 + \frac{0.5}{N_{th}-1} & \text{if } \frac{N}{N_{th}} < r(i) \leq \frac{2N}{N_{th}} \\ \ldots & \ldots \\ 0.5 + \frac{0.5(N_{th}-2)}{N_{th}-1} & \text{if } \frac{(N_{th}-2)N}{N_{th}} < r(i) \leq \frac{(N_{th}-1)N}{N_{th}} \\ 1 & \text{if } \frac{(N_{th}-1)N}{N_{th}} < r(i) \leq N \end{cases}$$

where $r(i)$ represents the rank of the node when they are sorted according to their out-degree in Case I and their in-degree in Case II.

An example of network generation for two cases, out-degrees and in-degrees and relative threshold values of the nodes are shown in Figure 2.7.

We initialized the opinions of individuals as a Bernoulli distributed random variable with an initial probability ($p$), i.e. the opinion of the node $i$ ($s_i$) might equal to 1 with a probability $p$ and equal to 0 with a probability $1-p$. We assumed that the opinion change process is reversible; thus, individuals may change their opinions continuously rather than only once.

After generating the network, assigning thresholds, and initializing the opinions, we ran the opinion change simulations. The process of updating their opinions is as follows:

1. Picking a node $i$ randomly.

2. Calculating the weighted average of the opinions of its in-neighbors ($\bar{o}_i$). Here, weights are the multiple edges formed between node $i$ and its neighbors.

3. Updating the opinion of node $i$ ($s_i$) according to the criteria as follows:

   (a) **if** $s_i = 0$ and $\bar{o}_i - s_i > \phi_i$,

   **then** $s_i = 1$ in the next step.

   (b) **if** $s_i = 1$ and $\bar{o}_i - s_i < -\phi_i$,

   **then** $s_i = 0$ in the next step.

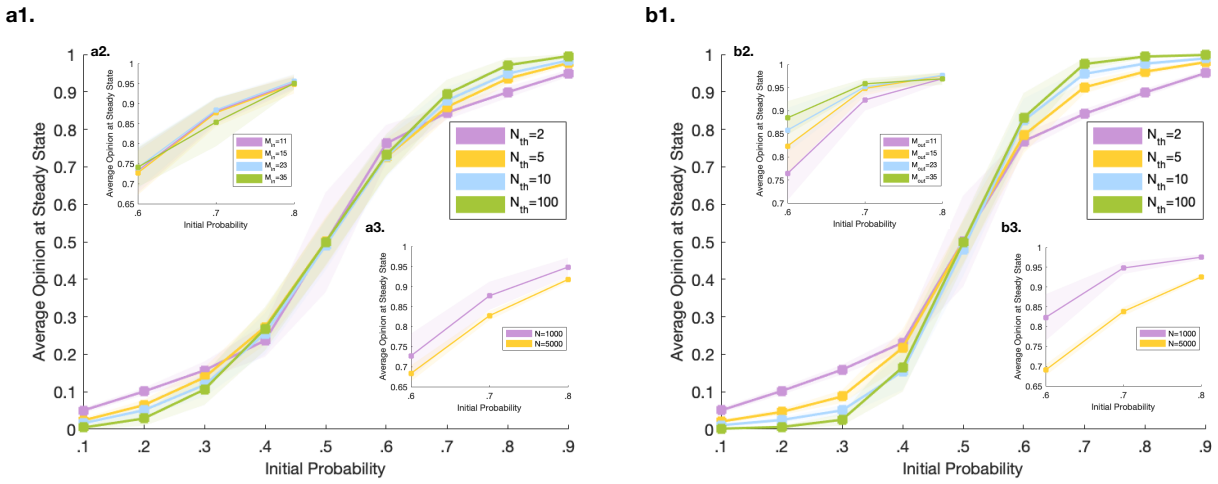


Figure 2.8: Simulation result of average opinion at steady state as a function of initial probability ($p$) a1. with varying threshold heterogeneity ($N_{th}$) when $N = 1000$ and $M_{in} = 15$, a2. with varying in-degree ($M_{in}$) when $N = 1000$ and $N_{th} = 10$ and a3. with varying seed size ($N$) when $M_{in} = 15$ and $N_{th} = 10$ if thresholds are out-degree dependent, and out-degrees are power-law distributed. Additionally, the simulation result of the average opinion at steady state as a function of $p$ b1. with varying $N_{th}$ when $N = 1000$ and $M_{in} = 15$, b2. with varying out-degree ($M_{out}$) when $N = 1000$ and $N_{th} = 10$ and b3. as a function $p$ when $M_{out} = 15$ and $N_{th} = 10$ if thresholds are in-degree dependent, and in-degrees are power-law distributed.

This Markovian chain is repeated until all possible opinion changes are made and individuals fix their opinion. We carried out all the simulations on MATLAB and repeated these simulations 50,000 times.

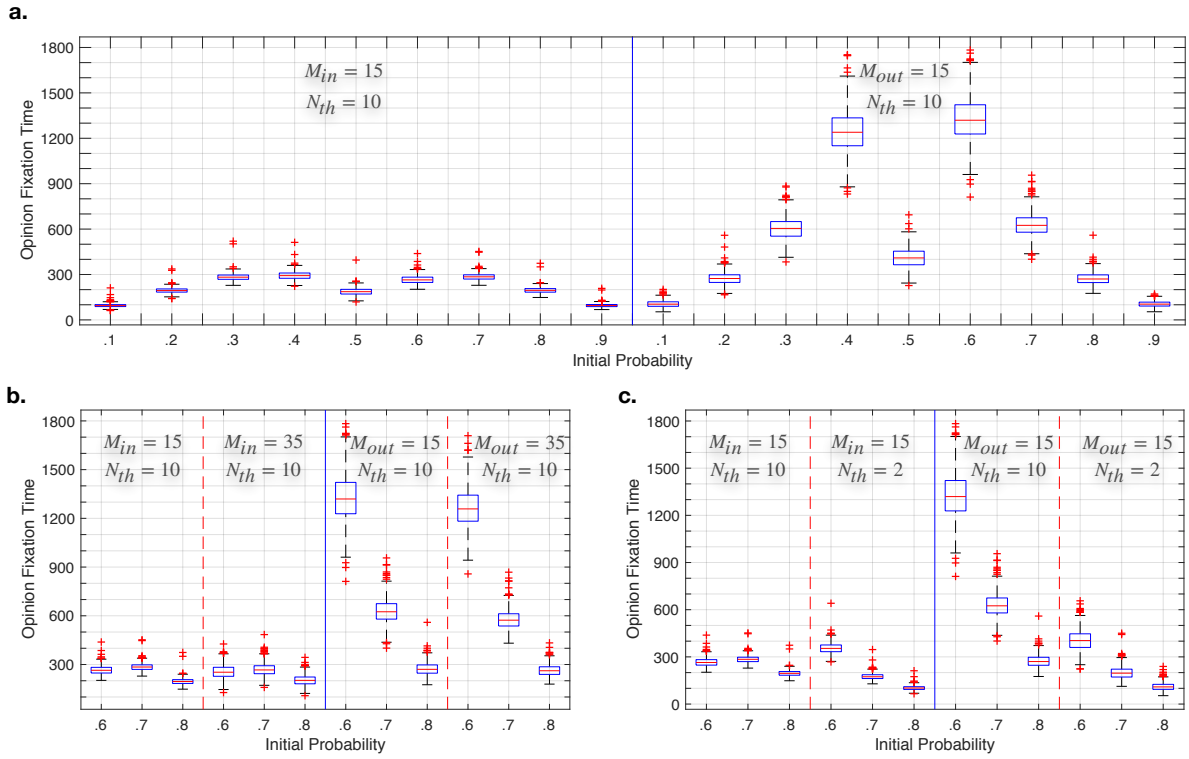


Figure 2.9: The comparison of fixation time of individuals as a function of the initial probability a. when thresholds are out-degree dependent (left) and in-degree dependent (right) b. with varying mean-degree ($M_{in}$/$M_{out}$) when thresholds are out-degree dependent (left) and in-degree dependent (right) c. with varying threshold heterogeneity ($N_{th}$) when thresholds are out-degree dependent (left) and in-degree dependent (right).

In the given study, we first aimed to analyze the effect of in-degree and out-degree dependence of thresholds on the average opinion at steady state ($\bar{s}$). Therefore, after all the individuals fix their

opinions in a network, we averaged their opinions by using the equation below:

$$\bar{s} = \frac{1}{N}\sum_{i}^{N} s_i \tag{2.5}$$

where $s_i$ is the opinion of node $i$ at steady state. We conducted our simulations to measure $\bar{s}$ as a function of the initial probability ($p$) with a varying mean-degree ($M_{in}/M_{out}$), seed size ($N$), and threshold heterogeneity $N_{th}$. Line plots in Figure 2.8 represent the expected value of 50,000 Monte Carlo simulations, and shaded areas with the same colors denote the relative one standard deviation from the expected value of these simulations. Here, Figure 4.a1-4.a3 shows the simulation results when thresholds are out-degree dependent and out-degrees are power-law distributed, while in-degrees are kept constant. Figure 4.b1-4.b3, on the other hand, indicates the simulation results when thresholds are in-degree dependent and power-law distributed, while out-degrees are kept constant.

Figure 2.9 shows the time elapsed until all individuals fix their opinion ($t_f$) as a function of $p$ with varying $M_{in}/M_{out}$ and varying $N_{th}$. We did not simulate the effect of varying $N$ on $t_f$ since it is already clear that increasing the seed size would cause more deviation in the opinions and increases $t_f$.

Figure 2.8a1 and 2.8b1 show $\bar{s}$ as a function of $p$ at various $N_{th}$ values. Since the standard deviation of the simulations are highest in the range $0.35 \lesssim p \lesssim 0.65$, we especially focus on the results when $p \lesssim 0.35$ and $p \gtrsim 0.65$. In general, the system is more likely to reach a consensus when thresholds are in-degree dependent, and there is a clear asymmetry before and after $p = 0.5$ in both cases. Therefore, we just focused on the region $0.6 \leq p \leq 0.8$ for further analysis. Although threshold heterogeneity of nodes in the system has a slight effect in the resulting average opinion when thresholds are out-degree dependent, we can conclude that the probability that the system reaches a consensus increases as the threshold heterogeneity increases; this increase is more pronounced

when thresholds are in-degree dependent, e.g. $\bar{s} = 0.8412$ when $N_{th} = 2$, while $\bar{s} = 0.9742$ when $N_{th} = 100$ at $p = 0.7$ (Figure 2.8b1). This can be explained as follows: When $N_{th} = 2$, thresholds are distributed as 0.5 or 1, and a node which has opinion 0 can change its opinion from 0 to 1 when 8 neighbors or all of its neighbors have opinion 1 if $N_{th} = 2$, respectively. On the other hand, thresholds may take values of $0.500, 0.625, 0.750, 0.875$ or 1.000 when $N_{th} = 5$, and a node can change its opinion when 8, 10, 12, 14 or all of its neighbors have opinion 1 if $N_{th} = 5$, respectively. When the initial probability is higher than 0.7, one may expect that a node has more than 10.5 ($M_{in}xp = 15x0.7$) neighbors who have opinion 1 initially, and exceeding thresholds are easier when thresholds are not equal to 1. Therefore, the number of nodes which have opinion 1 is higher at the steady state when the threshold heterogeneity is higher.

When it comes to the effect of heterogeneity on the opinion fixation time, $t_f$ increases with increasing $N_{th}$ when thresholds are in-degree dependent. When thresholds are out-degree dependent, the effect of $N_{th}$ on $f_t$ is very minimal and the relation between $N_{th}$ and $t_f$ depends on $p$, thus, increasing $N_{th}$ causes the people to fix their opinions later when $p \gtrsim 0.7$, while the effect is opposite when $0.6 \gtrsim p \gtrsim 0.7$.

Figure 2.8a2 and 2.8b2 show $\bar{s}$ as a function of $p$ at various $M_{in}$ and $M_{out}$ values. Results show that the change in the mean-degree has no prominent effect on the average opinion at the steady state when thresholds are out-degree dependent; however, increasing the mean-degree seems to facilitate reaching a consensus when thresholds are in-degree dependent if $p \lesssim 0.7$. In the same situation, if $p \gtrsim 0.7$, $\bar{s}$ values are very close to each other. Since the standard deviations of the results are high, we can conclude that the mean degree does not affect average opinion at a steady state when thresholds are in-degree dependent or out-degree dependent. This is not surprising when we redefine the threshold model. The threshold model takes the ratio of the node's threshold to the average opinion of his neighbors and changes the node's opinion if the ratio is higher than 1. The ratio does not change with changing mean-degree when the initial, $\bar{s}$, is not affected from

$M_{in}$ and $M_{out}$. We would expect $t_f$ to increase because when the number of links between nodes increased and caused more changes in ideas, but the results show that the change in mean-degree has no effect on $t_f$ when thresholds are in-degree or out-degree dependent.

Increasing node size in the network decreases $\bar{s}$ significantly when thresholds are in-degree dependent, whereas it has very little effect when thresholds are out-degree dependent. The effect of seed size on $\bar{s}$, when $0.6 \leq p \leq 0.8$, shows that there is more diversity in the opinions when the seed size is higher, e.g. $\bar{s} = 0.9480$ when $N = 1000$, while $\bar{s} = 0.7155$ when $N = 5000$ at $p = 0.7$. Low standard deviation in the Monte Carlo simulations also demonstrates the consistency of simulation results in every trial.

We can easily argue that, our study is novel because the degree-dependency of thresholds is inferred by using real world Twitter data. Social data analysis shows that the threshold of a node does not only depend on its out-degree but also depend on its in-degree. Although the examples of out-degree dependent threshold models can be found in some studies, we also examined the results of opinion change simulations of the in-degree dependent threshold model. This study also investigates the effect of heterogeneity in thresholds reaching a consensus for the first time. Our simulations demonstrated that the system is more likely to reach a consensus when thresholds are in-degree dependent, rather than out-degree dependent. However, people change their opinion more and fix their opinion later in this case. Thresholds with higher heterogeneity are more likely to come to a consensus, but reaching a consensus takes more time than thresholds with lower heterogeneity, and this change is more significant when threshold are correlated with in-degree of nodes. Additionally, increasing seed size in the network makes the formation of a consensus more difficult regardless of the dependence of threshold to the in-degree or out-degree. We also note that as mean degree increases, diversity in opinions of individuals decrease when thresholds are in-degree dependent, while it has no effect when thresholds are out-degree dependent.

*Effects of Network Topology in Social Contagion Analysis*

Networks are representations of the connection patterns of complex systems in which entities might be proteins, individuals, economic goods, etc. Topological structures and different properties of diverse complex networks have been investigated for decades. Most importantly, the characterization of the mixing patterns of these network structures helps us to understand the evolutionary, functional and dynamic process of those complex systems [111]. If nodes in a network tend to associate with other similar nodes, this pattern is called assortative mixing (also known as *homophily*). The concept of assortativity is extensively studied since its introduction by Newman [112] in 2002. Although its application areas are diverse, the assortativity of a network is generally determined by the Pearson correlation coefficient between the degree distribution of its nodes. Previous studies show that non-social networks generally show a disassortatively-mixed pattern, i.e. metabolic pathways, protein-protein interactions, power-grid, World-Wide-Web [113] or yeast genes and proteins [114]; however, brain connections are assortatively mixed [115] despite its non-social property. Social networks, on the other hand, tend to be assortative, i.e. Facebook [116], Flickr, mySpace [117]; however, there are some exceptions such as disassortative mixing patterns on Twitter [118] and Youtube [117]. In such platforms where social networks are established, it is not surprising that people interact with other people similar to them. This similarity might be based on age, race, language, education or number of connections established. Fisher et al. argued that social networks are assortative only when they are built as a group-based network [119]. Although measuring assortativity will not give an idea about the variation of all entities in a network, it is useful in understanding the average mixing behavior of them; thus, it plays an important role in understanding the dynamics of epidemic spreading, signal connections, information diffusion or consensus formation in a system.

In our previous study [120], we were focusing on the effect of the average mixing behavior of

heterogeneous agents on consensus formation. It is important to obtain a better understanding of consensus formation, since beliefs and opinions in social groups, including the society, constantly evolve as societal dynamics introduce paradigmatic shifts over time. Fashion trends, cultural changes, the rise and fall of political ideologies, marketing practices and technology innovations are good examples for these paradigm shifts leading to consensus formation. Simultaneous to these external influences in the society; internal communication patterns, such as online social networking activities of individuals, can also influence opinion formation, adoption, and dissemination of agents. For instance, it would be unexpected for an individual to adopt an opposing opinion in a network that predominantly supports another opinion. These internal communication patterns strongly depend on the network topology. Consensus formation of multi-agent systems agents have attracted researchers from many different disciplines. This concept is applied in many areas from spacecraft [121] to robotic teams [122]. There are applications of consensus strategies in decision-making, the polarization of people in the examples of political affiliation [123] and rumor spreading [124]. The multiplicity and diversity of uses necessitate a better understanding of the consensus formation process.

Despite the necessity of assigning heterogeneity to thresholds in Linear Threshold Model (LTM), this heterogeneity is poorly-defined among researchers, which leads to extensive use of uniform [64], [65], [66] and binary [4] thresholds in many studies. Arguably, this assumption of homogeneous or binary thresholds is an oversimplification of reality and may produce misleading results. To remedy this oversimplification and thereby provide more holistic and possibly more accurate models, many studies employed more complex threshold functions such as the tent-like function [9], the truncated normal distribution function [10] or the sigmoid function [11]. In the current study, we employ LTM to understand the dynamics of opinion formation and control the threshold heterogeneity with a parameter $N_{th}$ during the simulations.

Although the main analysis here was to understand the effect of the assortativity of the network on

the dynamics of consensus formation; we also investigated the effect of threshold heterogeneity to justify the robustness and scalability of the results. The heterogeneity of the agents is yielded by the diversity of their thresholds.

We first generated a random network using a configuration model, in which out-degree distribution is assigned as random numbers drawn from power-law distribution in the form of $\sqrt{N}x^{\gamma}$. Here, $\gamma = 3$ and $N$ denotes the number of nodes in a network, that equals to 1000. Furthermore, we keep the in-degree as constant ($k_{in} = 17$), motivated by Dunbar number, i.e. individuals have a cognitive limit on the number of their social relationships [125]. This random network tends to be neutral (uncorrelated) or slightly disassortative. To tune the magnitude of the assortativity, we applied the Xulvi Brunet-Sokolov rewiring algorithm [126]. This algorithm chooses two linked node pairs at each time step, i.e. $i, j$ and $m, n$ where $A_{ij}, A_{mn} = 1$ and $A$ denotes the adjacency matrix. Then, it orders these four nodes according to their degree, i.e. Suppose that $k_i < k_m < k_j < k_n$. To increase the assortativity, first two nodes and last two nodes i.e. $A_{ij}, A_{mn} = 0$ and $A_{im}, A_{jn} = 1$; to decrease the assortativity, first node with the last node and second node with the third node are rewired by destroying the previous linkage, i.e. $A_{ij}, A_{mn} = 0$ and $A_{in}, A_{mj} = 1$. This process continues until the desired assortativity is obtained. Note that, this algorithm does not change the overall degree distribution, thus mean a degree in the network; however, a rewired network may exhibit different geometrical and transport properties. The Xulvi Brunet-Sokolov algorithm considers only the out-degree distribution of the directed graph since the in-degree is constant.

In the next step, we initialized the opinions of individuals as a Bernoulli distributed random variable with an initial probability ($p$), i.e. the opinion of the node $i$ ($s_i$) might equal to 1 with a probability $p$ and equal to 0 with probability $(1 - p)$. This probability value of $p$ has a range of 0.2 to 0.8 in the current study.

The heterogeneity of the agents is yielded by the heterogeneity in their thresholds of adopting a new

opinion. For this purpose, we assigned thresholds as a uniformly distributed random variable ($\phi_i \in unif(0.5,1)$) throughout the interval defined by $N_{th}$ which takes value from the set of $2,5,10,100$ and increasing $N_{th}$ yield more heterogeneity among agents. Thresholds of the agents are randomly assigned from the subset defined by:

$$\phi_i \in \{0.5, 0.5+\frac{0.5}{N_{th}-1}, ..., 0.5+\frac{0.5(N_{th}-2)}{N_{th}-1}, 1\} \tag{2.6}$$

After generating the network and bringing its assortativity to the desired degree, initializing the opinions and assigning thresholds, we run the opinion change simulations. The process of updating opinions is as follows as in [82]:

1. Picking a node $i$ randomly.
2. Calculating the weighted average of the opinions of its in-neighbors ($\bar{o}_i$). Here, weights are the multiple edges formed between node $i$ and its neighbors.
3. Updating the opinion of node $i$ ($s_i$) according to the criteria as follows:
   (a) **if** $s_i = 0$ and $\bar{o}_i - s_i > \phi_i$,
   **then** $s_i = 1$ in the next step.
   (b) **if** $s_i = 1$ and $\bar{o}_i - s_i < -\phi_i$,
   **then** $s_i = 0$ in the next step.

This Markovian chain is repeated until individuals fix their opinion. After all the individuals fix their opinions in the network, we averaged their opinions by using the equation below:

$$\bar{s} = \frac{1}{N}\sum_{i}^{N} s_i(\infty) \tag{2.7}$$

where $s_i(\infty)$ is the opinion of node $i$ at steady-state and $N$ is the seed size, i.e. number of nodes in the network. We conducted our simulations to measure $\bar{s}$ as a function of the initial probability ($p$) with a varying assortativity ($r$) and varying threshold heterogeneity $N_{th}$.

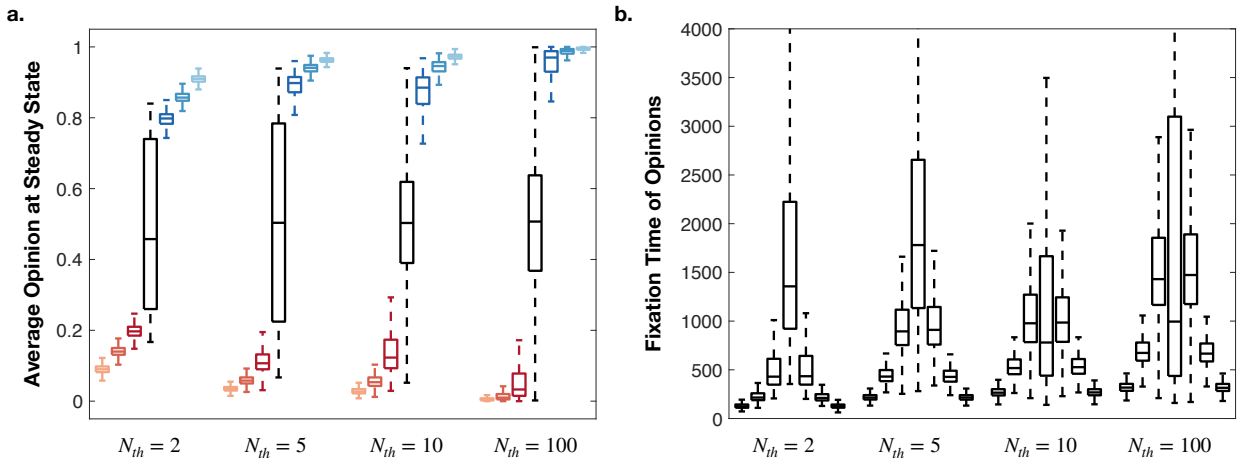


Figure 2.10: a. Average opinion at steady state ($\bar{s}$) b. Fixation time of opinions ($t_F$) when $N = 1000$, $r = 0$ and $N_{th} = \{2, 5, 10, 100\}$. For each $N_{th}$ seven boxplots show the variation in $p = 0.2, 0.3, ..., 0.8$.

Box plots in Figure 2.10 show the distribution of repeated experiments on the average opinion at the steady-state ($\bar{s}$) (left) and the time elapsed until all individuals fix their opinion ($t_F$) (right) when $N = 1000$. We fixed assortativity coefficient of the network as neutral ($r = 0$) since many studies in the literature generates Barabasi's scale-free and/or Erdos-Renyi networks, which are tend to show uncorrelated mixing pattern. Each figure includes 4 groups of box plots, in which groups represent various $N_{th}$, and $p$ varies from 0.2 to 0.8 in each group. Since average opinion shows the sample mean of the opinions at steady-state, the values closer to either 0 or 1 show the dominance of one of the opinions, i.e. the system is more likely to reach a consensus. Figure 3a shows that $p$ determines the dominance of the opinions; when $p \leq 0.4$, $\bar{s}$ take values close to 0, while $p \geq 0.6$ it approaches to 1. Furthermore, there is a clear asymmetry before and after $p = 0.5$ in all cases. As $p$ closes to 0.5, system has mix of both opinions rather than reaching a consensus. Figure 3b, on the other

hand, shows the relatively long duration of opinion change process when opinions are initialized halfway ($p = 0.5$). Although threshold heterogeneity of nodes in the system has a slight effect in the resulting average opinion when thresholds are out-degree dependent, we can conclude that the probability that the system reaches a consensus slightly increases as the threshold heterogeneity increases; however, the time elapsed until all nodes fix their opinions increases significantly with increasing $N_{th}$.

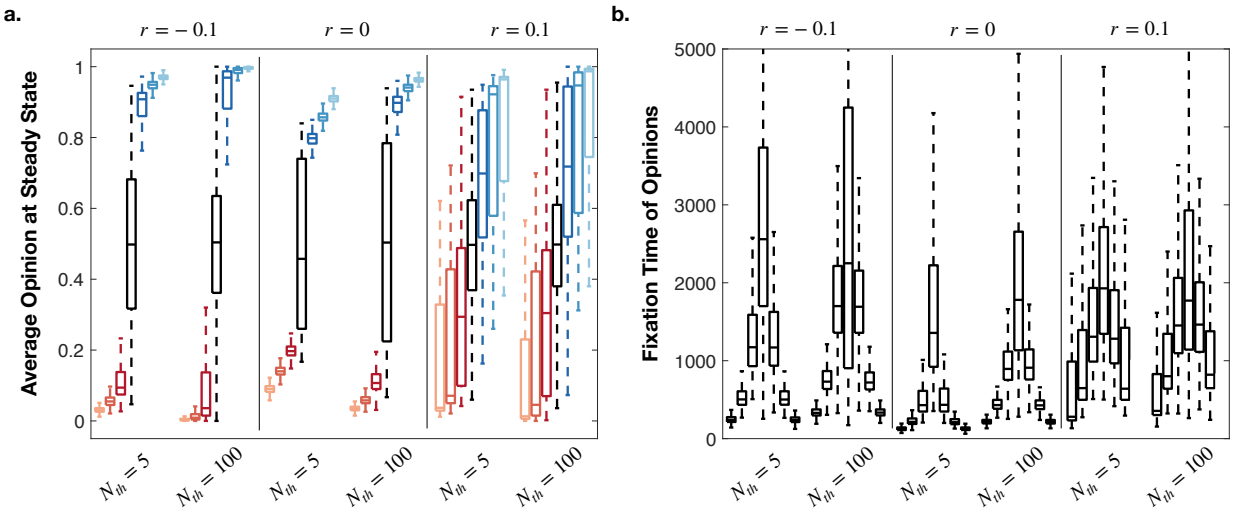


Figure 2.11: a. Average opinion at steady state ($\bar{s}$) b. Fixation time of opinions ($t_F$) when $N = 1000$, $r = -0.1$ in dissortative, $r = 0$ in neutral and $r = 0.1$ in assortative mixing. For each $N_{th=5}$ or $N_{th=100}$, and seven boxplots show the variation in $p = 0.2, 0.3, ..., 0.8$.

Figure 2.11a, on the other hand, shows the effect of rewiring the network before opinion update simulations, when network is assortative ($r = 0.1$), neutral ($r = 0$) and disassortative ($r = -0.1$). All simulations are carried out at $N_{th} = 5$ and $N_{th} = 10$ for each mixing pattern to understand the moderator effect of the threshold heterogeneity. Results show that the increase in the assortativity coefficient of a network has a prominent effect on the average opinion at the steady state at both threshold heterogeneity. The system is more likely to reach a consensus when network is disassortatively mixed and this effect is more prominent when thresholds are more heteroge-

neous. Surprisingly, $t_F$ reaches its minimum value when network is neutral. Figure 2.11b shows that bringing the network to the steady-state takes more time when degree distribution of its nodes either positively or negatively correlated. Again, this unexpected effect is more prominent when threshold heterogeneity is high.

To sum up, it is important to understand the dynamics of consensus formation in multi-agent system studies. Opinion formation and change depends on either the external effects, i.e. change in belief, ideologies and/or technology, or internal effects, i.e. change in interactions due to evolving network structure, thresholds to adopt a new opinion. The mixing pattern of the networks has been studied for many years, however, its effect on the dynamics of consensus formation is not analyzed in detail. Here, we investigated the sensitivity of dynamics of consensus formation to the assortativity of the network in the existence of heterogeneous agents. The contribution of the paper is as follows: We examined the effect of assortative mixing in networks on the dynamics of consensus formation with multi agent-based simulations. During the simulations we tested the effect of assortativity coefficient of network, initial probabilities of the different opinions and threshold heterogeneity of the agents in the network structure. We concluded that the system is more likely to reach a consensus when the network is disassortatively mixed or neutral; however, the likelihood of the consensus significantly decreases when the network is assortatively mixed. Surprisingly, the time elapsed until all nodes fix their opinions is slightly lower when the network is neutral compared to either assortative or disassortative networks. Reaching the consensus is more likely but more time-consuming when thresholds of agents in the system are more heterogeneous. This slight effect of heterogeneity is observed every cases regardless of the mixing pattern of the nodes; however, its positive effect reaching a consensus is more pronounced when the system is disassortatively mixed.

# CHAPTER 3: QUANTUM PROBABILISTIC APPROACHES

Since quantum theory is very comprehensive in its representations, computations, and inferences; their explanation and applications require a very detailed description. In this chapter, we just aim to briefly describe the fundamentals of quantum theory and its application in behavioral systems. For the sake of simplicity, we will focus on finite-state systems, although quantum approaches can facilitate modeling continuous state systems due to their more advanced representation compared to classical approaches. For more detailed explanations, the approaches that are used in the formulation of probability theory, and their applications in different disciplines can be found in [19, 18]. To compare the differences in classical and quantum approaches, we will focus on two main postulates which are sample space and events by using a simple example to illustrate them in the decision-making concept.

## Sample Spaces

Regardless of using the classical or quantum approach, probabilistic approaches aim to assign marginal probabilities to each event in the sample space. More fundamentally, the two approaches differ in their representation. The classical approach uses set-theoretic representation and its sample space is defined as a set of possible events, e.g. $\{m_0, m_1\}$. On the other hand, the quantum approach uses vector space representation and its sample space is a plane space spanned by the orthogonal basis vectors, e.g. $|m_0\rangle$ and $|m_1\rangle$. This *braket* notation is also called Dirac notation and is commonly used in the representation of quantum states as in Figure 3.1.

The differences in classical and quantum sample space representations mainly stem from the assumptions that are used in these approaches. The classic probabilistic theory assumes a sample

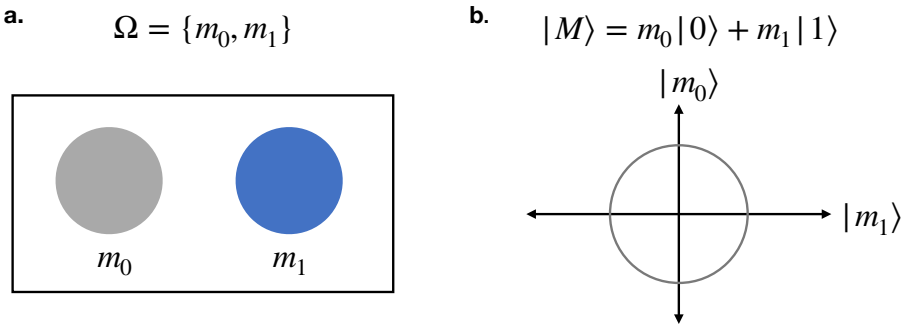


Figure 3.1: A graphical representation of sample spaces in **a.** classical approach, **b.** quantum approach.

space in which the outcome of the events are mutually exclusive, i.e. $\Omega = \{m_0, m_1\}$. In quantum probabilistic theory, on the other hand, events are modeled as subspaces of a Hilbert space in which each orthogonal basis vector corresponds to an elementary outcome, i.e. $|M\rangle = m_0|0\rangle + m_1|1\rangle$, where

$$M = \begin{bmatrix} m_0 \\ m_1 \end{bmatrix}$$

An inner product of vector $M$ is obtained with the multiplication of $|M\rangle$ with its complex conjugate ($|M\rangle^* = \langle M|$) as follows:

$$\langle M|M\rangle = \begin{pmatrix} m_0 \\ m_1 \end{pmatrix} \begin{pmatrix} m_0 & m_1 \end{pmatrix} = \begin{pmatrix} |m_0|^2 & |m_0||m_1|^* \\ |m_1||m_0|^* & |m_1|^2 \end{pmatrix} = \begin{pmatrix} \psi_{m_0}\psi_{m_0}{}^* & \psi_{m_0}\psi_{m_1}{}^* \\ \psi_{m_1}\psi_{m_0}{}^* & \psi_{m_1}\psi_{m_1}{}^* \end{pmatrix} \tag{3.1}$$

Events

As we are familiar with, representing the set of outcomes as mutually exclusive events in classical theory enables us to easily define more complex events that require intersection, union, and/or distribution of individual events. In general, the conjunction (intersection) of two independent events is represented by $(m_0 \cap m_1)$ and the disjunction (union) is by $(m_0 \cup m_1)$. Furthermore, a distributive axiom is also applicable in classical theory, i.e. $m_0 \cap (m_1 \cup m_2) = (m_0 \cap m_1) \cup (m_0 \cap m_2)$, since it obeys a set theory.

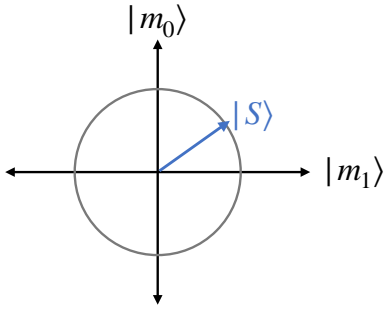


Figure 3.2: A graphical representation of sample spaces and their superposition in a Hilbert State.

In the quantum approach, on the other hand, mutually exclusive events are represented by orthonormal basis vectors contained in the Hilbert space. This geometric approach enables us to define a superposition state which comprises the occurrence of different events at the same time. For example, Figure 3.2 shows a superposition state of happening both events of $m_0$ and $m_1$ and computed as follows:

$$|S\rangle = \frac{e^{\theta_{m_0}}}{\sqrt{2}}|m_0\rangle + \frac{e^{\theta_{m_1}}}{\sqrt{2}}|m_1\rangle = \frac{e^{\theta_{m_0}}}{\sqrt{2}}\psi_{m_0} + \frac{e^{\theta_{m_1}}}{\sqrt{2}}\psi_{m_1} \tag{3.2}$$

Here, the exponential term $(e^{i\theta_{m_0}})$ is called global phase factor of the quantum probability ampli-

tude. The probability ($Pr(m_0)$) is related with a quantum probability amplitude ($e^{i\theta_{m_0}}|m_0\rangle$) which corresponds to the amplitude of a wave function, and this relation to the classical probability is obtained by multiplying this amplitude with its complex conjugate, i.e. $|e^{i\theta_{m_0}}|^2 = e^{i\theta_{m_0}}|m_0\rangle e^{-i\theta_{m_0}}|m_0\rangle^*$. This connection is obtained via Born's rule as follows:

$$Pr(m_0) = |e^{i\theta_{m_0}}\psi_{m_0}|^2 \tag{3.3}$$

Interference Effect in Quantum Probabilistic Approach

Although the result of an individual event probability in the classical probability theory converges to that in the quantum approach, the computation of the union of mutually exclusive events differs in these two methods. The quantum-like approach yields an extra term, *"interference effect"*, which does not exist in classical probability theory. To illustrate, suppose that we aim to obtain the union of three mutually exclusive events by using classical probability formula, which is given by:

$$Pr(A \cup B \cup C) = Pr(A) + Pr(B) + Pr(C) \tag{3.4}$$

The quantum counterpart of the classical probability of the union of three mutually exclusive events is obtained by using Born's rule in Eq. 3.11:

$$
\begin{aligned}
Pr(A \cup B \cup C) &= |e^{i\theta_A}\psi_A + e^{i\theta_B}\psi_B + e^{i\theta_C}\psi_C|^2 \\
&= e^{i\theta_A}\psi_A.e^{-i\theta_A}\psi_A + e^{i\theta_A}\psi_A.e^{-i\theta_B}\psi_B + e^{i\theta_A}\psi_A.e^{-i\theta_C}\psi_C \\
&+ e^{i\theta_B}\psi_B.e^{-i\theta_A}\psi_A + e^{i\theta_B}\psi_B.e^{-i\theta_B}\psi_B + e^{i\theta_B}\psi_B.e^{-i\theta_C}\psi_C \\
&+ e^{i\theta_C}\psi_C.e^{-i\theta_A}\psi_A + e^{i\theta_C}\psi_C.e^{-i\theta_B}\psi_B + e^{i\theta_C}\psi_C.e^{-i\theta_C}\psi_C
\end{aligned}
\tag{3.5}
$$

Knowing that,

$$
cos(\theta_1 - \theta_2) = \frac{e^{\theta_1-\theta_2} + e^{-\theta_1+\theta_2}}{2} \tag{3.6}
$$

Eq. 3.5 reduces to:

$$
\begin{aligned}
Pr(A \cup B \cup C) = |\psi_A|^2 + |\psi_B|^2 + |\psi_C|^2 + 2\big(&|\psi_A||\psi_B|cos(\theta_A - \theta_B) \\
&+ |\psi_A||\psi_C|cos(\theta_A - \theta_C) + |\psi_B||\psi_C|cos(\theta_B - \theta_C)\big)
\end{aligned}
\tag{3.7}
$$

The additional terms in Eq. 3.7 compared to Eq. 3.4 are called as *"interference terms"* which does not exist in classical probability theory [30, 29, 21, 31].

## Related Previous Works as a Motivational Source

### *An Example of Quantum-Like Approach in Decision-Making Analysis*

Artificial intelligence (AI) algorithms are proving increasingly useful in numerous situations since they can perform more complex computations by handling bigger data sets than humans may com-

prehend. Nowadays, AI-centered technologies are utilized for a wide range of activities including optimization of healthcare systems, medical diagnosis, robot controls, automated trading systems [127]. Furthermore, automated algorithms are not only used for prediction purposes but also considered as a decision-maker because it is believed that these algorithms may simulate decision-making processes more objectively. However, data used to train AI algorithms for learning may include biased measurements or historically biased human systematic errors. Missing data values or selection biases may also result in biased learning outcomes. Moreover, the prediction method might be biased against the minority groups by itself since it aims to optimize the aggregate error which is mainly more favored to majority groups.

Nowadays, AI algorithms rank job candidates in receiving jobs, rate students in college admissions, predict the likelihood of criminality of individuals and/or estimates the risk in giving loans. With the increasing demand for using artificial intelligence algorithms in making decisions that affect people's lives, the need for a fairness-oriented design in automated decision-making systems emerges as a major concern. These concerns about algorithmic fairness have also caused a lot of controversy in recent years. One of the most remarkable examples is that recent studies showed that the United States criminal justice system is falsely biased against the likelihood of criminality of African-American people compared to that of white people [128]. Surprisingly, some big tech companies are also showed to have gender discrimination in their automated decision-making systems. For example, Amazon's AI hiring system is more likely to hire males than females in hiring job candidates for software development and technical positions [129]. Also, Google's ad-targeting algorithms make recommendations of executive jobs positions more to male compared to female users [130]. [127] also discusses some real-world examples of algorithmic biases in AI chatbots, employment matching, flight routing, and automated legal aid for immigration algorithms, and search and advertising placement algorithms.

Since these automated systems may affect people's lives in almost everything, there is great im-

portance in assessing and improving the ethics of the decisions made by these automated systems. Therefore, researchers have introduced various tools to measure fairness in an algorithm or system. For example, Aequitas offers a toolkit that measures the fairness of models used for making estimations for different population subgroups. Additionally, IBM launched AI Fairness 360 (AIF360) toolkit to help industrial applications of algorithmic fairness research studies. In all these examples, fairness metrics are calculated either for different groups or individuals. The most common measures of algorithmic fairness classification tasks are disparate impact, demographic parity, and equalized odds. Disparate impact [131] and demographic parity [132] aims to quantify the legal notion of disparate impact by considering true positive rates for different groups. Equalized odds [133], on the other hand, is designed to measure differences between predictions for different groups by considering both false-positive rates and true positive rates of the two groups.

Although there is a great interest in algorithmic fairness among machine learning and deep learning researchers, and their studies focused on the optimization of the trade-off between fairness and accuracy in recent years [134, 135, 136, 137, 138, 139, 140]; whereas, understanding the sources of unfairness in decision-making is an essential challenge. To tackle this problem, researchers proposed fair causal learning approaches, which enable us to model cause and effects knowledge structure, to discover the sources of the bias, and to prevent unfair decision-making by amplifying transparency and explainability of AI algorithms. Loftus et al. discuss the importance of causal graphs in designing fair algorithms in detail [140]. They argue that mitigation of bias is only possible when the causal sources are examined thoroughly. Thus, they review extant fairness notions and show a methodology to combine these with causal techniques such as counterfactual fairness. Additionally, these causal interventions are carried out to address contrastive fairness in algorithmic decision-making [141]. [142] developed a novel methodology to get a fair classifier when the causal model is not complete by linking causal inference to multiple dependencies. Despite using traditional fairness measures in causal algorithms, [143] brought new definitions, i.e. fair on aver-

age causal effect (FACE), and fair on average causal effect on the treated (FACT) for more robust estimation in fair causal learning.

These studies consider fair causal learning problems based on the assumption that the underlying probabilistic model of the world is known; whereas, it is well-known that humans do not obey the classical probability rules in making decisions due to emotional changes, subconscious feelings, and subjective biases, and this yields uncertainty in underlying probabilistic models. In this study, we draw from quantum theory and convert classical probability rules to more generalized concept of quantum probability rules. The reason behind this attempt can be explained as follows: In quantum theory, the uncertainty principle states that one cannot assign the exact position and momentum of a physical system at the same time. Therefore, these quantities are determined with some characteristic uncertainties. There are a lot of examples of quantum decision making modeling in cognitive science due to the same reasons [144, 145]. In our previous study [146], we aim to employ quantum-like approach to classical Bayesian framework to generate more fair causal learning framework because we argue that transforming classical probability values as complex quantum amplitudes allow us to model the uncertainties in the underlying probabilistic model of the world is more efficiently.

We study a Bayesian setting in which decision-maker (DM) tries to maximize its expected utility, and consider the fairness of the decision simultaneously. A Bayesian framework for the decision-making problem can be seen in Figure 3.3. Here, $x$, $y$ and $z$ represents observations, the outcome, and sensitive variable(s), respectively. The joint probability distributions of $x, y$ and $z$ are depend on an unknown parameter $\theta$. The conditional probability distribution of action $a$ given $x$ is also conditioned by the selected policy $\pi$. With the given belief $\beta$, the DM tries to maximize its objective function that comprises expected utility $u$ and fairness $f$. In this Bayesian framework, we consider the same strategy as in [147]: At each discrete time step $t$, the DM's policy acknowledge the current action $a_t \in \mathscr{A}$, by observing some data $x_t \in \mathscr{X}$ depending on its current belief

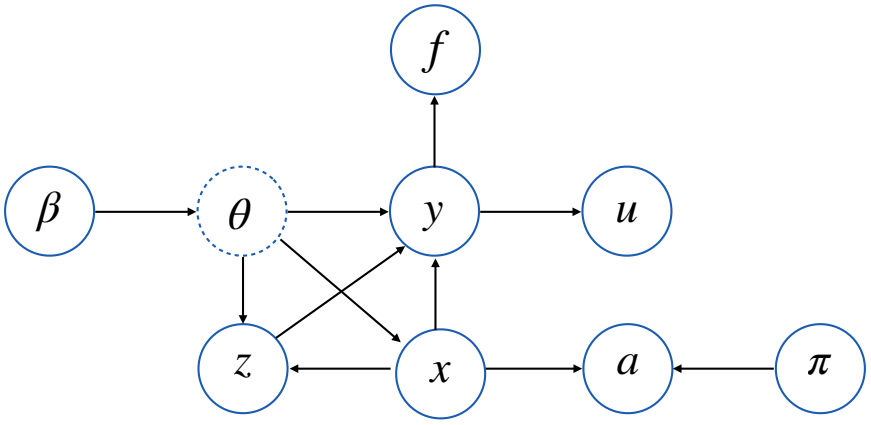


Figure 3.3: A decision problem with observations $x$, the outcome $y$, and sensitive variable(s) $z$. The joint probability distributions of $x, y$ and $z$ are depend on an unknown parameter $\theta$. The conditional probability distribution of action $a$ given $x$ is also conditioned by the selected policy $\pi$. With the given belief $\beta$, the DM tries to maximize its objective function that comprises expected utility $u$ and fairness $f$.

$\beta_t$ and makes a decision $\pi(a_t|\beta_t, x_t)$. Therefore, the stochasticity of the model parameters in $\beta$ will influence the outcomes in each time step and yield a stochastic outcome in the case of higher uncertainty. Here, we assume that $\beta$ has a probability distribution $\mathscr{P} \triangleq \{P_\theta|\theta \in \Theta\}$ that contains the actual law of $P^*_\theta = P$ for some $\theta^*$. The trade-off between utility and fairness is satisfied with the following criteria:

$$\max_{\pi}(1-\lambda)\mathbb{E}^{\pi}_{P}u - \lambda\mathbb{E}^{\pi}_{P}f \tag{3.8}$$

Here, $P$ denotes the underlying probability distribution and $\lambda$ is a multiplier used to adjust trade-off between fairness and utility, i.e. $\lambda = 0$ has no emphasis on fairness, while $\lambda = 1$ considers maximizing fairness only. The fairness is measured with disparate impact as in [128], and the decision rule is assumed to be fair if the decision rule is independent for all sensitive variables, i.e.,

$y \perp\!\!\!\perp z$.

For the same decision problem, [147] introduces two balance models that considers model uncertainty by taking all possible decisions into account to maximize DM's objective. In Bayesian balance model, the deviation from balance of policy $\pi$ is measured with respect to each possible parameter $\theta$, and the outcomes are weighed to prevent extreme unfairness and lowest utility.

**Definition 1.** *A decision rule $\lambda(.)$ is $(\alpha, p)$-Bayes balanced with respect to $\beta$ if $\forall a, y, z$:*

$$f(\pi) \triangleq \int_{\Theta} \leq \sum_{a,y,z} \left| \sum_{x} \pi(a|x)[\mathbb{P}_{\theta}(x,z|y) - \mathbb{P}_{\theta}(x|y)\mathbb{P}_{\theta}(z|y)] \right|^{p} d\beta(\theta) \leq \alpha^{p} \tag{3.9}$$

In marginal balance approach, on the other hand, a single point estimate for the model is considered instead of using a fully Bayesian approach, i.e., $\mathbb{P}_{\beta} \triangleq \int_{\Theta} \mathscr{P}_{\theta} d\beta(\theta)$.

**Definition 2.** *A decision rule $\lambda(.)$ is $(\alpha, p)$-marginal balanced with respect to $\beta$ if $\forall a, y, z$:*

$$\sum_{a,y,z} \left| \sum_{x} \pi(a|x)[\mathbb{P}_{\beta}(x,z|y) - \mathbb{P}_{\beta}(x|y)\mathbb{P}_{\beta}(z|y)] \right|^{p} \leq \alpha \tag{3.10}$$

Since quantum theory is very comprehensive in its representations, computations, and inferences; their explanation and applications require a very detailed description. For the sake of simplicity, we will focus on finite-state systems, although quantum approaches can facilitate modeling continuous state systems due to their more advanced representation compared to classical approaches. The differences in classical and quantum sample space representations mainly stem from the assumptions that are used in these approaches. The classic probabilistic theory assumes a sample space in which the outcome of the events are mutually exclusive. In quantum probabilistic theory, on the other hand, events are modeled as subspaces of a Hilbert space in which each orthogonal basis vector corresponds to an elementary outcome. To employ quantum-like probabilistic approach,

we represent probabilistic entities as complex probability amplitudes by employing Inverse Born Problem (IBP). This transition using Born's rule can be seen in this expression:

$$Pr(A) \propto |e^{i\theta_A}\psi_A|^2 \tag{3.11}$$

As we mentioned before, we assumed that $\beta$ has a probability distribution $\mathscr{P} \triangleq \{P_\theta|\theta \in \Theta\}$ that contains the actual law of $P^*_\theta = P$ for some $\theta^*$. Therefore, for the application of balance gradient descent, we need to focus on the following expression as in Eq. 3.12:

$$f(\pi) \triangleq \int_\Theta \leq \sum_{a,y,z} \left| \sum_x \pi(a|x)\Delta_\theta(x,y,z) \right|^p d\beta(\theta) \leq \alpha^p \tag{3.12}$$

where $\Delta_\theta(x,y,z) = [\mathbb{P}_\theta(x,z|y) - \mathbb{P}_\theta(x|y)\mathbb{P}_\theta(z|y)]$ in Bayes balanced approach. Identifying delta expression with its quantum counterpart is possible with integrating Eq. 3.11 in Eq.3.12:

$$\begin{aligned}
&\left| e^{i\theta_{x,z|y}}\Psi_\theta(x,z|y) - e^{i\theta_{x|y}}\Psi_\theta(x|y)e^{i\theta_{z|y}}\Psi_\theta(z|y) \right|^2 \\
&= \left| e^{i\theta_{x,z|y}}\Psi_\theta(x,z|y) - e^{i\theta_{x|y}}\Psi_\theta(x|y)e^{i\theta_{z|y}}\Psi_\theta(z|y) \right| \\
&\cdot \left| e^{i\theta_{x,z|y}}\Psi_\theta(x,z|y) - e^{i\theta_{x|y}}\Psi_\theta(x|y)e^{i\theta_{z|y}}\Psi_\theta(z|y) \right|^* \\
&= e^{i\theta_{x,z|y}}\Psi_\theta(x,z|y).e^{-i\theta_{x,z|y}}\Psi_\theta(x,z|y) + e^{i\theta_{x,z|y}}\Psi_\theta(x,z|y).e^{-i\theta_{x|y}}\Psi_\theta(x|y)e^{i\theta_{z|y}}\Psi_\theta(z|y) \\
&+ e^{-i\theta_{x,z|y}}\Psi_\theta(x,z|y).e^{i\theta_{x|y}}\Psi_\theta(x|y)e^{i\theta_{z|y}}\Psi_\theta(z|y) \\
&+ e^{i\theta_{x|y}}\Psi_\theta(x|y)e^{i\theta_{z|y}}\Psi_\theta(z|y).e^{-i\theta_{x|y}}\Psi_\theta(x|y)e^{i\theta_{z|y}}\Psi_\theta(z|y) \\
&= |\Psi_\theta(x,z|y)|^2 + |\Psi_\theta(x|y)\Psi_\theta(z|y)|^2 + |\Psi_\theta(x,z|y)|.|\Psi_\theta(x|y)\Psi_\theta(z|y)|e^{i(\theta_{x,z|y}-\theta_{x|y}\theta_{z|y})} \\
&+ |\Psi_\theta(x|y)\Psi_\theta(z|y)|^2 + |\Psi_\theta(x,z|y)|.|\Psi_\theta(x|y)\Psi_\theta(z|y)|e^{i(\theta_{x|y}\theta_{z|y}-\theta_{x,z|y})}
\end{aligned} \tag{3.13}$$

Knowing that

$$cos(\theta_1 - \theta_2) = \frac{e^{i(\theta_1-\theta_2)}e^{i(\theta_2-\theta_1)}}{2} \tag{3.14}$$

Then Eq. 3.13 can be rewritten as:

$$\begin{aligned} &|\Psi_\theta(x,z|y)|^2 + |\Psi_\theta(x|y)\Psi_\theta(z|y)|^2 \\ &\pm 2|\Psi_\theta(x,z|y)|.|\Psi_\theta(x|y)\Psi_\theta(z|y)|cos(\theta_{x,z|y} - \theta_{x|y}\theta_{z|y}) \end{aligned} \tag{3.15}$$

Therefore, we can redefine delta expression in quantum counterpart of Bayes balanced approach as in Eq. 3.15.

**Definition 3.** *A decision rule $\lambda(.)$ is $(\alpha, p)$-Quantum Bayes balanced with respect to $\beta$ if $\forall a, y, z$:*

$$f(\pi) \triangleq \int_\Theta \leq \sum_{a,y,z} \left| \sum_x \pi(a|x) \left[ |\Psi_\theta(x,z|y) - \Psi_\theta(x|y)\Psi_\theta(z|y)|^2 \right] \right|^p d\beta(\theta) \leq \alpha^p \tag{3.16}$$

which satisfies

$$f(\pi) \triangleq \int_\Theta \leq \sum_{a,y,z} \left| \sum_x \pi(a|x) \left[ \mathbb{P}_\theta(x,z|y) + \mathbb{P}_\theta(x|y)\mathbb{P}_\theta(z|y) - 2cos\theta\sqrt{\mathbb{M}} \right] \right|^p d\beta(\theta) \leq \alpha^p \tag{3.17}$$

where

$$\mathbb{M} = \mathbb{P}_\theta(x,z|y)\mathbb{P}_\theta(x|y)\mathbb{P}_\theta(z|y) \tag{3.18}$$

The aim of this study was to compare and contrast performances of our Quantum Bayes balanced framework with the extant approaches of marginal and Bayes balanced approaches given in [147]

when the underlying probabilistic model of the world is not known. For this purpose, we have used ProPublica COMPAS (Correctional Offender Management Profiling for Alternative Sanctions) data set [148, 149, 150]. ProPublica risk assessment data set includes a number of previous felonies, charge degree, age, race, and gender of 7214 individuals as features and a binary outcome variable that shows whether an inmate recidivated within two years after release from prison. We assigned race and gender as sensitive attributes, while the remaining attributes are used as observations for policy. For the non-binary features, we applied discretization by assigning the average value as a threshold, and the values higher than the threshold are assigned as 1, while the rest is assigned as 0. Randomly selected 6000 observations are used for training, whereas, remaining 1214 are tested for validation purposes.

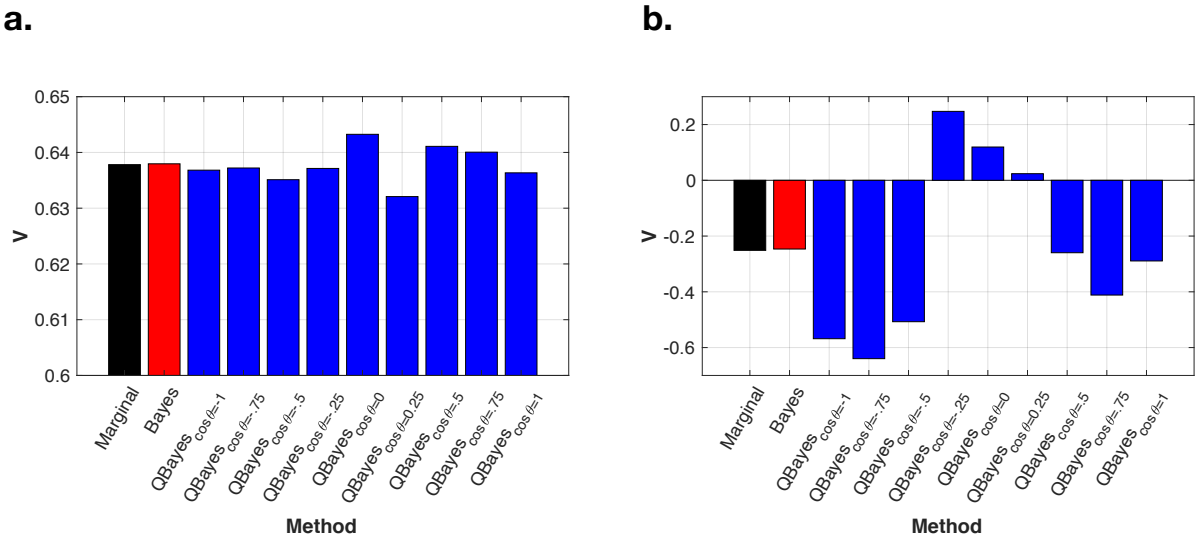


Figure 3.4: The results of the optimization criteria given in Eq. 3.8 by using marginal-balanced (black bar), Bayes-balanced (red bar) and quantum Bayes balanced (blue bars) with varying interference values when **a.** $\lambda = 0$, **a.** $\lambda = 0.25$.

Figure 3.4 shows the results of the optimization criteria given in Eq. 3.8 by using marginal-balanced (black bar), Bayes-balanced (red bar) and quantum Bayes balanced (blue bars) with

varying interference values ($cos\theta$). Since the aim is to maximize the utility and minimize the deviation from the fairness criterion, the higher values are more favorable. In Figure 3.4.a, $\lambda = 0$, that means fairness is not taken into account and the gradient descent algorithm tries to maximize utility only. We realized that the Bayesian approach performs slightly better than the classical marginal approach. The superiority of the performance of the quantum Bayesian approach varies with respect to the specified interference effect. When $cos\theta = 0$, a higher score is obtained, i.e. A higher utility is obtained in the decision-making process. When we assign more importance to fairness in the objective function as $\lambda = 0.25$ in Figure 3.4.b, we could not observe a significant difference in the results obtained via marginal and Bayesian approaches. However, in some definite interference values ($-0.25 \lessapprox cos\theta \lessapprox 0.25$), the quantum Bayes balanced approach gives significantly better results with satisfying higher utility and less deviation from fairness.

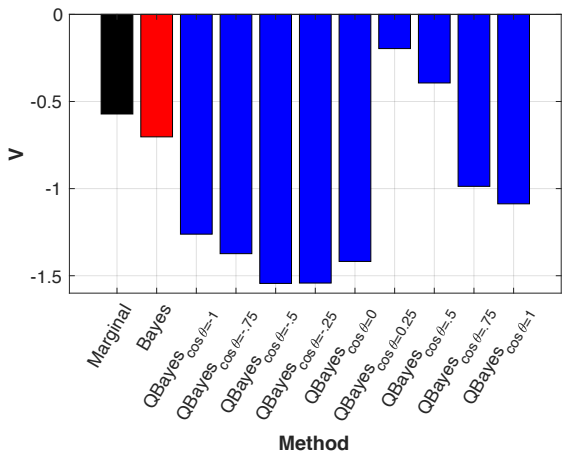


Figure 3.5: The results of the optimization criteria given in Eq. 3.8 by using marginal-balanced (black bar), Bayes-balanced (red bar) and quantum Bayes balanced (blue bars) with varying interference values when $\lambda = 0.5$.

Figure 3.5 shows the results of the optimization criteria given in Eq. 3.8 by using marginal-balanced (black bar), Bayes-balanced (red bar) and quantum Bayes balanced (blue bars) with vary-

ing interference values ($cos\theta$) when equal importance is given to utility and fairness ($\lambda = 0.5$). Here, we observed that the Bayesian balanced approach decreases the objective function compared to the marginal balanced approach, and quantum Bayesian balanced with interference term $-1 \lessapprox cos\theta \lessapprox 0$ yields even smaller values. However, results demonstrated that the quantum Bayesian approach performs better when the range of interference term between $\sim$0.25 to $\sim$0.5.

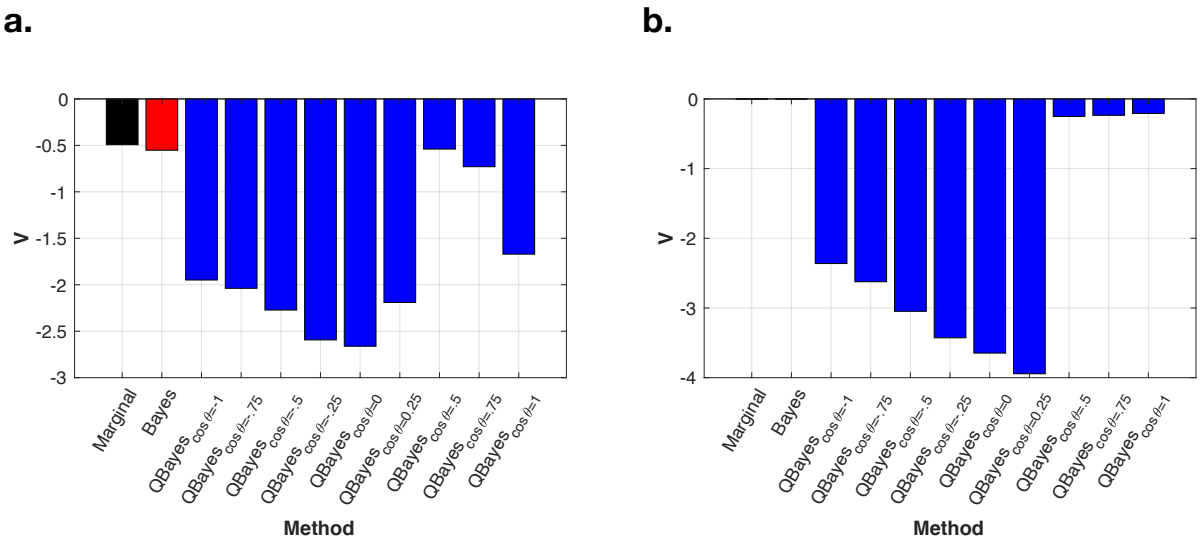


Figure 3.6: The results of the optimization criteria given in Eq. 3.8 by using marginal-balanced (black bar), Bayes-balanced (red bar) and quantum Bayes balanced (blue bars) with varying interference values when **a.** $\lambda = 0.75$, **a.** $\lambda = 1$.

Figure 3.6 shows the results of the optimization criteria given in Eq. 3.8 by using marginal-balanced (black bar), Bayes-balanced (red bar) and quantum Bayes balanced (blue bars) with varying interference values ($cos\theta$) when the optimization function weight more on fairness than utility. Although the quantum Bayes balanced approach may show relatively similar results when $cos\theta = 0.5$ compared to the Bayesian approach, the marginal approach performs better than both. When the optimization of the decision making is only keep the deviation on fairness as low as possible, the quantum Bayesian approach falls short regardless of the interference value. It should

be noted that, better results in the quantum Bayesian approach are observed when interference is $0.5 \lessapprox cos\theta \leq 1$.

To sum up, here, we introduced the quantum Bayesian approach as a candidate for fair decision-making in causal learning, motivated by the human decision-making literature in cognitive science. We demonstrated that the quantum Bayesian perspective creates well-performing fair decision rules under high uncertainty on the well-known COMPAS data set when the optimization function aims to maximize the utility and minimize the deviation from the fairness at the same time. Whereas, when the aim of the DM to make a fair decision only, marginal and Bayes balanced approaches perform better than their quantum counterpart.Although our approach yields very promising results, it should be noted that computational complexity of Bayesian methods are raised significantly with the increasing number of data points and features. This complexity increase is much more higher when quantum Bayesian approaches are employed, since these methods bring extra interference terms. The most efficient way to tackle this problem is to discover heuristics that predict the interference terms. Then, our method will be as fast as classical Bayesian approaches in the existence of larger data sets. Future studies may aim to find a heuristic to predict optimum interference value in the quantum approach, and adapting the quantum framework to different AI methodologies.

# CHAPTER 4: FUNDAMENTALS OF ENTROPY MEASURES

The second law of thermodynamics states that the total entropy of an isolated system (the thermal energy per unit temperature that is unavailable for doing useful work) can never decrease. This concept of entropy that was introduced by Rudolf Clausius in 1865 [151] as a term in the field of thermodynamics, later adapted into statistical physics and information theory to characterize the uncertain, ambiguous and disordered behavior of stochastic processes [152]. After Clasius' definition of entropy as a thermodynamic concept, Shannon [153, 153] argued that this concept can be extended into different disciplines due to its probabilistic nature in defining the randomness of stochastic processes, and proposed Shannon entropy [154] as a uncertainty measure. Later, the entropy measure proposed by Renyi et al. [155], called Renyi entropy, has been applied in diverse areas including quantum information, information theory, and fractal theory. Another non-extensive measure of Tsallis entropy which is an extension of Boltzman entropy [156] has also gained a lot of attention. Recently, a new entropy named Deng entropy [157] has been proposed to solve uncertainty of the stochastic processes based on the given evidence. [40] describes the similarities and differences of these entropy measures to better explain their use areas.

For a random variable $X$ over a probability space $\Omega$, Shannon entropy is defined for continuous and discrete variables as follows, respectively:

$$\begin{aligned} S(X) &= -\int_{\Omega} p(x) log_2(p(x)) dx \\ S(X) &= -\sum_{x \in \Omega} p(x) log_2(p(x)) \end{aligned} \tag{4.1}$$

where $p(x)$ denotes the probability distribution. Although this measure performs well in the existence of finite storage capacity of transmitting channel in communication, it falls short in infinite storage capacity. To address this, Renyi [158] proposed a new measure, called Renyi entropy,

which is defined for discrete variables as follows:

$$S_\alpha(X) = \frac{1}{1-\alpha} ln(\sum_{k=1}^{n} p_k^\alpha) \tag{4.2}$$

where $\alpha \neq 1$ and $\alpha \geq 0$. When the order of $\alpha$ equals to 1, Renyi entropy degenerates into Shannon entropy.

On the contrary of Shannon and Renyi entropy measures which yields exponential equilibrium distribution, Tsallis extended these definitions and proposed a new entropy measure which can be used with any non-negative real number, which yields a power-law equilibrium distribution [159]. The formula of Tsallis entropy for a non-negative real number $q$ is as follows:

$$S_q(X) = \frac{1 - \sum_{i=1}^{n} p_i^\alpha}{q-1} \tag{4.3}$$

where $q \neq 1$ and $q \geq 0$. When the order of $q$ equals to 1, Tsallis entropy degenerates into Shannon entropy.

Belief entropy, named as Deng entropy, on the other hand, can be described as a combination of a measure of total non-specificity in the basic probability assignment indicating the degree of belief in $A_i \in P(X)$ and a measure of discord of the mass function among various focal elements. Its formula is:

$$H_d = -\sum_i m(A_i) ln \frac{m(A_i)}{2^{|A_i-|} - 1} \tag{4.4}$$

Belief Entropy as an Uncertainty Measure of Stochastic Processes

[160] utilized the belief entropy to calculate the interference effects caused by phase differences in quantum-like Bayesian networks for the first time. To prove the effectiveness of the proposed

model, Prisoner's dilemma game is one of the simplest yet efficient example of the cooperation between two individuals. In this game, each individual chooses to either cooperate or betray to the other without knowing their actions, and each joint action will yield different payoffs. In the example given in [160] the payoff matrix is defined as follows:

Table 4.1: Payoff Matrix.

| A/B | 0 | 1 |
|---|---|---|
| 0 | 4/4 | 2/5 |
| 1 | 5/2 | 3/3 |

Numerical results for the experiments of Prisoner's Dilemma game with the payoff table given in Table 4.1 are given in [161] by averaging the correspondingly probabilities as an average of four different sources. Accordingly, the probabilities of the second player chooses to betray when she knows the first player chose to betray or cooperate are equal to 0.87 and 0.74, respectively. Although the classical probability theory computes the result as 0.8050, experimental results show that the probability of the second player chooses to betray when she does not know the action of the first player is found to be equal to 0.64, violating the law of total probability.

In the light of aforementioned probability values, interference effect in quantum-like Bayesian network aims to find a heuristic for the calibration of $cos(\theta_1 - \theta_2)$ in Equation 3.6. For this purpose, [160] firstly defines the belief degree as an estimate of the phase difference as follows:

$$D_b = cos(\theta_i - \theta_j) \tag{4.5}$$

where $\theta_i$ and $\theta_j$ are angles in the interference term in Equation 3.7.

Since the vectors of two possible answers of player's actions in Prisoner's dilemma game can be

described as:

$$\begin{bmatrix} \alpha_T \\ \beta_T \end{bmatrix} = \begin{bmatrix} \psi_{P_N=T} \cdot \psi_{Parents=T} \\ \psi_{P_N=T} \cdot \psi_{Parents=F} \end{bmatrix}, \begin{bmatrix} \alpha_F \\ \beta_F \end{bmatrix} = \begin{bmatrix} \psi_{P_N=F} \cdot \psi_{Parents=T} \\ \psi_{P_N=F} \cdot \psi_{Parents=F} \end{bmatrix} \tag{4.6}$$

Therefore,

$$\begin{bmatrix} \alpha_T \\ \beta_T \end{bmatrix} = \begin{bmatrix} \sqrt{0.5}.\sqrt{0.26} \\ \sqrt{0.5}.\sqrt{0.13} \end{bmatrix} = \begin{bmatrix} 0.3606 \\ 0.2550 \end{bmatrix} \tag{4.7}$$

$$\begin{bmatrix} \alpha_F \\ \beta_F \end{bmatrix} = \begin{bmatrix} \sqrt{0.5}.\sqrt{0.74} \\ \sqrt{0.5}.\sqrt{0.87} \end{bmatrix} = \begin{bmatrix} 0.6083 \\ 0.6595 \end{bmatrix} \tag{4.8}$$

Later, the belief distance that measures the deviation from neutral probability of 0.5 is calculated as follows:

$$B_{d_x} = |\alpha_x + \frac{\alpha_x - \beta_x}{\alpha_x + \beta_x - 1}| \tag{4.9}$$

where $|\alpha_x - 0.5| < |\beta_x - 0.5|$. Thus, the belief distance in the aforementioned numerical example of Prisoner's dilemma game can be calculated as:

$$B_{d_T} = |0.6083 + \frac{0.6083 - 0.6595}{0.6083 + 0.6595 - 1}| = 0.4171 \tag{4.10}$$

$$B_{d_F} = |0.3606 + \frac{0.3606 - 0.2550}{0.3606 + 0.2550 - 1}| = 0.6353 \tag{4.11}$$

Finally the belief degree is calculated by using Deng entropy as follows:

$$D_b = \sum_x B_{d_x} log \frac{B_{d_x}}{2^{|A_i|} - 1} \tag{4.12}$$

Here, $|A_i|$ represents the number of possible actions which is equal to 2 in our example since players have chances of either cooperation or betrayal. Thus,

$$D_b = 0.4171log\frac{0.4171}{2^1-1} + 0.6353log\frac{0.6353}{2^1-1} = -0.9420 \tag{4.13}$$

The quantity of belief degree is used as a heuristic for the interference term and the conditional probability in a quantum Bayesian network is calculated by:

$$P(X|e) = \delta \sum_{i=1}^{|Y|} |\prod_{x}^{N} \psi(X_x|Parents(X_x,e,y=i))|^2 + 2Interference \tag{4.14}$$

Therefore,

$$\begin{aligned}
P(P2 = Defect) &= \delta[|\psi_{P2=D|P1=D}|^2 + |\psi_{P2=D|P1=C}|^2 + 2|\psi_{P2=D|P1=D}|.|\psi_{P2=D|P1=C}|.cos(\theta_1-\theta_2)] \\
&= \delta[0.5(0.87) + 0.5(0.74) + 2\sqrt{0.5(0.87)}\sqrt{0.5(0.74)} - 0.9420] = \delta 0.04917 \\
P(P2 = Cooperate) &= \delta[|\psi_{P2=C|P1=D}|^2 + |\psi_{P2=C|P1=C}|^2 + 2|\psi_{P2=C|P1=D}|.|\psi_{P2=C|P1=C}|.cos(\theta_1-\theta_2)] \\
&= \delta[0.5(0.13) + 0.5(0.26) + 2\sqrt{0.5(0.13)}\sqrt{0.5(0.26)} - 0.9420] = \delta 0.02182
\end{aligned} \tag{4.15}$$

And the final result is:

$$\begin{aligned}
P(P2 = Cooperate) &= \frac{\delta 0.04917}{\delta 0.04917 + \delta 0.02182} = 0.6926 \\
P(P2 = Cooperate) &= \frac{\delta 0.02182}{\delta 0.04917 + \delta 0.02182} = 0.3074
\end{aligned} \tag{4.16}$$

# CHAPTER 5: METHODOLOGY

Proposed Framework: Quantum Social Contagion

In the context of network theory, a complex network, $G\langle V,E\rangle$, is defined as the set of vertices (nodes) ($V=\{v_1,v_2,...,v_n\,|n\in N\}$) and edges between them ($E_{v_i,v_j}=(v_i,v_j)$ where $(i,j\in N; i\neq j)$. To exemplify the social contagion mechanism in this study, we integrate a quantum-like point of view to the classical message-passing approach [8], that generalizes the well-known susceptible-adopted-recovered (SAR) model, to fully describe the mechanisms of information (or behavior) spreading on a complex network with $N$ nodes and a degree distribution $P(k)$. In this model, each individual in a network falls into one of three states: *susceptible*, *adopted* and *recovered*. An individual in a *susceptible* state ($S$) does not adopt the information yet. *Adopted* individuals ($A$) adopts the information and tries to transmit it to its every *susceptible* neighbors with a probability $\lambda$ at each time step. After each successful transmission, the *susceptible* individual, who receives information from his *adopted* neighbor, updates his cumulative units of information, i.e. $m\Rightarrow m+1$. It should be noted that non-redundant, thus non-Markovian, information transmission is considered to focus on a more legit scenario, i.e. information can be transmitted only once from an *adopted* individual to a specific *susceptible* individual who records each successful transmission at each time step. A *susceptible* individual becomes *adopted* if its cumulative units of information exceeds its threshold. Simultaneously, each adopted individual may lose his interest in the information and becomes *recovered* with a probability $\gamma$. Since *recovered* individuals will not further participate in information spreading, a steady-state is reached if all individuals in the network become *recovered* or there is no chance for individuals to change their current states. We initialize the social contagion model with small fraction of individuals ($\rho_0$) assigned as *adopted*, and the rest as *susceptible* in the network. In the rest of this study, $S(t)$, $A(t)$, and $R(t)$ represent the fractions of susceptible,

adopted, and recovered individuals at the time step $t$, respectively.

*Edge-Based Compartmental Theory for Quantum Social Contagion Analysis*

In the current study, we employ an edge-based compartmental theory to understand the dynamics of the quantum social contagion approach inspired by numerous studies [24, 4, 9]. Suppose that $u, (u \in V)$ is an individual who is in the susceptible state, i.e. He can receive information from his neighbors but cannot transfer since he has not adopted information yet. Let $v, (v \in V)$ be a randomly chosen neighbor of $u$ ($E_{u,v} \neq 0$). If we define $\theta(t)$ as the probability that the individual $v$ has not transmitted information to an individual $u$ by time $t$, the probability that individual $u$ with degree $k_u$ has received $m$ pieces information from his distinct neighbors by time $t$ will be binomially distributed and expressed as:

$$\tau_m(k_u, t) = \binom{k_u}{m} \theta(t)^{(k_u - m)} (1 - \theta(t))^m \tag{5.1}$$

The quantum counterpart of this step is intuitively the same, because the binomial distribution property holds true. Since we have defined $\theta(t)$ as the probability that the individual $v$ has not transmitted information to an individual $u$ by time $t$, the quantum probability of the same event can be calculated by using Born's rule in Eq. 3.11 as follows:

$$|\sqrt{\theta(t)} e^{\theta(t)}|^2 = (\sqrt{\theta(t)} e^{\theta(t)}).(\sqrt{\theta(t)} e^{-\theta(t)}) = \theta(t) \tag{5.2}$$

Similarly, the probability of a successful transmission is equal to:

$$|\sqrt{1 - \theta(t)} e^{(1-\theta(t))}|^2 = (\sqrt{1 - \theta(t)} e^{(1-\theta(t))}).(\sqrt{1 - \theta(t)} e^{(\theta(t)-1)}) = 1 - \theta(t) \tag{5.3}$$

Therefore, we get exactly the same outcome (Eq.5.1) as in the classical theory. Furthermore, if the individual $u$ could receive enough pieces of information from his distinct neighbors to exceed his threshold ($\phi_u$), i.e. $m \geq \phi_u$, he will adopt the information and try to transmit it to his susceptible neighbors in the next time step. Otherwise, he will keep his susceptible state in the next time step. Thus, the probability of individual $u$ with degree $k_u$ being susceptible is:

$$\begin{aligned} s_u(k_u,t) &= \sum_{\phi_u} F(\phi_u) \sum_{m=0}^{\phi_u-1} \tau_m(k_u,t) \\ &= \sum_{\phi_u} F(\phi_u) \sum_{m=0}^{\phi_u-1} \binom{k_u}{m} \theta(t)^{(k_u-m)} (1-\theta(t))^m \end{aligned} \tag{5.4}$$

where $F(\phi_u)$ denotes the information adoption threshold function.

We obtain the fraction of susceptible individuals at time $t$ by combining Eqs. 5.4 with the degree distribution of the network as:

$$\begin{aligned} S(t) &= \sum_{k_u} P(k_u) s_u(k_u,t) \\ &= \sum_{k_u} P(k_u) \sum_{\phi_u} F(\phi_u) \sum_{m=0}^{\phi_u-1} \binom{k_u}{m} \theta(t)^{(k_u-m)} (1-\theta(t))^m \end{aligned} \tag{5.5}$$

We can follow a similar strategy to calculate the probability of individual $v$ with degree $k_v$ being susceptible state. Being in susceptible state, the individual $u$ is unable to transmit the information to its neighbor $v$. Thus, the individual $v$ can receive information from his $k_v - 1$ distinct neighbors. Taking all possible values of receiving $m$ pieces of cumulative information and $\phi_v$ into consideration, we obtain:

$$
\begin{aligned}
s_v(k_v,t) &= \sum_{\phi_v} F(\phi_v) \sum_{m=0}^{\phi_v-1} \tau_m(k_v,t) \\
&= \sum_{\phi_v} F(\phi_v) \sum_{m=0}^{\phi_v-1} \binom{k_v-1}{m} \theta(t)^{(k_v-m-1)} (1-\theta(t))^m
\end{aligned}
\tag{5.6}
$$

Recall that, the transfer between states of individuals occur not only between susceptible and adopted states; but also adopted and recovered states. Adopted individuals may lose their interest in the transmission process and move into the recovered state with a predefined probability. Thus, the following set of ordinary differential equations (ODEs) define the time dependence of the individuals in each compartment in the system described above.

$$
\begin{aligned}
\frac{dA(t)}{dt} &= -\frac{dS(t)}{dt} - \gamma A(t) \\
\frac{dR(t)}{dt} &= \gamma A(t)
\end{aligned}
\tag{5.7}
$$

By computing $\theta(t)$, we can solve the equations for $S(t)$, and also $A(t)$ and $R(t)$, and investigate the system dynamics. In edge-based compartmental theory, we have not made any assumption about the state of individual $v$; therefore, $\theta(t)$ may consist of three possible outcomes which are mutually exclusive in classical approach:

$$
\theta(t) = \xi_S(t) + \xi_A(t) + \xi_R(t) \tag{5.8}
$$

where $\xi_S(t)$ ($\xi_A(t)$, $\xi_R(t)$) represents the probability that a neighbor $v$ in the susceptible (adopted, recovered) state, and has not transmitted the information to individual $u$ by time $t$.

To employ quantum probability rules, we can use Born's rule in Eq. 3.11 and write counterpart of Eq. 5.8 as follows (see Eq. 3.7):

$$\begin{aligned}\theta(t) &= |e^{i\theta\psi_{\xi_S(t)}} + e^{i\theta\psi_{\xi_A(t)}} + e^{i\theta\psi_{\xi_R(t)}}|^2 \\ &= |\psi_{\xi_S(t)}|^2 + |\psi_{\xi_A(t)}|^2 + |\psi_{\xi_R(t)}|^2 + 2\Big[|\psi_{\xi_S(t)}||\psi_{\xi_A(t)}|cos(\theta_{\xi_S(t)} - \theta_{\xi_A(t)}) \\ &+ |\psi_{\xi_S(t)}||\psi_{\xi_R(t)}|cos(\theta_{\xi_S(t)} - \theta_{\xi_R(t)}) + |\psi_{\xi_A(t)}||\psi_{\xi_R(t)}|cos(\theta_{\xi_A(t)} - \theta_{\xi_R(t)})\Big]\end{aligned} \tag{5.9}$$

Here, the amplitude $|\psi_{\xi_S(t)}|^2$ refers to $P(\xi_S(t))$, $|\psi_{\xi_A(t)}|^2$ to $P(\xi_A(t))$ and $|\psi_{\xi_R(t)}|^2$ to $P(\xi_R(t))$. The angle $\theta_{\xi_S(t)} - \theta_{\xi_A(t)}$ corresponds to the phase of the inner product between $|\xi_S(t)|$ and $|\xi_A(t)|$. Note that there is no direct transition from susceptible state to recovered state, so $cos(\theta_{\xi_S(t)} - \theta_{\xi_R(t)})$ will be equal to 0. By recalling inverse Born's rule again, we can finalize the relation above as:

$$\begin{aligned}\theta(t) &= \xi_S(t) + \xi_A(t) + \xi_R(t) \\ &+ \sqrt{\xi_S(t)\xi_A(t)}cos(\theta_{\xi_S(t)} - \theta_{\xi_A(t)}) + \sqrt{\xi_A(t)\xi_R(t)}cos(\theta_{\xi_A(t)} - \theta_{\xi_R(t)})\end{aligned} \tag{5.10}$$

Herein, the additional terms are called as interference terms that does not exist in classical probability theory. From this point, we will call $\sqrt{\xi_S(t)\xi_A(t)}cos(\theta_{\xi_S(t)} - \theta_{\xi_A(t)})$ as SA interference term and $\sqrt{\xi_A(t)\xi_R(t)}cos(\theta_{\xi_A(t)} - \theta_{\xi_R(t)})$ as AR interference term for the sake of simplicity.

Later, we draw from statistical network science to make the connection between these two individuals $u$ and $v$. In the case of the existence of an uncorrelated network, the probability of an edge connecting individual $v$ with a degree $k_v$ to one of its neighbors, e.g., individual $u$ with degree $k_u$, is equal to $k_v P(k_v)/\langle k \rangle$, where $\langle k \rangle$ is the mean degree. Thus, it can be obtained that:

$$\begin{aligned}\xi_S(t) &= \frac{\sum_{k_v} k_v P(k_v) s_v(k_v,t)}{\langle k \rangle} \\ &= \frac{\sum_{k_v} k_v P(k_v) \sum_{\phi_v} F(\phi_v) \sum_{m=0}^{\phi_v - 1} \tau_m(k_v,t)}{\langle k \rangle} \\ &= \frac{\sum_{k_v} k_v P(k_v) \sum_{\phi_v} F(\phi_v) \sum_{m=0}^{\phi_v - 1} \binom{k_v - 1}{m} \theta(t)^{(k_v - 1 - m)} (1-\theta(t))^m}{\langle k \rangle}\end{aligned} \tag{5.11}$$

$\theta(t)$ is a time-dependent variable, and it will not accomplish its definition after any successful transmission. Therefore, we need to consider its time-dependence to fully understand the systems dynamics from the beginning till the steady-state. If we suppose that an adopted individual transmits behavioral information with probability $\lambda$, the decrease in $\theta(t)$ can be written as:

$$\frac{d\theta(t)}{dt} = -\lambda \xi_A(t) \tag{5.12}$$

At time $t$, the behavioral information is not transmitted with probability $1-\lambda$ and the adopted individuals move into recovered state with probability $\gamma$, simultaneously. Then;

$$\frac{d\xi_R(t)}{dt} = \gamma(1-\lambda)\xi_A(t) \tag{5.13}$$

Substituting Eqs. 5.12 into 5.13 and integrating it with the initial conditions of $\theta(0) = 1$ and $\xi_R(0) = 0$, we can obtain:

$$\xi_R(t) = \frac{\gamma(1-\lambda)[1-\theta(t)]}{\lambda} \tag{5.14}$$

*Binomial Threshold Distribution*

Since the quantum-like social contagion is a novel approach, and it introduces a complexity via its additional interference terms. Because the heterogeneity of individuals in information adoption is significant, we assume that $F(\phi_u)$ can be represented as a binomial distribution. In other words, individuals may have either a relatively lower threshold ($T_a = 1$) with probability $p$, or a relatively higher threshold ($T_b > 1$) with probability $1-p$. Thus;

$$F(\phi_u) = \begin{cases} T_a, & \text{with probability } p \\ T_b, & \text{with probability 1-}p \end{cases} \tag{5.15}$$

We obtain the fraction of susceptible individuals at time $t$ by combining Eqs. 5.4 and 5.15 with the degree distribution of the network as:

$$\begin{aligned} S(t) &= \sum_{k_u} P(k_u) s_u(k_u, t) \\ &= \sum_{k_u} P(k_u) \left[ p\theta(t)^{k_u} + (1-p) \sum_{m=0}^{T_B-1} \binom{k_u}{m} \theta(t)^{(k_u-m)} (1-\theta(t))^m \right] \end{aligned} \tag{5.16}$$

We can follow a similar strategy to calculate the probability of individual $v$ with degree $k_v$ being susceptible state. Taking all possible values of receiving $m$ pieces of cumulative information and $\phi_v$ into consideration, we obtain:

$$s_v(k_v, t) = p\theta(t)^{(k_v-1)} + (1-p) \sum_{m=0}^{T_B-1} \binom{k_v}{m} \theta(t)^{(k_v-m-1)} (1-\theta(t))^m \tag{5.17}$$

Then, the rest of the methodology is followed from Eq. 5.17 till the end. Finally, we obtain $\xi_A(t)$ inserting Eqs. 5.11 and 5.14 into 5.9. Substituting the resulting equation of $\xi_A(t)$ into Eq. 5.12, we derive the time evolution of $\theta(t)$. Furthermore, the dynamics of quantum social contagion can be described with the ODE equations in Eq. 5.7. When $t \to \infty$, we find the final adoption size $R(\infty)$ once the degree distribution is known.

*Belief-Entropy-Based Heuristic*

In this study, we propose belief entropy as a heuristic for the calculation of interference term in Equation 5.10.

$$D_i j = cos(\theta_i - \theta_j) = -\sum_i m(x_i) ln \frac{m(x_i)}{2^{|x_i - 1} - 1} \tag{5.18}$$

where $|x_i|$ represents the number of possible actions which is equal to three in our example since individuals can be in one of three states. $m(.)$ denotes the function of belief mass in Dempster-Shafer evidence theory. Accordingly,

$$D_{SA} = cos(\theta_{\xi_S(t)} - \theta_{\xi_A(t)}) = -m(x_{SA}) lnm(x_{SA}) \tag{5.19}$$

where

$$m(x_{SA}) = \alpha \left| \xi_S(t) + \frac{\xi_S(t) - \xi_A(t)}{\xi_S(t) + \xi_A(t) - 1} \right| \tag{5.20}$$

It should be noted that masses of all the members of the set add up to a total of 1. Therefore, $\alpha$ is used as a normalization parameter.

$$\alpha \left( \left| \xi_S(t) + \frac{\xi_S(t) - \xi_A(t)}{\xi_S(t) + \xi_A(t) - 1} \right| + \left| \xi_A(t) + \frac{\xi_A(t) - \xi_R(t)}{\xi_A(t) + \xi_R(t) - 1} \right| \right) = 1 \tag{5.21}$$

Accordingly, Equation 5.10 can be rewritten as:

$$\begin{aligned}\theta(t) &= \xi_S(t) + \xi_A(t) + \xi_R(t) + \sqrt{\xi_S(t)\xi_A(t)}D_{SA} + \sqrt{\xi_A(t)\xi_R(t)}D_{AR} \\ &= \xi_S(t) + \xi_A(t) + \xi_R(t) - \sqrt{\xi_S(t)\xi_A(t)}m(x_{SA})lnm(x_{SA}) - \sqrt{\xi_A(t)\xi_R(t)}m(x_{AR})lnm(x_{AR})\end{aligned} \tag{5.22}$$

Co-evolution of Two Quantum Social Contagions

In this section, we will explain the mathematical modeling of co-evolution of two quantum social contagions by using edge-based compartmental theory inspired by [162]. During this process, suppose that there are two behavior (information), i.e., $b \in \{1,2\}$ successively disseminate in the network. To exemplify the social contagion mechanism in this study, we integrate a quantum-like point of view to the classical message-passing approach [8] that generalizes the well-known susceptible-adopted-recovered (SAR) model, to fully describe the mechanisms of information (or behavior) spreading on a complex network. In this approach, each individuals of the network of $N$ nodes and a degree distribution $P(k)$ falls into one of three states: *susceptible*, *adopted* and *recovered*. These states represent:

- An individual in a *susceptible* state ($S$) does not adopt the behavior yet,
- An individual in an *adopted* state observed the behavior and adopted it already and tries to transmit it to his *susceptible* neighbors,
- An individual in a *recovered* state adopted the behavior once but lose interest and will not further participate in spreading.

First of all, we focus on the spreading of first behavior (information) ($b_1$). Suppose that $u, (u \in V)$ is an individual who is in the adopted state and all other individuals are in susceptible state, i.e. They can receive information from his neighbors but cannot transfer since they have not adopted information yet. In each time step, $u$ tries to transmit to information to all his susceptible neighbors with the probability of $\lambda_1$. Let $v, (v \in V)$ be a randomly chosen neighbor of $u$ ($E_{u,v} \neq 0$). Once the influence successful and $u$ transmit information to $v$, he loses his interest in spreading by probability $\gamma_1$, and goes to recovered state and $v$ increase his cumulative piece of information $m$ by 1. The probability of individual $v$ with degree $k_v$ adopts $b_1$ can be identified with:

$$\pi(k_v, m) = 1 - (1 - \tau_1)^m \tag{5.23}$$

where $m$ is the cumulative number of $b_1$ that individual $v$ has received from adopted neighbors, while $\tau_1$ is the unit of adopting probability for each reception of $b_1$. Since each adopted individual will try to transmit the information $b_1$ during the process, individual $v$ will update his cumulative piece of information each time until it exceeds his threshold.

Later, following the dynamical process of $b_1$, a random seed node is selected to be in the adopted state for behavior 2 ($b_2$) and the rest of the nodes set to be in the susceptible state for $b_2$. The dynamical properties of $b_1$ and $b_2$ are analogous; however, transmission probability is equal to $\lambda_2$ instead of $\lambda_1$, and the recovery probability is equal to $\gamma_2$ instead of $\gamma_1$. Furthermore, let $X_u$ represents the final state of individual $u$ for $b_1$ and $X_u = S$ means that individual $u$ did not adopt $b_1$ yet, while $X_u = R$ means that individual $u$ has adopted $b_1$. Additionally, the susceptible individual $u$ of degree $k_u$ receives the $p^{th}$ piece of $b_2$, and the cumulative number of pieces of received $b_2$ is $m$, then individual $u$ adopts $b_2$ with a probability:

$$\Psi(k_v, m, X) = \begin{cases} 1-(1-\tau_2)^m, X_u = S \\ 1-(1-\alpha\tau_2)^m, X_u = R \end{cases} \tag{5.24}$$

Here, $\tau_2$ represents the unit adopting probability for each reception of $b_2$. Also, when a node has adopted $b_1$, i.e., $X_u = R$, the actual unit adoption probability $\tau_2$ converts to $\alpha\tau_2$, where $\alpha \in [0, \frac{1}{\tau_2}]$ is a parameter that is used to adjust the adoption synergy between $b_1$ and $b_2$. For example, $\alpha = 0$ means that if an individual adopted $b_1$ it never adopts $b_2$. Furthermore, $\alpha = \frac{1}{\tau_2}$ means that if an individual adopted $b_1$ needs to receive only one piece of $b_2$ to adopt $b_2$. On the other hand, $\alpha = 1$ means that adopting $b_1$ has no impact on adopting $b_2$.

During the spread of $b_1$, we employ an edge-based compartmental theory to understand the dynamics of the quantum social contagion approach as in the previous subsection. Again, we focus on a single individual, - called $u$, who is in the susceptible state and one of its neighbor $v$, where $E_{u,v} \neq 0$. Let $\theta_1(t)$ is the probability that the individual $v$ has not transmitted $b_1$ to the individual $u$ by time $t$, then the probability that individual $u$ with degree $k_u$ has received $m$ pieces of $b_1$ from his distinct neighbors by time $t$ will be binomially distributed and computed as:

$$\tau(k_u, t) = \binom{k_u}{m} \theta_1(t)^{(k_u - m)} (1-\theta_1(t))^m \tag{5.25}$$

If the individual $u$ could receive enough pieces of information from his distinct neighbors, he will adopt the information and try to transmit it to his susceptible neighbors in the next time step. Otherwise, he will keep his susceptible state in the next time step. Thus, the probability of individual $u$ with degree $k_u$ being susceptible is:

$$
\begin{aligned}
s_u(k_u,t,b_1) &= \sum_{m=0}^{k_u} \tau(k_u,t) \prod_{i=0}^{m} (1-\pi(k_u,i)) \\
&= \sum_{m=0}^{k_u} \binom{k_u}{m} \theta_1(t)^{(k_u-m)} (1-\theta_1(t))^m \prod_{i=0}^{m} (1-\pi(k_u,i))
\end{aligned}
\tag{5.26}
$$

Thus, we obtain the fraction of susceptible individuals at time $t$ by combining Eqs. 5.26 with the degree distribution of the network as:

$$
\begin{aligned}
S1(t) &= \sum_{k_u} P(k_u) s_u(k_u,t,b_1) \\
&= \sum_{k_u} P(k_u) \sum_{m=0}^{k} \binom{k_u}{m} \theta_1(t)^{(k_u-m)} (1-\theta_1(t))^m \prod_{i=0}^{m} (1-\pi(k_u,i))
\end{aligned}
\tag{5.27}
$$

Being in susceptible state, the individual $u$ is unable to transmit the information to its neighbor $v$. Thus, the individual $v$ can receive information from his $k_v - 1$ distinct neighbors. If we consider all the possible values of receiving $m$ pieces of cumulative information and $\phi_v$ values, we obtain the following:

$$
\begin{aligned}
s_v(k_v,t,b_1) &= \sum_{m=0}^{k_v-1} \tau(k_v,t) \prod_{i=0}^{m} (1-\pi(k_v,i)) \\
&= \sum_{m=0}^{k_v-1} \binom{k_v-1}{m} \theta_1(t)^{(k_v-m-1)} (1-\theta_1(t))^m \prod_{i=0}^{m} (1-\pi(k_v,i))
\end{aligned}
\tag{5.28}
$$

Taking into consideration the fact that individuals transfer between states not only from susceptible to adopted states, but also from adopted to recovered states; the following set of ordinary differ-

ential equations (ODEs) define the time dependence of the individuals in each compartment in the system described above

$$\begin{aligned} \frac{dA_1(t)}{dt} &= -\frac{dS_1(t)}{dt} - \gamma_1 A_1(t) \\ \frac{dR_1(t)}{dt} &= \gamma_1 A_1(t) \end{aligned} \tag{5.29}$$

As aforementioned above, in edge-based compartmental theory, we have not made any assumption about the state of individual $v$; therefore, $\theta_1(t)$ may consist of three possible outcomes which are mutually exclusive in classical approach:

$$\theta_1(t) = \xi_{S1}(t) + \xi_{A1}(t) + \xi_{R1}(t) \tag{5.30}$$

where $\xi_{S1}(t)$ ($\xi_{A1}(t)$, $\xi_{R1}(t)$) represents the probability that a neighbor $v$ in the susceptible (adopted, recovered) state, and has not transmitted $b_1$ to individual $u$ by time $t$.

By utilizing the using the Born's rule in Eq. 3.11 and using the similar assumption in Eq. 5.9, we can derive the quantum counterpart of Eq. 5.30 as follows:

$$\begin{aligned} \theta_1(t) = {} & \xi_{S1}(t) + \xi_{A1}(t) + \xi_{A1}(t) \\ & + \sqrt{\xi_{S1}(t)\xi_{A1}(t)}cos(\theta_{\xi_{S1}(t)} - \theta_{\xi_{A1}(t)}) + \sqrt{\xi_{A1}(t)\xi_{R1}(t)}cos(\theta_{\xi_{A1}(t)} - \theta_{\xi_{R1}(t)}) \end{aligned} \tag{5.31}$$

Here, the amplitude $|\psi_{\xi_{S1}(t)}|^2$ refers to $P(\xi_{S1}(t))$, $|\psi_{\xi_{A1}(t)}|^2$ to $P(\xi_{A1}(t))$ and $|\psi_{\xi_{R1}(t)}|^2$ to $P(\xi_{R1}(t))$. The angle $\theta_{\xi_{S1}(t)} - \theta_{\xi_{A1}(t)}$ corresponds to the phase of the inner product between $|\xi_{S1}(t)|$ and $|\xi_{A1}(t)|$. Also, the additional terms are called as interference terms that does not exist in classical probability theory. From this point, we will call $\sqrt{\xi_{S1}(t)\xi_{A1}(t)}cos(\theta_{\xi_{S1}(t)} - \theta_{\xi_{A1}(t)})$ as SA1

interference term and $\sqrt{\xi_{A1}(t)\xi_{R1}(t)}cos(\theta_{\xi_{A1}(t)} - \theta_{\xi_{R1}(t)})$ as AR1 interference term for the sake of simplicity.

To calculate $\theta_1(t)$, lets recall that individual $u$ and individual $v$ with a degree $k_v$ are connected to each other. In the case of the existence of an uncorrelated network, the probability of an edge connecting individual $v$ to one of its neighbors, e.g., individual $u$ with degree $k_u$, is equal to $k_v P(k_v)/\langle k \rangle$, where $\langle k \rangle$ is the mean degree. Thus, it can be obtained that:

$$\begin{aligned} \xi_{S1}(t) &= \frac{\sum_{k_v} k_v P(k_v) s_v(k_v, t, b_1)}{\langle k \rangle} \\ &= \frac{\sum_{k_v} k_v P(k_v) \sum_{m=0}^{k_v-1} \binom{k_v-1}{m} \theta_1(t)^{(k_v-m-1)} (1-\theta_1(t))^m \prod_{i=0}^{m} (1-\pi(k_v, i))}{\langle k \rangle} \end{aligned} \tag{5.32}$$

We assume that the adoption transmits $b_1$ with probability $\lambda_1$, so the decrease in $\theta_1(t)$ can be expressed by:

$$\frac{d\theta_1(t)}{dt} = -\lambda_1 \xi_{A1}(t) \tag{5.33}$$

At time $t$, $b_1$ is not transmitted with probability $1-\lambda_1$ and the adopted individuals move into recovered state with probability $\gamma_1$, simultaneously. Then;

$$\frac{d\xi_{R1}(t)}{dt} = \gamma_1 (1-\lambda_1) \xi_{A1}(t) \tag{5.34}$$

Substituting Eqs. 5.33 into 5.34 and integrating it with the initial conditions of $\theta_1(0) = 1$ and $\xi_{R1}(0) = 0$, we obtain:

$$\xi_{R1}(t) = \frac{\gamma_1(1-\lambda_1)[1-\theta_1(t)]}{\lambda_1} \tag{5.35}$$

In the second part of the analysis, we will model the spread of the second behavior (information), $b_2$. Let $\omega(X)$ be the probability of the state of a random individual in terms of $b_1$. Here, $X = S$ and $X = R$ indicates that indicates that the individual has not adopted and has adopted $b_1$, respectively. Therefore, $\omega(S) = 1 - R1$ and $\omega(R) = R1$. For $b_2$, the transmission probability is depend on the actual state of the individual for $b_1$ as identified in Eq. 5.40. Now, the probability of individual $u$ with degree $k_u$ being susceptible can be investigated under two steps. First, there is a chance for individual $u$ has not adopted $b_1$ and does not adopt $b_2$ by time $t$. Second, there is a chance for individual $u$ has adopted $b_1$ and does not adopt $b_2$ by time $t$. Combining both gives us the probability of individual $u$ with degree $k_u$ being susceptible as follows:

$$\begin{aligned} s_u(k_u,t,b_2) &= \sum_{X\in\{S,R\}} \omega(X) \sum_{m=0}^{k_u} \tau(k_u,t) \prod_{i=0}^{m} (1-\psi(k_u,i,X)) \\ &= \sum_{X\in\{S,R\}} \omega(X) \sum_{m=0}^{k_u} \binom{k_u}{m} \theta_2(t)^{(k_u-m)} (1-\theta_2(t))^m \prod_{i=0}^{m} (1-\psi(k_u,i,X)) \end{aligned} \tag{5.36}$$

where $F(\phi_u)$ denotes the information adoption threshold function.

Thus, we obtain the fraction of susceptible individuals at time $t$ for the second behavior $b_2$ by combining Eqs. 5.26 with the degree distribution of the network as:

$$
\begin{aligned}
S2(t) &= \sum_{k_u} P(k_u) s_u(k_u, t, b_2) \\
&= \sum_{k_u} P(k_u) \sum_{X \in \{S,R\}} \omega(X) \sum_{m=0}^{k_u} \binom{k_u}{m} \theta_2(t)^{(k_u - m)} (1 - \theta_2(t))^m \prod_{i=0}^{m} (1 - \psi(k_u, i, X))
\end{aligned}
\tag{5.37}
$$

As explained in the derivation of Eq. 5.38, being in susceptible state, the individual $u$ is unable to transmit the information to its neighbor $v$. Thus, the individual $v$ can receive information from his $k_v - 1$ distinct neighbors. If we consider all the possible values of receiving $m$ pieces of cumulative information and $\phi_v$ values, we obtain the following:

$$
\begin{aligned}
s_v(k_v, t, b_2) &= \sum_{m=0}^{k_v - 1} \tau(k_v, t) \prod_{i=0}^{m} (1 - \pi(k_v, i)) \\
&= \sum_{m=0}^{k_v - 1} \binom{k_v - 1}{m} \theta_2(t)^{(k_v - m - 1)} (1 - \theta_2(t))^m \prod_{i=0}^{m} (1 - \psi(k_v, i, X))
\end{aligned}
\tag{5.38}
$$

Then, we repeat the same procedure to calculate $\theta_2$. Since $\theta_2$ is obtained with the summation of $\xi_{S2}(t)$, $\xi_{A2}(t)$ and $\xi_{R2}(t)$, where each represents the probability that a neighbor $v$ in the susceptible (adopted, recovered) state, and has not transmitted $b_2$ to individual $u$ by time $t$, we calculate the probability of an edge connecting individual $v$ to one of its neighbors as follows:

$$
\begin{aligned}
\xi_{S2}(t) &= \frac{\sum_{k_v} k_v P(k_v) s_v(k_v, t, b_2)}{\langle k \rangle} \\
&= \frac{\sum_{k_v} k_v P(k_v) \sum_{m=0}^{k_v - 1} \binom{k_v - 1}{m} \theta_2(t)^{(k_v - m - 1)} (1 - \theta_2(t))^m \prod_{i=0}^{m} (1 - \psi(k_v, i, X))}{\langle k \rangle}
\end{aligned}
\tag{5.39}
$$

where

$$\Psi(k_v, m, X) = \begin{cases} 1-(1-\tau_2)^m, X_u = S \\ 1-(1-\alpha\tau_2)^m, X_u = R \end{cases} \tag{5.40}$$

Inserting Eqs. 5.39 and into main $\theta_2$ function yields $\xi_A(t)$ in classical theory as follows:

$$\begin{aligned} \xi_{A2(t)} &= \theta_2(t) - \frac{\sum_{k_v} k_v P(k_v) s_v(k_v, t, b_2)}{\langle k \rangle} - \frac{\gamma_2(1-\lambda_2)[1-\theta_2(t)]}{\lambda_2} \\ &= \theta_2(t) - \frac{\sum_{k_v} k_v P(k_v) \sum_{m=0}^{k_v-1} \binom{k_v-1}{m} \theta_2(t)^{(k_v-m-1)} (1-\theta_2(t))^m \prod_{i=0}^{m} (1-\psi(k_v, i, X))}{\langle k \rangle} \\ &- \frac{\gamma_2(1-\lambda_2)[1-\theta_2(t)]}{\lambda_2} \end{aligned} \tag{5.41}$$

Then, the time evolution of $\theta_2(t)$ in classical theory is found to be equal to:

$$\frac{d\theta_2(t)}{dt} = -\lambda_2 \left[ \theta_2(t) - \frac{\sum_{k_v} k_v P(k_v) s_v(k_v, t, b_2)}{\langle k \rangle} \right] - \gamma_2(1-\lambda_2)[1-\theta_2(t)] \tag{5.42}$$

In quantum counterpart of this calculation; however, is more complex due to the interference terms in 3.7. In this case, we insert Eqs. 5.39 into Eq. 5.10 to obtain $\xi_A 2(t)$ by using the quantum approach:

$$\begin{aligned} \theta_2(t) &= \frac{\sum_{k_v} k_v P(k_v) s_v(k_v, t, b_2)}{\langle k \rangle} + \xi_{A2}(t) + \frac{\gamma_2(1-\lambda_2)[1-\theta_2(t)]}{\lambda_2} \\ &+ \sqrt{\frac{\sum_{k_v} k_v P(k_v) s_v(k_v, t, b_2)}{\langle k \rangle} \xi_{A2}(t)} cos(\theta_{\xi_{S2}(t)} - \theta_{\xi_{A2}(t)}) \\ &+ \sqrt{\xi_{A2}(t) \frac{\gamma_2(1-\lambda_2)[1-\theta_2(t)]}{\lambda_2}} cos(\theta_{\xi_{A2}(t)} - \theta_{\xi_{R2}(t)})\lambda) \end{aligned} \tag{5.43}$$

# CHAPTER 6: RESULTS

In this study, we aim to answer five research questions given in Introduction section. Every question will be investigated under relative subsections. To understand the analyses and organization in this section, recall the following research question:

- To better model the complexity of human decision-making and explain existing paradoxes and fallacies, researchers developed numerous quantum-like approaches [18, 19, 15, 20, 21, 22]. Does the quantum-like approach model the dynamics of social contagion better?

- The most challenging task in employing social contagion analyses is to model heterogeneity of the individuals in their adoption threshold. Current studies that use the classical approach demonstrated the existence of discontinuous phase transitions in the final spreading size versus transmission probability. What type of phase transitions are observed when agents are modeled as quantum decision-makers?

- The variability of the social contagion dynamics with changing network properties (assortativity, density, clustering, degree distribution, etc.) is highly studied among researchers [37, 38]. Does the superiority/incapacity of quantum-based probabilistic models in social contagion analyses over classical models vary with changing network properties?

- Quantum-like probabilistic models yield extra interference terms compared to classical approaches. Some studies that utilized quantum-like approaches in decision-making systems tunes these parameters manually [30], [39]; while others do automatically by using a static heuristic [32] and/or dynamic heuristic [21]. Can a heuristics based on entropy measures be an alternative to the extant heuristics in the literature?

- Despite the great interest in modeling a contagion of single behavior, there might be compet-

ing or cooperating contagions in the complex network in real case scenarios. Does quantum contagion is applicable for these complex contagions, or is it too complex to handle?

## Comparison of Quantum-Like and Classical Approaches in Modeling Social Contagion

As aforementioned in the Introduction section, human inference is deterministic and jumps between state-like steps over time according to classical approaches. In contrast, quantum-like approaches are based on the aspect that human minds simultaneously hold competing beliefs. Despite bringing more generalizable and realistic point of view, quantum-like approaches are more complex and time-inefficient. Thus, in this section, we will first focus on the scenario in which individuals are homogeneous, i.e. all individuals have same threshold value ($T_a = T_b = 1$ in Equation 5.15). Later, we will integrate binomial threshold distribution ($T_a \neq T_b$ in Equation 5.15).

### *Homogeneous Adoption Threshold*

Here, we aim to compare and contrast the dynamics and performances of classical social contagion along with its quantum counterpart. In fact, the differences in these two approaches stem from the definition of $\theta(t)$ in Eqs. 5.8 and 5.10; therefore, we first investigated the graphical solution of fixed point equation $d\theta(t)/dt$ at steady-state, i.e. $t \to \infty$ with different threshold values on random regular networks in Figure 6.1.

Figure 6.1a shows the graphical solution of the fixed point of equation $d\theta(t)/dt$ when all agents have same adoption threshold $T_a = T_b = 1$ and the classical social contagion model is utilized. Results show that there is only one nontrivial solution regardless of the value of $\lambda$, and the increasing $\lambda$ yield the solution on lower $\theta(\infty)$. Since only the maximum solution is physically meaningful in such situations, we plotted the physically meaningful solutions of $\theta(t)$ for each possible $\lambda$ values

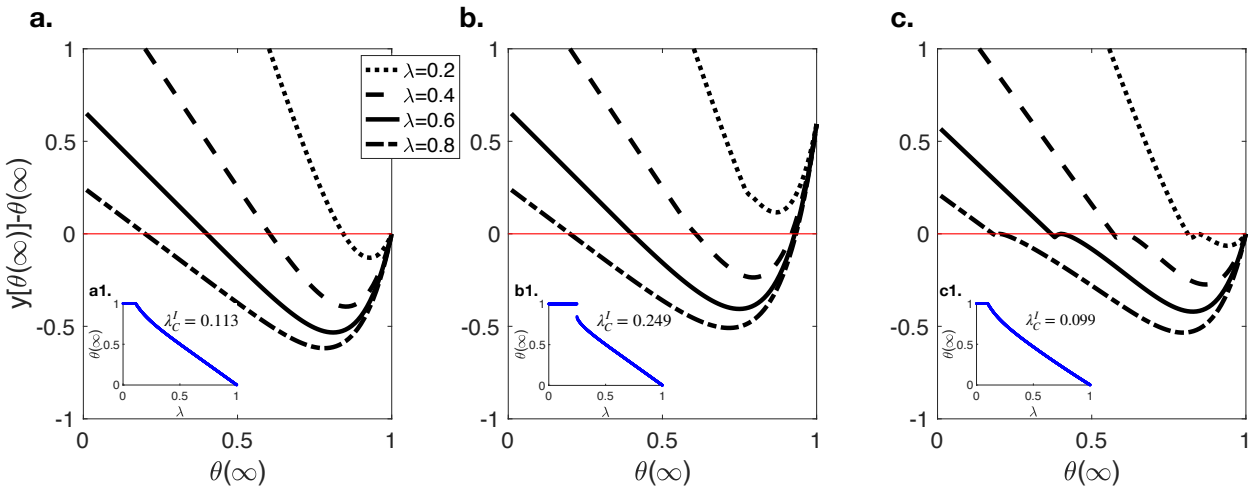


Figure 6.1: The graphical solution of fixed point of equation $d\theta(t)/dt$ at steady-state in the existence of homogeneous agents ($T_b = 1$) on random regular networks ($\langle k \rangle = 10$ and $p = 0.3$) when a. no interference term (classical method), b. $cos(\theta_{\xi_S(t)} - \theta_{\xi_A(t)}) = 0.5$, c. $cos(\theta_{\xi_A(t)} - \theta_{\xi_R(t)}) = 0.2$. The physically meaningful solutions of $\theta(t)$ for each possible $\lambda$ values are shown in the subplots a1, b1 and c1, respectively.

by using the classical approach in Figure 6.1a1. The solution for $\theta(\infty)$ shows a continuous change after the critical transmission probability ($\lambda_c^I = 0.113$). It means that the final adoption size $R(\infty)$ grows continuously with the increasing $\lambda$. The quantum approach, on the other hand, yields two interference terms: SA ($cos(\theta_{\xi_S(t)} - \theta_{\xi_A(t)})$) and AR ($cos(\theta_{\xi_S(t)} - \theta_{\xi_A(t)})$) interference terms. Figure 6.1b and 6.1c show the graphical solution of fixed point of equation $d\theta(t)/dt$ at steady-state when $T_b = 2$ and only SA and AR interference terms are observed, respectively. The change in $\theta(\infty)$ with respect to $\lambda$ in the existence of SA and AR interference is also plotted in Figure 6.1b1 and 6.1c1. Results show that the SA interference term makes the pattern discontinuous, i.e. $R(\infty)$ increases discontinuously with the increasing $\lambda$ and jump to another point at critical transmission probability ($\lambda_c^I = 0.249$). In the existence of AR interference term, on the other hand, same continuous change pattern is observed as in classical social contagion; however, at lower critical transmission probability ($\lambda_c^I = 0.099$).

*Heterogeneous Adoption Threshold*

In the previous subsection, we investigated the dynamics and performances of classical social contagion along it quantum counterpart when all individuals have same adoption threshold ($T_A = T_B = 1$). Here, to implement the heterogeneity of agents in a social contagion analysis we used binomial threshold distribution defined in Equation 5.15. To understand the effect of threshold heterogeneity, we repeated our experiments on two different threshold values, e.g., $T_b = 2$ and $T_b = 4$.

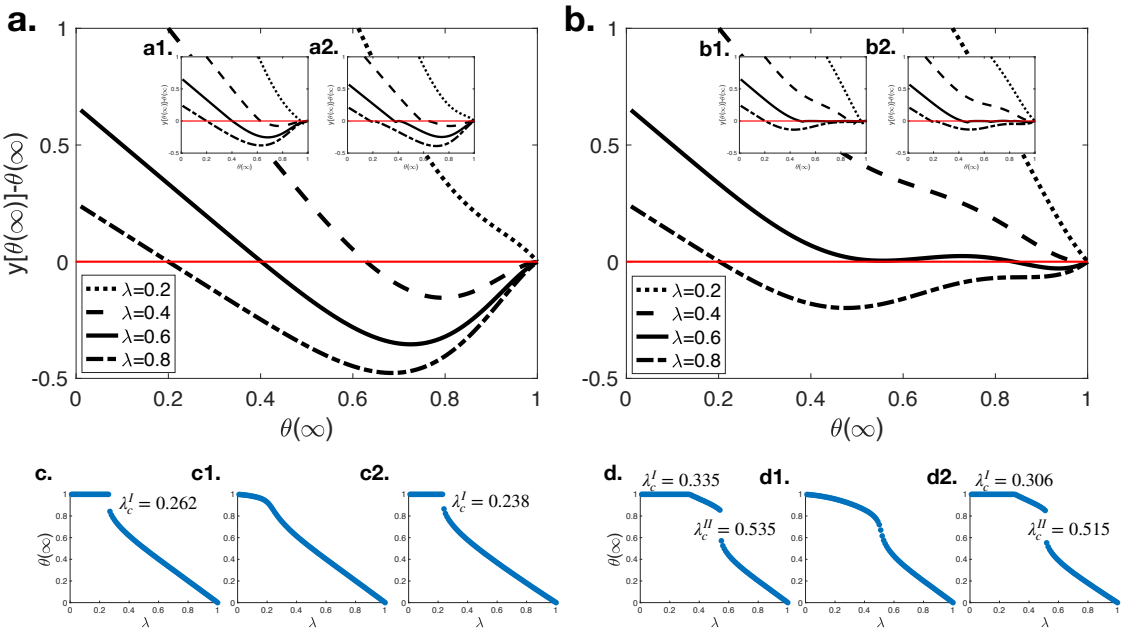


Figure 6.2: The graphical solution of fixed point of equation $d\theta(t)/dt$ at steady-state when a. $T_b = 2$ and b. $T_b = 4$ on random regular networks ($\langle k \rangle = 10$ and $p = 0.3$). The physically meaningful solutions of $\theta(t)$ for each possible $\lambda$ values are shown when c. $T_b = 2$ and d. $T_b = 4$. Subplots a1, b1 and c1 show the relative solutions when $cos(\theta_{\xi_S(t)} - \theta_{\xi_A(t)}) = 0.2$, while subplots a2, b2 and c2 do when $cos(\theta_{\xi_A(t)} - \theta_{\xi_R(t)}) = 0.2$

Figure 6.2a shows the graphical solution of fixed point of equation $d\theta(t)/dt$ when $T_b = 2$. Results show that, as in the case of homogeneous adoption threshold distribution, there is only one

nontrivial solution when $\lambda$ is small; however, at moderate $\lambda$ values there are cases in which two nontrivial solutions are observed. In such a case, only the maximum solution is physically meaningful. In Figure 6.2c, we plotted the physically meaningful solutions of $\theta(t)$ for each possible $\lambda$ values by using the classical approach. The solution for $\theta(\infty)$ show a discontinuous change and jump to another point at critical transmission probability ($\lambda_c^I = 0.262$). Therefore, $R(\infty)$ grows discontinuously with the increasing $\lambda$. The quantum approach, on the other hand, yields two interference terms: SA ($cos(\theta_{\xi_S(t)} - \theta_{\xi_A(t)})$) and AR ($cos(\theta_{\xi_S(t)} - \theta_{\xi_A(t)})$) interference terms. Figure 6.2a1 (6.2a2) shows the graphical solution of fixed point of equation $d\theta(t)/dt$ at steady-state when $T_b = 2$ and only SA (AR) interference is observed. The change in $\theta(\infty)$ with respect to $\lambda$ in the existence of SA (AR) interference is also plotted in Figure 6.2c1 (6.2c2). Results show that the SA interference term makes the pattern continuous, i.e. $R(\infty)$ increases continuously with the increasing $\lambda$. In the existence of AR interference term, on the other hand, same discontinuous change pattern is observed as in classical social contagion; however, at lower critical transmission probability ($\lambda_c^I = 0.238$).

For the case of $T_b = 4$ (Figure 6.2b), $\theta(\infty)$ decreases continuously and a continuous phase transition observed at the first critical transmission probability ($\lambda_c^I = 0.335$), then another discontinuous change occurs at the second critical transmission probability ($\lambda_c^{II} = 0.535$) in the classical approach (Figure 6.2d). It means that, $R(\infty)$ first increases continuously and then a discontinuous pattern is observed, which is called as hybrid phase transition. W. Wang et al. [4] explains this situation as follows: In the existence of more than one critical transmission probability, two different types of information adoption occur: i) Local adoption in which the information is adopted by a small fraction of individuals, ii) Global adoption in which the information is adopted by a finite fraction of individuals. When $\lambda < \lambda_c^I$, individuals adopt information locally, while a global adoption is observed when $\lambda > \lambda_c^{II}$. In the case of $\lambda_c^I < \lambda < \lambda_c^{II}$, individuals who have lower thresholds adopt behavior globally while individuals who have higher thresholds adopt behavior locally. In

the quantum social contagion model, SA interference term makes $R(\infty)$ growth continuous with increasing $\lambda$, while AR term displays same pattern as in classical approach with lower the critical transmission probabilities, i.e. ($\lambda_c^I = 0.306$ and $\lambda_c^{II} = 0.515$).

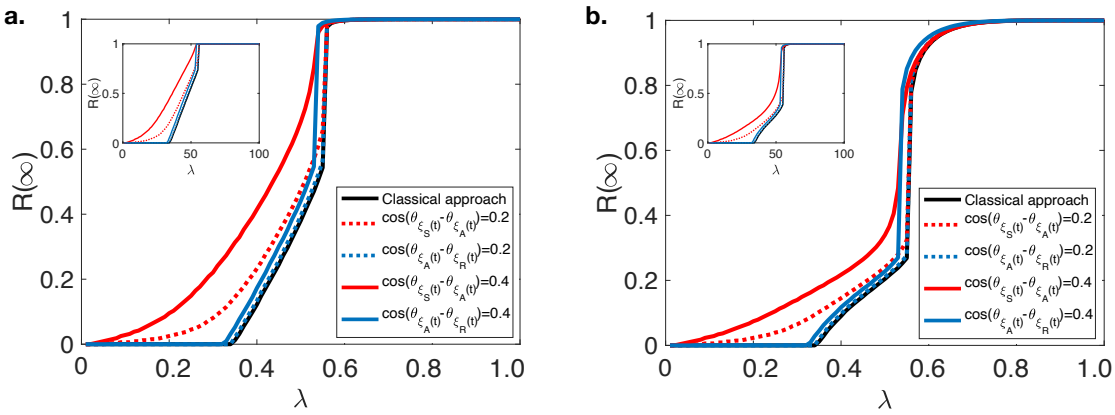


Figure 6.3: The final information adoption size $R(\infty)$ versus $\lambda$ with classical (black solid line), various $cos(\theta_{\xi_S(t)} - \theta_{\xi_A(t)}) = 0.2$ and 0.4 (red dash and solid lines) and $cos(\theta_{\xi_A(t)} - \theta_{\xi_R(t)}) = 0.2$ and 0.4 (blue dash and solid lines) when a. $T_b = 2$ and b.$T_b = 4$ on random regular networks ($\langle k \rangle = 10$ and $p = 0.3$). Subplots show the same simulations when $\langle k \rangle = 15$.

Figure 6.3 shows $R(\infty)$ versus $\lambda$ by using classical approach and varying strength of SA and AR interference terms in Equation 5.10 when $T_b = 2$ (Figure 6.3a) and $T_b = 4$ (Figure 6.3b). As we mentioned, classical approaches show a hybrid phase transition in both cases. This hybrid phase transition pattern is also observed when only AR interference exists; however, a second-order (continuous) phase transition is observed in the existence of SA interference. We observed the similar pattern until $T_b \geq 6$ only, since after this level the fraction of individuals who have lower adoption threshold were not enough to persuade individuals who have higher adoption threshold in the system. Furthermore, the phase transition becomes continuous even in the classical approach also when $T_b = 1$, since the model reduces to the traditional SAR model [2]. The mini subplots on the left-top corner of each figure shows same dynamics when mean-degree ($\langle k \rangle$) of RNN is increased, and same conclusions are observed. Therefore, we can conclude that our results are

robust to the changes in $\langle k \rangle$ of RNNs.

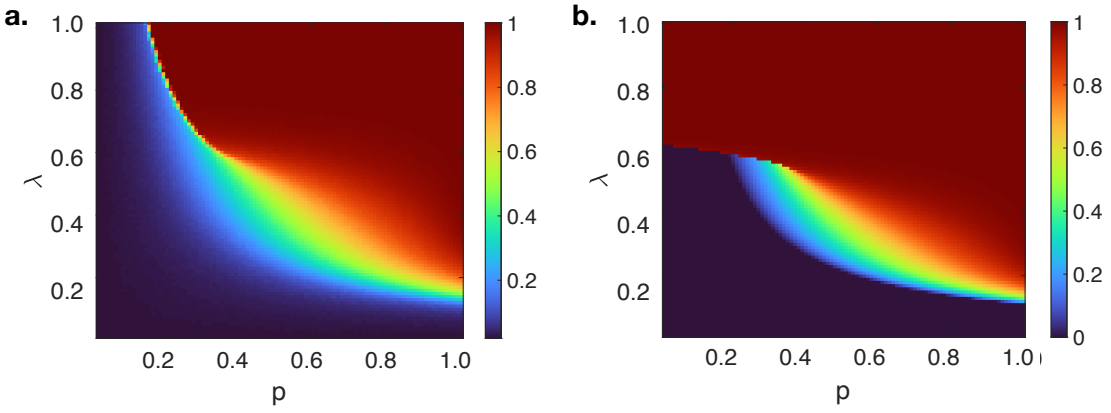


Figure 6.4: The dependence of $R(\infty)$ on $p$ and $\lambda$ on random regular networks with $\langle k \rangle = 10$ and $T_b = 4$ as a result of a. numerical simulations, b. theoretical analysis by using a classical approach.

For the comparison of performances of classical and quantum approaches in this study, extensive numerical simulations are performed on uncorrelated random regular networks (RRNs) with $N = 10,000$, $\langle k \rangle = 10$ and $\gamma = 1.0$. Figure 6.4 shows the fraction of adopted individuals with varying behavioral information transmission probability ($\lambda$) and initial fraction of adopted individuals ($p$). The theoretical solutions of $R(\infty)$ described in Figure 6.2 can be seen at $\lambda p$ plane more clearly. A first continuous, then a discontinuous increase in $R(\infty)$ shows a hybrid phase transition. This crossover phenomena in the increase of $R(\infty)$ with respect to $p$ separates the $\lambda p$ plane into three different regions: i) region I ($p \leq 0.15$), only negligibly small fraction of individuals adopt the information (local information adoption), ii) region II with a first-order phase transition ($0.15 < p \leq 0.42$), a definite fraction of individuals adopt the information above $\lambda_c^I$, iii) region III with a second order phase transition ($p > 0.42$), a global adoption is observed above $\lambda_c^I$. On the other hand, a theoretical analysis by using a classical approach fails to model spreading mechanism in region I when $p$ is small, because $\theta(\infty)$ is observed to be equal to 1 until a fixed value although it has gradually decreasing pattern in numerical simulations. This results with an overestimation

of final adoption size in this region. Moreover, a smooth transitions of $R(\infty)$ on the $\lambda p$ plane in region II in numerical simulations are also modeled with a redundant sharp transitions in the classical approach.

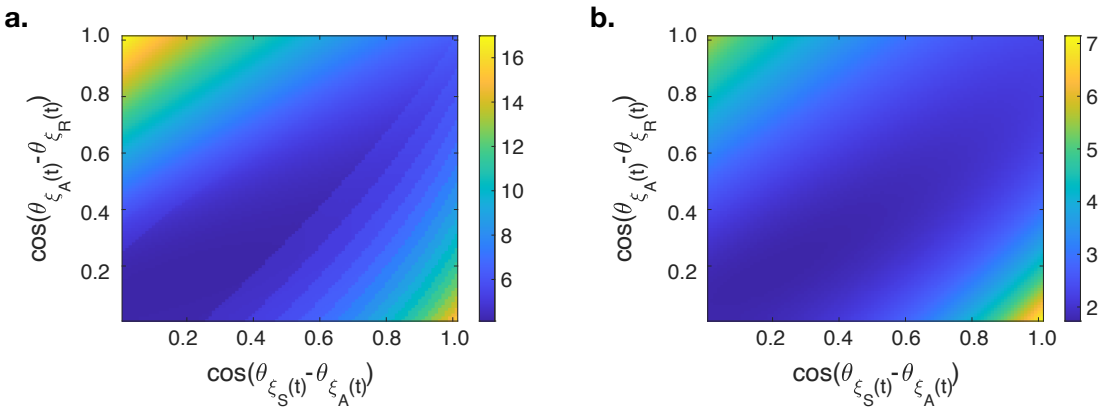


Figure 6.5: The dependence of error between $R(\infty)$ numerical simulations and theoretical analysis by using a quantum-like approach on $cos(\theta_{\xi_S(t)} - \theta_{\xi_A(t)})$ and $cos(\theta_{\xi_A(t)} - \theta_{\xi_R(t)})$ interference terms when a. $p = 0.3$, b. $p = 0.6$.

The squared difference of $R(\infty)$ versus $\lambda$ from 0.01 to 1.00 (0.01 increments) between results obtained via theoretical analysis and numerical simulations using a quantum-like approach with varying interference terms are shown in Figure 6.5. The origin point represents the squared error when classical approach is used since both interference terms are equal to zero ($e^2_{p=0.3} = 4.1707$ and $e^2_{p=0.6} = 1.7643$). Regardless of the initial fraction of adopted individuals ($p$), the minimum errors are observed near to the diagonal of interference terms plane, and the minimum value is obtained when $cos(\theta_{\xi_S(t)} - \theta_{\xi_A(t)}) = 0.15$ and $cos(\theta_{\xi_A(t)} - \theta_{\xi_R(t)}) = 0.16$ ($e^2_{p=0.3} = 4.1229$ and $e^2_{p=0.6} = 1.7326$). These results demonstrate that quantum-like approach in edge-based compartmental model of message passing approach in the modeling of social contagion performs better compared to the classical method since it can better predict the final adoption size at close to the critical transmission probabilities.

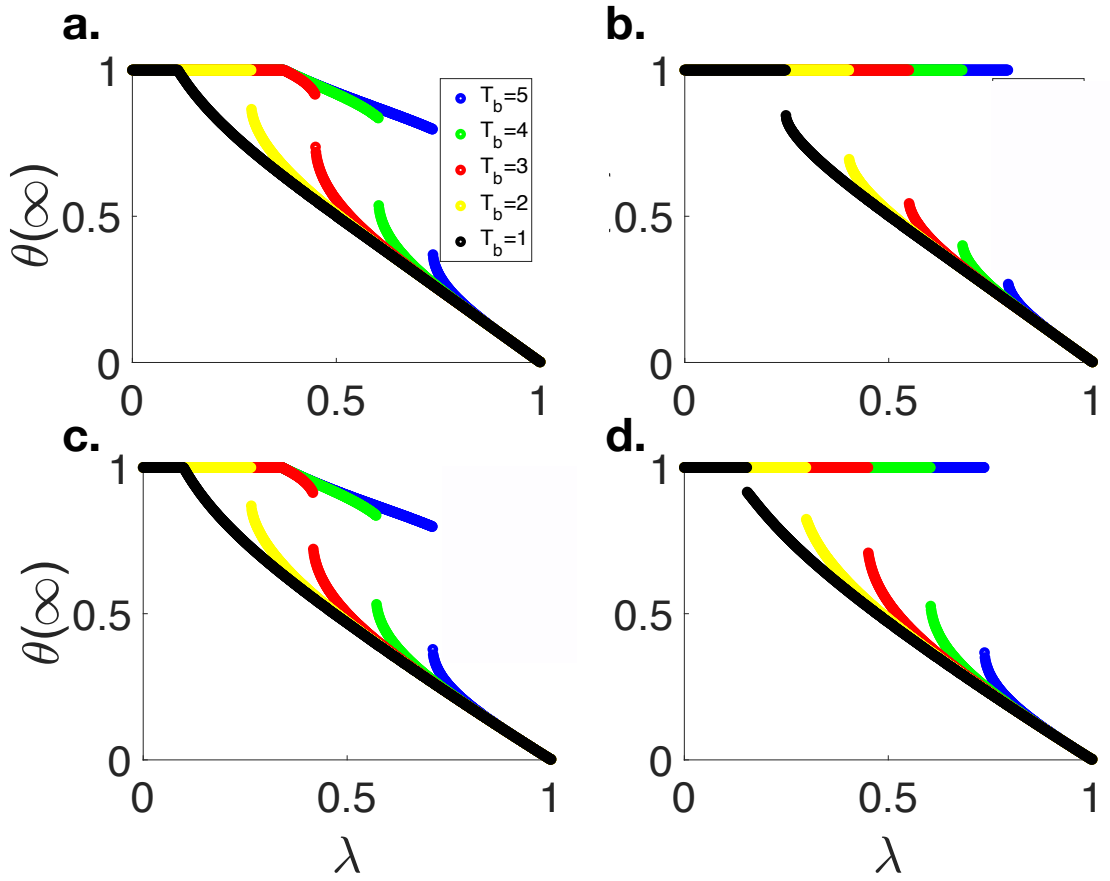


Figure 6.6: The physically meaningful solutions of fixed point of equation $d\theta(t)/dt$ at steady-state for each possible $\lambda$ values on random regular networks ($\langle k \rangle = 10$ and $p = 0.3$) with varying $T_b$ when a. $cos(\theta_{\xi_S(t)} - \theta_{\xi_A(t)}) = 0$ and $cos(\theta_{\xi_A(t)} - \theta_{\xi_R(t)}) = 0$, b. $cos(\theta_{\xi_S(t)} - \theta_{\xi_A(t)}) = 0.5$ and $cos(\theta_{\xi_A(t)} - \theta_{\xi_R(t)}) = 0$, c. $cos(\theta_{\xi_S(t)} - \theta_{\xi_A(t)}) = 0$ and $cos(\theta_{\xi_A(t)} - \theta_{\xi_R(t)}) = 0.5$, d. $cos(\theta_{\xi_S(t)} - \theta_{\xi_A(t)}) = 0.5$ and $cos(\theta_{\xi_A(t)} - \theta_{\xi_R(t)}) = 0.5$

In the comparison of phase transitions in social contagion dynamics when classical and quantum approaches are utilized, we first observed the case in which individuals have homogeneous adoption threshold values. Here, we observed that the final adoption size $R(\infty)$ grows continuously with the increasing $\lambda$ in the utilization of classical approach. Whereas, SA interference term in the quantum approach makes the pattern discontinuous and $R(\infty)$ increases discontinuously with the

increasing $\lambda$ and jump to another point at critical transmission probability. In the existence of AR interference term, on the other hand, same continuous change pattern is observed as in classical social contagion; however, at lower critical transmission probability. In the case of heterogeneous adoption threshold, $\theta(\infty)$ decreases continuously and a continuous phase transition observed at the first critical transmission probability, then another discontinuous change occurs at the second critical transmission probability even in the classical approach. It means that, $R(\infty)$ first increases continuously and then a discontinuous pattern is observed, which is called as hybrid phase transition.

Table 6.1: Critical Transmission Probabilities ($\lambda_c^I(\lambda_c^{II})$) of Social Contagion on Random Regular Networks ($\langle k \rangle = 10$ and $p = 0.3$) With Varying $T_b$

| | $T_b = 1$ | $T_b = 2$ | $T_b = 3$ | $T_b = 4$ | $T_b = 5$ |
|---|---|---|---|---|---|
| $cos(\theta_{\xi_S(t)} - \theta_{\xi_A(t)}) = 0$<br>$cos(\theta_{\xi_A(t)} - \theta_{\xi_R(t)}) = 0$ | 0.113 | 0.293 | 0.373 (0.450) | 0.373 (0.605) | 0.373 (0.737) |
| $cos(\theta_{\xi_S(t)} - \theta_{\xi_A(t)}) = 0.5$<br>$cos(\theta_{\xi_A(t)} - \theta_{\xi_R(t)}) = 0$ | 0.249 | 0.404 | 0.551 | 0.682 | 0.794 |
| $cos(\theta_{\xi_S(t)} - \theta_{\xi_A(t)}) = 0$<br>$cos(\theta_{\xi_A(t)} - \theta_{\xi_R(t)}) = 0.5$ | 0.100 | 0.266 | 0.343 (0.419) | 0.343 (0.573) | 0.343 (0.711) |
| $cos(\theta_{\xi_S(t)} - \theta_{\xi_A(t)}) = 0.5$<br>$cos(\theta_{\xi_A(t)} - \theta_{\xi_R(t)}) = 0.5$ | 0.155 | 0.300 | 0.452 | 0.605 | 0.737 |

To understand the dependence of phase transitions in a social contagion process with quantum decision makers, we have plotted the physically meaningful solutions of fixed point of equation $d\theta(t)/dt$ at steady-state for each possible $\lambda$ values on random regular networks ($\langle k \rangle = 10$ and $p = 0.3$) with varying $T_b$ in 6.6. Critical transmission probabilities for each $T_b$ are also recorded in Table 6.1. Figure 6.6a shows the case in which classical approach is utilized. In the case of homogeneous adoption threshold, a continuous phase transition exists ($T_b = 1$ shown with a black line). When the difference between threshold values are relatively lower between two groups ($T_b = 2$ shown in yellow line), e.g., a group who has a low and high threshold values, only a discontinuous phase transition is observed. In higher threshold values ($T_b \geq 2$), on the other hand,

a hybrid phase transition occurred. When there is only SA interference in the quantum-like social contagion model, a discontinuous phase transition is observed regardless of the threshold value (Figure 6.6b). However, the existence of only AR interference term in the quantum-like social contagion model exhibits same phase transition patterns with that of classical model, - only a small changes in the critical transmission probability values are observed (Table 6.6). The existence of both interference terms prevented the hybrid phase transition in the classical model and only a discontinuous phase transition is observed.

The Variability of The Social Contagion Dynamics With Changing Network Properties

The previous section showed the physically meaningful solutions of fixed point of equation $d\theta(t)/dt$ at steady-state for each possible $\lambda$ values on random regular networks ($\langle k \rangle = 10$ and $p = 0.3$) with varying $T_b$ in Figure 6.6. We have repeated same experiments to understand the effect of initial probability $p$ and the mean-degree $\langle k \rangle$ in this section. Therefore, Figure 6.7 shows the results when there is no interference term (6.7a), only SA interference term (6.7b), only AR interference term (6.7c) and when both interference exist (6.7d) when $\langle k \rangle$ is increased from 10 to 15. The critical transmission probabilities observed in these analyses are also written in Table 6.2.

Table 6.2: Critical Transmission Probabilities ($\lambda_c^I(\lambda_c^{II})$) of Social Contagion on Random Regular Networks ($\langle k \rangle = 15$ and $p = 0.3$) With Varying $T_b$

| | $T_b = 1$ | $T_b = 2$ | $T_b = 3$ | $T_b = 4$ | $T_b = 5$ |
|---|---|---|---|---|---|
| $cos(\theta_{\xi_S(t)} - \theta_{\xi_A(t)}) = 0$<br>$cos(\theta_{\xi_A(t)} - \theta_{\xi_R(t)}) = 0$ | 0.073 | 0.190 | 0.241 (0.291) | 0.241 (0.398) | 0.241 (0.497) |
| $cos(\theta_{\xi_S(t)} - \theta_{\xi_A(t)}) = 0.5$<br>$cos(\theta_{\xi_A(t)} - \theta_{\xi_R(t)}) = 0$ | 0.166 | 0.271 | 0.374 | 0.470 | 0.559 |
| $cos(\theta_{\xi_S(t)} - \theta_{\xi_A(t)}) = 0$<br>$cos(\theta_{\xi_A(t)} - \theta_{\xi_R(t)}) = 0.5$ | 0.065 | 0.171 | 0.218 (0.265) | 0.218 (0.366) | 0.218 (0.463) |
| $cos(\theta_{\xi_S(t)} - \theta_{\xi_A(t)}) = 0.5$<br>$cos(\theta_{\xi_A(t)} - \theta_{\xi_R(t)}) = 0.5$ | 0.101 | 0.195 | 0.294 | 0.398 | 0.496 |

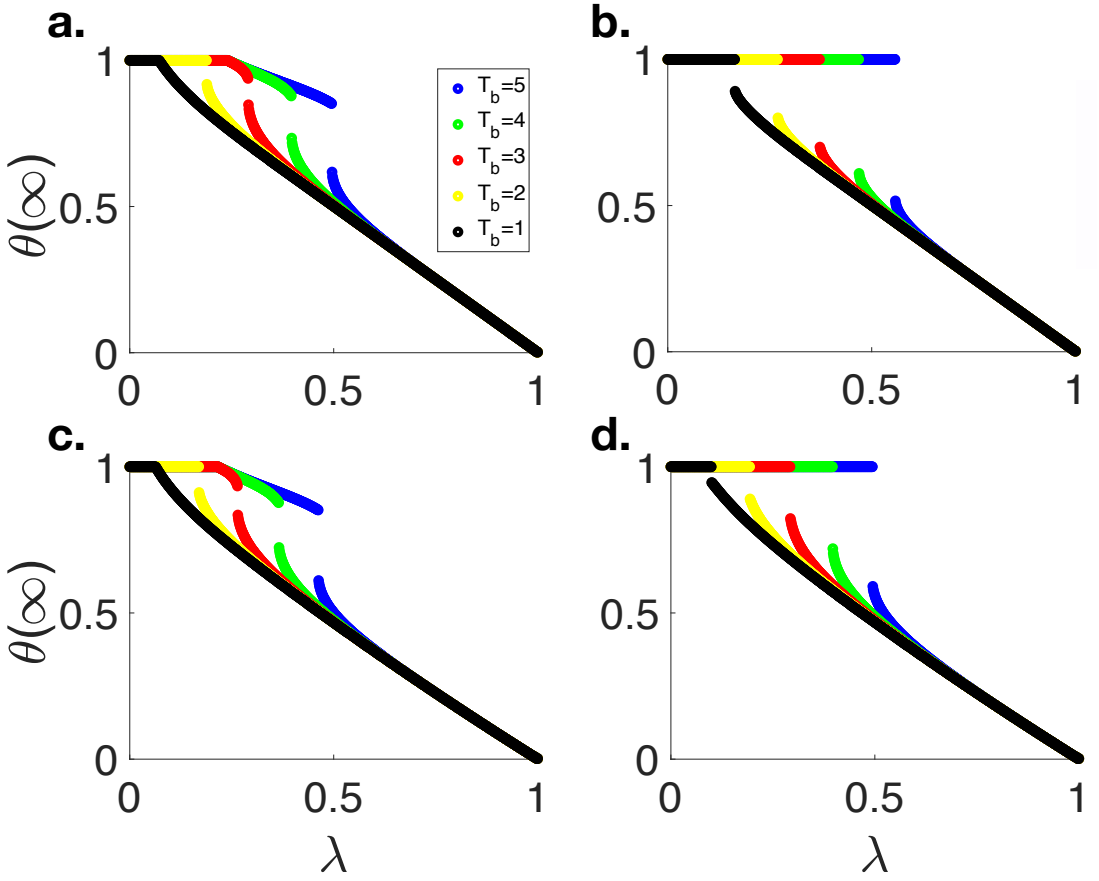


Figure 6.7: The physically meaningful solutions of fixed point of equation $d\theta(t)/dt$ at steady-state for each possible $\lambda$ values on random regular networks ($\langle k \rangle = 15$ and $p = 0.3$) with varying $T_b$ when a. $cos(\theta_{\xi_S(t)} - \theta_{\xi_A(t)}) = 0$ and $cos(\theta_{\xi_A(t)} - \theta_{\xi_R(t)}) = 0$, b. $cos(\theta_{\xi_S(t)} - \theta_{\xi_A(t)}) = 0.5$ and $cos(\theta_{\xi_A(t)} - \theta_{\xi_R(t)}) = 0$, c. $cos(\theta_{\xi_S(t)} - \theta_{\xi_A(t)}) = 0$ and $cos(\theta_{\xi_A(t)} - \theta_{\xi_R(t)}) = 0.5$, d. $cos(\theta_{\xi_S(t)} - \theta_{\xi_A(t)}) = 0.5$ and $cos(\theta_{\xi_A(t)} - \theta_{\xi_R(t)}) = 0.5$

Results demonstrated that phase transition do not depend on the mean-degree and same types of phase transitions are observed. Whereas, critical transmission probabilities are affected with the changing mean degree of random regular networks. Increasing mean degree unexpectedly lowered the critical transmission probabilities, since increasing connectivity between individuals will increase the likelihood of global adoption.

Later, we showed the physically meaningful solutions of fixed point of equation $d\theta(t)/dt$ at steady-

state for each possible $\lambda$ values on random regular networks ($\langle k \rangle = 15$ and $p = 0.6$) with varying $T_b$ in Figure 6.8 and the critical transmission probabilities are also given in Table 6.3.

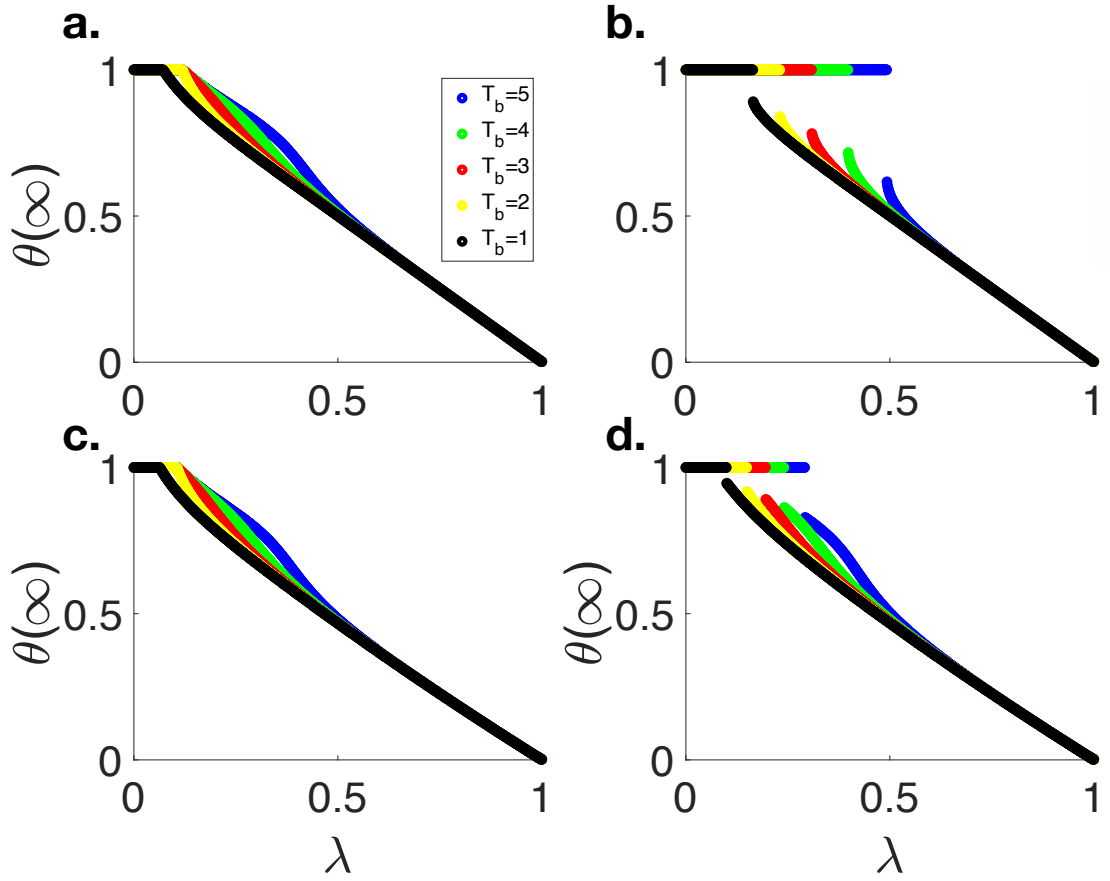


Figure 6.8: The physically meaningful solutions of fixed point of equation $d\theta(t)/dt$ at steady-state for each possible $\lambda$ values on random regular networks ($\langle k \rangle = 15$ and $p = 0.6$) with varying $T_b$ when a. $cos(\theta_{\xi_S(t)} - \theta_{\xi_A(t)}) = 0$ and $cos(\theta_{\xi_A(t)} - \theta_{\xi_R(t)}) = 0$, b. $cos(\theta_{\xi_S(t)} - \theta_{\xi_A(t)}) = 0.5$ and $cos(\theta_{\xi_A(t)} - \theta_{\xi_R(t)}) = 0$, c. $cos(\theta_{\xi_S(t)} - \theta_{\xi_A(t)}) = 0$ and $cos(\theta_{\xi_A(t)} - \theta_{\xi_R(t)}) = 0.5$, d. $cos(\theta_{\xi_S(t)} - \theta_{\xi_A(t)}) = 0.5$ and $cos(\theta_{\xi_A(t)} - \theta_{\xi_R(t)}) = 0.5$

Here, results show that increasing initial probability extinguished the hybrid phase transitions, i.e. one single critical transmission probability is observed in every cases. Regardless of $T_b$, a continuous phase transition is observed when the classical approach is utilized (Figure 6.8a) or there is only AR interference exist in the quantum social contagion (Figure 6.8c). The existence

of SA interference term, on the other, triggers a discontinuous phase transition in quantum social contagion (Figure 6.8b and Figure 6.8c).

Table 6.3: Critical Transmission Probabilities ($\lambda_c^I(\lambda_c^{II})$) of Social Contagion on Random Regular Networks ($\langle k \rangle = 15$ and $p = 0.6$) With Varying $T_b$

| | $T_b = 1$ | $T_b = 2$ | $T_b = 3$ | $T_b = 4$ | $T_b = 5$ |
|---|---|---|---|---|---|
| $cos(\theta_{\xi_S(t)} - \theta_{\xi_A(t)}) = 0$<br>$cos(\theta_{\xi_A(t)} - \theta_{\xi_R(t)}) = 0$ | 0.073 | 0.121 | 0.121 | 0.121 | 0.121 |
| $cos(\theta_{\xi_S(t)} - \theta_{\xi_A(t)}) = 0.5$<br>$cos(\theta_{\xi_A(t)} - \theta_{\xi_R(t)}) = 0$ | 0.166 | 0.232 | 0.310 | 0.399 | 0.494 |
| $cos(\theta_{\xi_S(t)} - \theta_{\xi_A(t)}) = 0$<br>$cos(\theta_{\xi_A(t)} - \theta_{\xi_R(t)}) = 0.5$ | 0.065 | 0.108 | 0.108 | 0.108 | 0.108 |
| $cos(\theta_{\xi_S(t)} - \theta_{\xi_A(t)}) = 0.5$<br>$cos(\theta_{\xi_A(t)} - \theta_{\xi_R(t)}) = 0.5$ | 0.101 | 0.151 | 0.197 | 0.242 | 0.293 |

Belief Entropy as a Heuristic

Figure 6.5 shows the dependence of error between $R(\infty)$ numerical simulations and theoretical analysis by using a quantum-like approach on SA ($cos(\theta_{\xi_S(t)} - \theta_{\xi_A(t)})$) and AR ($cos(\theta_{\xi_A(t)} - \theta_{\xi_R(t)})$) interference terms on different initial probabilities $p$. Each data pint on heat map figures are calculated by taking the squared difference of $R(\infty)$ versus $\lambda$ from 0.01 to 1.00 (0.01 increments) between results obtained via theoretical analysis and numerical simulations using a quantum-like approach. Since the origin points represents when both interference terms are equal to zero, the error degenerates to the one between numerical simulations and the theoretical analysis when classical approach is used ($e^2_{p=0.3} = 4.1707$ and $e^2_{p=0.6} = 1.7643$). Since smaller error values are obtained when $cos(\theta_{\xi_S(t)} - \theta_{\xi_A(t)}) = 0.15$ and $cos(\theta_{\xi_A(t)} - \theta_{\xi_R(t)}) = 0.16$ ($e^2_{p=0.3} = 4.1229$ and $e^2_{p=0.6} = 1.7326$), we can easily argue that quantum-like approach in edge-based compartmental model of message passing approach in the modeling of social contagion performs better compared to the classical method since it can better predict the final adoption size at close to the critical

transmission probabilities.

Furthermore, we observed that the optimum value for both interference terms are obtained when $cos(\theta_{\xi_S(t)} - \theta_{\xi_A(t)}) = 0.15$ and $cos(\theta_{\xi_A(t)} - \theta_{\xi_R(t)}) = 0.16$ regardless of the changing initial probability. Using belief entropy in Equation 5.22 when $t \to \infty$ gives results of $cos(\theta_{\xi_S(t)} - \theta_{\xi_A(t)}) = 0.15$ and $cos(\theta_{\xi_A(t)} - \theta_{\xi_R(t)}) = 0.17$ which shows that our proposed method can be used in the prediction of interference terms in quantum-like social contagion.

## Quantum-Like Analysis of Interactive Social Contagions

In the previous section, we have performed extensive numerical simulations on uncorrelated random regular networks (RRNs) with $N = 10,000$, $\langle k \rangle = 10$ and $\gamma = 1.0$ for the comparison of performances of classical and quantum approaches in this study. We have demonstrated that a hybrid phase transition is observed and the crossover phenomena in the increase of $R(\infty)$ with respect to $p$ separates the $\lambda\, p$ plane into three different regions: i) region I: only negligibly small fraction of individuals adopt the information (local information adoption), ii) region II with a first-order phase transition: a definite fraction of individuals adopt the information, iii) region III with a second order phase transition, a global adoption is observed.

In this section, on the other hand, we examined the effect of the spread of behavior 1 $b_1$ on adoption of behavior 2 $b_2$ and what kind of phase transitions are observed on the same network. In these analyses, four different adoption regions are observed: i) Region I (orange colored): Both $b_1$ and $b_2$ are adopted by only negligibly small fraction of individuals, ii) Region II (brown colored): While a definite fraction of individuals adopt $b_1$, a negligibly small fraction of individuals adopted $b_2$, iii) Region III (light orange colored): While a definite fraction of individuals adopt $b_2$, a negligibly small fraction of individuals adopted $b_1$, iv) Region IV (black colored): A global adoption is

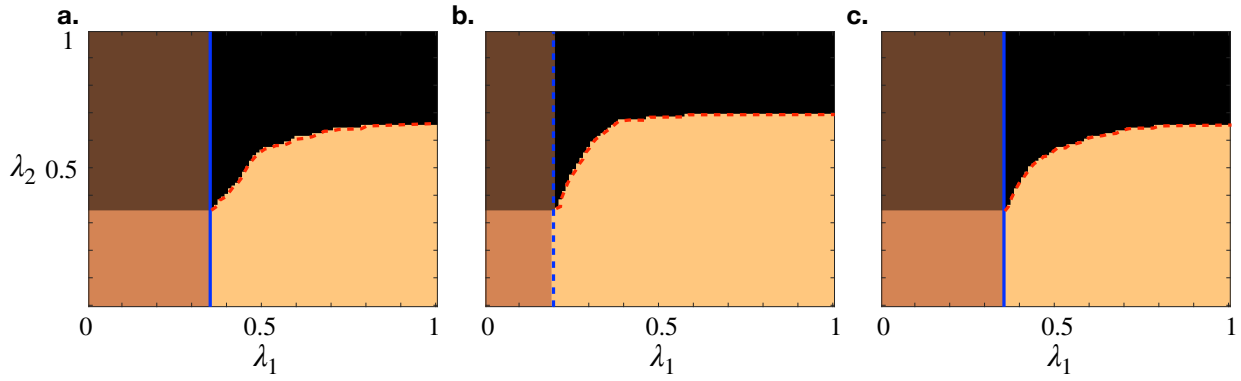


Figure 6.9: The phase diagram of the system that shows the impact of $b_1$ on the spread of $b_2$ on random regular networks with $\langle k \rangle = 10$ a. with numerical simulations, b. theoretical analysis by using a classical approach, c) theoretical analysis by using a quantum-like approach with $cos(\theta_{\xi_S(t)} - \theta_{\xi_A(t)}) = 0.16$ and $cos(\theta_{\xi_A(t)} - \theta_{\xi_R(t)}) = 0.15$ interference terms. Orange and black colored areas represent no behaviors adopted and two behaviors are widely adopted in these regions, respectively. Brown and light orange colored regions, respectively, represent only $b_1$ and only $b_2$, widely adopted. The blue and red lines represent the discontinuous critical information transmission rate $\lambda_{1c}^I$ of $b_1$ and critical information transmission rate $\lambda_{2c}^I$ of $b_2$.

observed for both $b_1$ and $b_2$. Figure 6.9.a shows that $R_1(\infty)$ discontinuously increases with $\lambda_2$ and displays an abrupt behavior with increasing above $\lambda_{1c}^I = 0.351$ when $\tau_1 = 0.3$. Although $R_2(\infty)$ discontinuously increases with $\lambda_2$ when $\tau_1 = 0.3$, no breakdown is observed in the spread of $b_1$. Liu et al. [162] explained this situation as follows: When the $b_1$ outbreak occurs, the probability of an individual adopted $b_1$ for each $b_2$ decreases; susceptible nodes have to have more $b_2$ to adopt the behavior, and so more nodes remain in a sub-critical state. Therefore, increasing $\lambda_1$ above $\lambda_{1c}^I = 0.351$ triggers $R_2(\infty)$ increase with more abruptly and outbreak information threshold $\lambda_{2c}^I$ of $b_2$.

When we define the results obtained with numerical simulations on RNNs as ground truth, we can easily compare and contrast the efficiency and accuracy of edge-based compartmental theoretical analysis by using a classical approach and a quantum-like approach. As aforementioned above, there are mainly four regions to describe the adoption behavior of two behavior: Region I is where

there is no outbreak (or global adoption) of either $b_1$ or $b_2$ when $\lambda_1^I < \lambda_{1c}^I$ and $\lambda_1^I < \lambda_{2c}^I$, while Region IV refers shows the 2D plane when there is outbreak (global adoption) for both $b_1$ or $b_2$ when $\lambda_1^I \geq \lambda_{1c}^I$ and $\lambda_1^I \geq \lambda_{2c}^I$. Although a quantum-like approach in Figure 6.9.c is able to compute these critical points, the use of a classical approach will underestimate the size of Region I and overestimate that of Region IV. These results demonstrated that quantum-like generalization of social contagion is able to model the co-diffusion of two synergistic behavior on a single network and yield better results compared to classical approach.

# CHAPTER 7: CONCLUSION AND FUTURE PLANS

The spread of ideas, attitudes or behavioral patterns among a group of individuals is called social contagion. Although this spread among individuals used to be regarded as a pathogen in a biological spreading, empirical studies demonstrated that social contagion is far more complex due to the social, cognitive, and behavioral differences of humans. The complexity of humans in a social contagion process is addressed by considering the heterogeneity of their adoption thresholds with the assumption of perfect rationality; however, numerous empirical studies demonstrate that humans violate the rules of classical probability while making decisions. In order to improve the modeling of human decision-making about the adoption of information and/or behavior, we employed a quantum-like approach in social contagion analysis as well as assigning individuals heterogeneous adoption thresholds. We believe that our method, so-called quantum contagion, is able to portray the complexity of individuals and better model a social contagion process. We integrate Inverse Born Problem (IBP) to represent classical probabilistic entities as complex probability amplitudes in a quantum-like message-passing approach. An edge-based compartmental theory is used to quantify the classical and quantum-theoretical models, and a large number of simulations on RRNs are carried out for the comparison of their performances. In this study, we have conducted several experiments to investigate i) the superiority of quantum-like approaches compared to classical ones in the existence of both homogeneous and heterogeneous agents, ii) the types of phase transitions in the final spreading size versus transmission probability when agents are modeled as quantum decision-makers, iii) the variability of the social contagion dynamics with changing network properties, iv) the efficiency of belief entropy measure as an alternative to the extant heuristics in the definition of interference terms in quantum-like social contagion model, v) the quantum social contagion dynamics when there are interactive social contagions on complex networks.

First, we examined the phase transitions in social contagion dynamics when adoption thresholds of individuals are homogeneous and heterogeneous separately. Later, we have conducted similar experiments when individuals are modeled as quantum decision-makers. For the analysis of heterogeneity in their adoption thresholds, we employed a two-state spreading threshold model in which individuals have a relatively low threshold ($T_A = 1$) with probability $p$, and a relatively high threshold ($T_B > 1$) with probability $1 - p$. The effect of threshold heterogeneity with varying network properties has been already investigated in previous studies. These studies showed that two different types of information adoption occur in the existence of more than one critical transmission probability: local and global adoption. The local adoption is observed when $\lambda < \lambda_c^I$ and information is adopted by a small fraction of individuals who has a lower adoption threshold. Whereas, the global adoption occurs when $\lambda > \lambda_c^{II}$ and information is adopted by a finite fraction of individuals. In the case of $\lambda_c^I < \lambda < \lambda_c^{II}$, individuals who have lower thresholds adopt behavior globally while individuals who have higher thresholds adopt behavior locally. Although edge-based compartmental theory can model social contagion dynamics in most cases, these analyses fall short when transmission rates are close to these critical transmission probabilities. In the classical social contagion model, the final adoption size ($R(\infty)$) grows discontinuously with the increasing behavioral information transmission probability ($\lambda$). Numerical investigations carried out on RRNs show that the quantum social contagion model performs better than the extant classical social contagion model since it is able to model the dynamics near the critical transmission probabilities. The quantum social contagion model displays the same hybrid phase transition pattern; however, both phase transitions are observed at lower critical transmission probability values. It means that local and global adoption behavior in the two-state spreading threshold model is observed earlier than the classical approach. The sharp discontinuous changes in final adoption size near the critical transmission probabilities are also observed smoother in the quantum approach. Testing our conclusions on different mean degrees of RNN and with a different initial fraction of adopted individuals also demonstrates the generalizability and robustness of our conclusions. The

optimum SA and AR interference values remain the same, as the initial fraction of adopted individuals changes. Thus, we argue that interference in quantum social contagion is not dependent on the initial fraction of adopted individuals on the network.

Second, we have carried out quantum social contagion experiments with changing mean degree $\langle k \rangle$ and initial probability $p$ of RNN. Based on the results, increasing initial probability caused hybrid phase transitions to be extinguished, meaning that only one critical transmission probability was observed in all cases. Regardless of $T_b$, a continuous phase transition is observed when the classical approach is utilized or there is only AR interference exist in the quantum social contagion. The existence of SA interference term, on the other, yielded a discontinuous phase transition in quantum social contagion. When it comes to the effect of mean degree of RNN on the social contagion dynamics, we observed that that phase transition do not depend on the mean-degree and same types of phase transitions are observed. Whereas, critical transmission probabilities are affected with the changing mean degree of random regular networks. Increasing mean degree unexpectedly lowered the critical transmission probabilities, since increasing connectivity between individuals will increase the likelihood of global adoption.

Although quantum-like generalization of social contagion models are able to portray the complexity of individuals and better model a social contagion process, the interference term brings an additional complexity that decreases the time-efficiency of these models. Additionally, this effect can be determined only by calibration with a real dataset, causing its application to become harder. Therefore, third, we have proposed a new heuristic approach based on belief entropy in the calculation of interference term that quantum social model includes. To test the effectiveness of the proposed approach, we have performed extensive numerical simulations on uncorrelated random regular networks (RRNs) and concluded that belief entropy can be used to compute the interference effect in the quantum-like generalization of social contagion models. We believe that these results will increase the use of quantum social contagion models in any application area without

having a concern of calibration or time complexity.

The purpose of this study is to better model the real-life social contagion dynamics to shed light on the control of viral disease, microfinance activities, false information, harmful emotions, and technology adoptions. Actually, the co-evolutionary dynamics of spreading mechanisms play an important role in the explanation of these real-world phenomena. The simultaneous evolution of different contagions at the same network may alter social contagion dynamics, and we may observe significant differences in different successive or competitive social contagions. Thus, lastly, we have initiated an analysis to compare classical and quantum-like social contagion models when there are two behavior successively spread in a single network. In this case, we have observed four regions to describe the adoption behavior of two behavior: Region I: when there is no outbreak (or global adoption) of either $b_1$ or $b_2$ when $\lambda_1^I < \lambda_{1c}^I$ and $\lambda_2^I < \lambda_{2c}^I$, Region II: when $b_1$ is globally adopted while $b_2$ is locally adopted as $\lambda_1^I \geq \lambda_{1c}^I$ and $\lambda_2^I < \lambda_{2c}^I$, Region III: when $b_2$ is globally adopted while $b_1$ is locally adopted as $\lambda_1^I < \lambda_{1c}^I$ and $\lambda_2^I \geq \lambda_{2c}^I$, and Region IV: when both $b_1$ and $b_2$ are globally adopted with $\lambda_1^I \geq \lambda_{1c}^I$ and $\lambda_2^I \geq \lambda_{2c}^I$. Comparing critical points obtained via theoretical analysis using classical and quantum-like approach demonstrated that quantum-like generalization of social contagion is able to model the co-diffusion of two synergistic behavior on a single network and yield better results compared to classical approach.

Although this study aims to propose a novel theoretical approach to the problem of social contagion dynamics, it can also portray useful insights for many applications since outcomes help us to better understand the real-world social contagion dynamics. One of the most appealing application areas related to social contagion is understanding the attributes and dynamics of information spread through intermediate users' set during this information exchange. Marketing companies or political campaigns may use these insights to better reach out to the certain amount of people. Additionally, although these models are called information diffusion models, these methods and the outcomes of this study can be used to model abstract values' contagiousness such as emotions or sentiments.

Thus, we can list another common application of information diffusion models on online social networks as sentiment (emotion) spreading. Furthermore, another important application area of social contagion models is the influence maximization problem, which can be defined as "the problem of finding a small set of seed nodes in a social network that maximizes the spread of influence under certain influence cascade models". These application areas can be expanded for other applications.

Future studies may aim to integrate quantum-like generalization of social contagion model on not only successive but also competing behavior (or information) in the same network. Moreover, the co-evolution of multiple social contagions more than two remains open for further exploration. We intend to continue our analyses in these directions. It should be noted that, despite the quantum-like approach in edge-based compartmental theory bringing heterogeneity due to the entangled structure of complex amplitudes in $\lambda$, we assumed that each adopted node has an equal chance to transmit the behavior to his susceptible neighbors. Thus, we ignored the influence variety of specific nodes in the spreading mechanism. Researchers can integrate IBP to other high-performance theoretical approaches for epidemic spreading such as dynamical message passing and/or edge-based mean-field theory; however, these techniques yield very complex equations, and the quantum-like approach may exacerbate its complexity to make this problem even more challenging to resolve [163].

# APPENDIX A: CALCULATION OF $\xi_A(t)$ AND TIME EVOLUTION OF $\theta(t)$ IN CLASSICAL AND QUANTUM APPROACH

Inserting Eqs. 5.11 and 5.14 into Eq. 5.8 yields $\xi_A(t)$ by using the classical approach and gives the following expression:

$$\xi_A(t) = \theta(t) - \frac{\sum_{k_v} k_v P(k_v) s_v(k_v,t)}{\langle k \rangle} - \frac{\gamma(1-\lambda)[1-\theta(t)]}{\lambda} \tag{A.1}$$

Substituting Eq.A.1 in Eq. 5.12 gives us the time evolution of $\theta(t)$ as:

$$\frac{d\theta(t)}{dt} = -\lambda \left[ \theta(t) - \frac{\sum_{k_v} k_v P(k_v) s_v(k_v,t)}{\langle k \rangle} \right] - \gamma(1-\lambda)[1-\theta(t)] \tag{A.2}$$

In quantum counterpart of this calculation; however, is more complex due to the interference terms in 3.7. In this case, we insert Eqs. 5.11 and 5.14 into Eq. 5.10 to obtain $\xi_A(t)$ by using the quantum approach:

$$\begin{aligned} \theta(t) = {} & \frac{\sum_{k_v} k_v P(k_v) s_v(k_v,t)}{\langle k \rangle} + \xi_A(t) + \frac{\gamma(1-\lambda)[1-\theta(t)]}{\lambda} \\ & + \sqrt{\frac{\sum_{k_v} k_v P(k_v) s_v(k_v,t)}{\langle k \rangle} \xi_A(t)} cos(\theta_{\xi_S(t)} - \theta_{\xi_A(t)}) \\ & + \sqrt{\xi_A(t) \frac{\gamma(1-\lambda)[1-\theta(t)]}{\lambda}} cos(\theta_{\xi_A(t)} - \theta_{\xi_R(t)})\lambda) \end{aligned} \tag{A.3}$$

Solving this quadratic equation for $\xi_A(t)$ yields 4 different roots, the physically meaningful one is as follows:

$$\xi_A(t) = \frac{1}{2}\Bigg[cos^2(\theta_{\xi_S(t)} - \theta_{\xi_A(t)})\frac{\sum_{k_v} k_v P(k_v) s_v(k_v,t)}{\langle k\rangle} - \sqrt{\Bigg(cos^4(\theta_{\xi_S(t)} - \theta_{\xi_A(t)})\Bigg(\frac{\sum_{k_v} k_v P(k_v) s_v(k_v,t)}{\langle k\rangle}\Bigg)^2$$

$$- 4cos^3(\theta_{\xi_S(t)} - \theta_{\xi_A(t)})cos(\theta_{\xi_A(t)} - \theta_{\xi_R(t)})\Bigg(\frac{\sum_{k_v} k_v P(k_v) s_v(k_v,t)}{\langle k\rangle}\Bigg)^{(3/2)}\sqrt{\Bigg(\frac{\gamma(1-\lambda)[1-\theta(t)]}{\lambda}\Bigg)}$$

$$+ 6cos^2(\theta_{\xi_S(t)} - \theta_{\xi_A(t)})cos^2(\theta_{\xi_A(t)} - \theta_{\xi_R(t)})\frac{\sum_{k_v} k_v P(k_v) s_v(k_v,t)}{\langle k\rangle}\frac{\gamma(1-\lambda)[1-\theta(t)]}{\lambda}$$

$$+ 4cos^2(\theta_{\xi_S(t)} - \theta_{\xi_A(t)})\theta(t)\frac{\sum_{k_v} k_v P(k_v) s_v(k_v,t)}{\langle k\rangle} - 4cos^2(\theta_{\xi_S(t)} - \theta_{\xi_A(t)})\Bigg(\frac{\sum_{k_v} k_v P(k_v) s_v(k_v,t)}{\langle k\rangle}\Bigg)^2$$

$$- 4cos^2(\theta_{\xi_S(t)} - \theta_{\xi_A(t)})\frac{\sum_{k_v} k_v P(k_v) s_v(k_v,t)}{\langle k\rangle}\frac{\gamma(1-\lambda)[1-\theta(t)]}{\lambda}$$

$$- 4cos(\theta_{\xi_S(t)} - \theta_{\xi_A(t)})cos^3(\theta_{\xi_A(t)} - \theta_{\xi_R(t)})\sqrt{\Bigg(\frac{\sum_{k_v} k_v P(k_v) s_v(k_v,t)}{\langle k\rangle}\Bigg)}\Bigg(\frac{\gamma(1-\lambda)[1-\theta(t)]}{\lambda}\Bigg)^{(3/2)}$$

$$- 8cos(\theta_{\xi_S(t)} - \theta_{\xi_A(t)})cos(\theta_{\xi_A(t)} - \theta_{\xi_R(t)})\theta(t)\sqrt{\Bigg(\frac{\sum_{k_v} k_v P(k_v) s_v(k_v,t)}{\langle k\rangle}\Bigg)}\sqrt{\Bigg(\frac{\gamma(1-\lambda)[1-\theta(t)]}{\lambda}\Bigg)}$$

$$+ 8cos(\theta_{\xi_S(t)} - \theta_{\xi_A(t)})cos(\theta_{\xi_A(t)} - \theta_{\xi_R(t)})\Bigg(\frac{\sum_{k_v} k_v P(k_v) s_v(k_v,t)}{\langle k\rangle}\Bigg)^{(3/2)}\sqrt{\Bigg(\frac{\gamma(1-\lambda)[1-\theta(t)]}{\lambda}\Bigg)}$$

$$+ 8cos(\theta_{\xi_S(t)} - \theta_{\xi_A(t)})cos(\theta_{\xi_A(t)} - \theta_{\xi_R(t)})\sqrt{\Bigg(\frac{\sum_{k_v} k_v P(k_v) s_v(k_v,t)}{\langle k\rangle}\Bigg)}\Bigg(\frac{\gamma(1-\lambda)[1-\theta(t)]}{\lambda}\Bigg)^{(3/2)}$$

$$+ cos^4(\theta_{\xi_A(t)} - \theta_{\xi_R(t)})\Bigg(\frac{\gamma(1-\lambda)[1-\theta(t)]}{\lambda}\Bigg)^2 + 4cos(\theta_{\xi_A(t)} - \theta_{\xi_R(t)})\theta(t)\Bigg(\frac{\gamma(1-\lambda)[1-\theta(t)]}{\lambda}\Bigg)$$

$$- 4cos^2(\theta_{\xi_A(t)} - \theta_{\xi_R(t)})\Bigg(\frac{\sum_{k_v} k_v P(k_v) s_v(k_v,t)}{\langle k\rangle}\Bigg)\Bigg(\frac{\gamma(1-\lambda)[1-\theta(t)]}{\lambda}\Bigg)$$

$$- 4^2 cos(\theta_{\xi_A(t)} - \theta_{\xi_R(t)})\Bigg(\frac{\gamma(1-\lambda)[1-\theta(t)]}{\lambda}\Bigg)^2\Bigg)$$

$$- 2cos(\theta_{\xi_S(t)} - \theta_{\xi_A(t)})cos(\theta_{\xi_A(t)} - \theta_{\xi_R(t)})\sqrt{\Bigg(\frac{\sum_{k_v} k_v P(k_v) s_v(k_v,t)}{\langle k\rangle}\Bigg)}\sqrt{\Bigg(\frac{\gamma(1-\lambda)[1-\theta(t)]}{\lambda}\Bigg)}$$

$$+ cos^2(\theta_{\xi_A(t)} - \theta_{\xi_R(t)})\Bigg(\frac{\gamma(1-\lambda)[1-\theta(t)]}{\lambda}\Bigg) + 2\theta(t) - 2\Bigg(\frac{\sum_{k_v} k_v P(k_v) s_v(k_v,t)}{\langle k\rangle}\Bigg) - 2\Bigg(\frac{\gamma(1-\lambda)[1-\theta(t)]}{\lambda}\Bigg)\Bigg] \tag{A.4}$$

# APPENDIX B: COPYRIGHT PERMISSION TO REUSE A PUBLISHED CONTENT

MDPI Copyright Permission

The following statement is taken from `https://www.mdpi.com/authors/rights`.

For all articles published in MDPI journals, copyright is retained by the authors. Articles are licensed under an open access Creative Commons CC BY 4.0 license, meaning that anyone may download and read the paper for free. In addition, the article may be reused and quoted provided that the original published version is cited. These conditions allow for maximum use and exposure of the work, while ensuring that the authors receive proper credit.

This thesis includes some contents and figures from the paper titled "Quantum Contagion: A Quantum-Like Approach for the Analysis of Social Contagion Dynamics with Heterogeneous Adoption Thresholds" [146].

Springer Copyright Permission

The following statement is taken from https://www.springer.com/gp/rights-permissions/obtaining-permissions/882. Authors have the right to reuse their article's Version of Record, in whole or in part, in their own thesis. Additionally, they may reproduce and make available their thesis, including Springer Nature content, as required by their awarding academic institution. Authors must properly cite the published article in their thesis according to current citation standards.

This thesis includes some contents and figures from the paper titled "The Degree-dependent Threshold Model: Towards a Better Understanding of Opinion Dynamics on Online Social Networks." Conference of the Computational Social Science Society of the Americas. Springer, Cham, 2021." [82]

This thesis includes some contents and figures from the paper titled "Effects of Assortativity on Consensus Formation with Heterogeneous Agents" Conference of the Computational Social Science Society of the Americas. Springer, Cham, 2022." [120]

This thesis includes some contents and figures from the paper titled "A Quantum Leap for Fairness: Quantum Bayesian Approach for Fair Decision Making. In International Conference on Human-Computer Interaction (pp. 489-499). Springer, Cham." [146]

# LIST OF REFERENCES


[1] Sara Levens, Omar ElTayeby, Tiffany Gallicano, Michael Brunswick, and Samira Shaikh. Using information processing strategies to predict message level contagion in social media. In *International Conference on Applied Human Factors and Ergonomics*, pages 3–13. Springer, 2019.

[2] Romualdo Pastor-Satorras, Claudio Castellano, Piet Van Mieghem, and Alessandro Vespignani. Epidemic processes in complex networks. *Reviews of modern physics*, 87(3):925, 2015.

[3] Duncan J Watts. A simple model of global cascades on random networks. *Proceedings of the National Academy of Sciences*, 99(9):5766–5771, 2002.

[4] Wei Wang, Ming Tang, Panpan Shu, and Zhen Wang. Dynamics of social contagions with heterogeneous adoption thresholds: crossover phenomena in phase transition. *New Journal of Physics*, 18(1):013029, 2016.

[5] Kerk F Kee. Adoption and diffusion. *The international encyclopedia of organizational communication*, pages 1–14, 2017.

[6] Mark Granovetter. Threshold models of collective behavior. *American journal of sociology*, 83(6):1420–1443, 1978.

[7] Jacob Goldenberg, Barak Libai, and Eitan Muller. Talk of the network: A complex systems look at the underlying process of word-of-mouth. *Marketing letters*, 12(3):211–223, 2001.

[8] Brian Karrer and Mark EJ Newman. Message passing approach for general epidemic models. *Physical Review E*, 82(1):016101, 2010.

[9] Xuzhen Zhu, Wei Wang, Shimin Cai, and H Eugene Stanley. Dynamics of social contagions with local trend imitation. *Scientific reports*, 8(1):7335, 2018.

[10] Panagiotis D Karampourniotis, Sameet Sreenivasan, Boleslaw K Szymanski, and Gyorgy Korniss. The impact of heterogeneous thresholds on social contagion with multiple initiators. *PloS one*, 10(11):e0143020, 2015.

[11] Clay Fink, Aurora C Schmidt, Vladimir Barash, John Kelly, Christopher Cameron, and Michael Macy. Investigating the observability of complex contagion in empirical social networks. In *Tenth International AAAI Conference on Web and Social Media*, 2016.

[12] Herbert A Simon. A behavioral model of rational choice. *The quarterly journal of economics*, 69(1):99–118, 1955.

[13] Leonard J Savage. *The foundations of statistics*. Courier Corporation, 1972.

[14] Amos Tversky and Daniel Kahneman. Judgment under uncertainty: Heuristics and biases. *science*, 185(4157):1124–1131, 1974.

[15] Vyacheslav I Yukalov, Elizaveta P Yukalova, and Didier Sornette. Information processing by networks of quantum decision makers. *Physica A: Statistical Mechanics and its Applications*, 492:747–766, 2018.

[16] Ece C Mutlu. Quantum probabilistic models using feynman diagram rules for better understanding the information diffusion dynamics in online social networks. In *Proceedings of the AAAI Conference on Artificial Intelligence*, volume 34, pages 13730–13731, 2020.

[17] Graham Loomes. Variability, noise, and error in decision making under risk. *The Wiley Blackwell handbook of judgment and decision making*, 2:658–695, 2015.

[18] Emmanuel Haven and Andrei Khrennikov. *Quantum social science*. Cambridge University Press, 2013.

[19] Jerome R Busemeyer and Peter D Bruza. *Quantum models of cognition and decision*. Cambridge University Press, 2012.

[20] Andrei Khrennikov, Irina Basieva, Emmanuel M Pothos, and Ichiro Yamato. Quantum probability in decision making from quantum information representation of neuronal states. *Scientific reports*, 8(1):1–8, 2018.

[21] Catarina Moreira and Andreas Wichert. Interference effects in quantum belief networks. *Applied Soft Computing*, 25:64–85, 2014.

[22] Mehrdad Ashtiani and Mohammad Abdollahi Azgomi. A survey of quantum-like approaches to decision making and cognition. *Mathematical Social Sciences*, 75:49–80, 2015.

[23] Yu-Xiao Zhu, Yan-Yan Cao, Ting Chen, Xiao-Yan Qiu, Wei Wang, and Rui Hou. Crossover phenomena in growth pattern of social contagions with restricted contact. *Chaos, Solitons & Fractals*, 114:408–414, 2018.

[24] Wei Wang, Xiao-Long Chen, and Lin-Feng Zhong. Social contagions with heterogeneous credibility. *Physica A: Statistical Mechanics and Its Applications*, 503:604–610, 2018.

[25] Wei Wang, Ming Tang, Hai-Feng Zhang, and Ying-Cheng Lai. Dynamics of social contagions with memory of nonredundant information. *Physical review e*, 92(1):012820, 2015.

[26] John Von Neumann, Oskar Morgenstern, and Harold William Kuhn. *Theory of games and economic behavior (commemorative edition)*. Princeton university press, 2007.

[27] Maurice Allais. Le comportement de l'homme rationnel devant le risque: critique des postulats et axiomes de l'école américaine. *Econometrica: Journal of the Econometric Society*, pages 503–546, 1953.

[28] Diedrik Aerts and Sven Aerts. Applications of quantum statistics in psychological studies of decision processes. *Foundations of Science*, 1(1):85–97, 1995.

[29] Andrei Khrennikov. Quantum-like brain:"interference of minds". *BioSystems*, 84(3):225–241, 2006.

[30] Andrei Khrennikov. Quantum-like model of cognitive decision making and information processing. *Biosystems*, 95(3):179–187, 2009.

[31] Andrei Yu Khrennikov and Emmanuel Haven. Quantum mechanics and violations of the sure-thing principle: The use of probability interference and other concepts. *Journal of Mathematical Psychology*, 53(5):378–388, 2009.

[32] Vyacheslav I Yukalov and Didier Sornette. Decision theory with prospect interference and entanglement. *Theory and Decision*, 70(3):283–328, 2011.

[33] Zheng Wang, Jerome R Busemeyer, Harald Atmanspacher, and Emmanuel M Pothos. The potential of using quantum theory to build models of cognition. *Topics in Cognitive Science*, 5(4):672–688, 2013.

[34] Masanari Asano, Irina Basieva, Andrei Khrennikov, Masanori Ohya, Yoshiharu Tanaka, and Ichiro Yamato. A model of epigenetic evolution based on theory of open quantum systems. *Systems and synthetic biology*, 7(4):161–173, 2013.

[35] Emmanuelle Tognoli and JA Scott Kelso. The metastable brain. *Neuron*, 81(1):35–48, 2014.

[36] Alexander Wendt. *Quantum mind and social science*. Cambridge University Press, 2015.

[37] Zi-Ke Zhang, Chuang Liu, Xiu-Xiu Zhan, Xin Lu, Chu-Xu Zhang, and Yi-Cheng Zhang. Dynamics of information diffusion and its applications on complex networks. *Physics Reports*, 651:1–34, 2016.

[38] Adrien Guille, Hakim Hacid, Cecile Favre, and Djamel A Zighed. Information diffusion in online social networks: A survey. *ACM Sigmod Record*, 42(2):17–28, 2013.

[39] Emmanuel M Pothos and Jerome R Busemeyer. A quantum probability explanation for violations of 'rational'decision theory. *Proceedings of the Royal Society B: Biological Sciences*, 276(1665):2171–2178, 2009.

[40] Mei Li, Xiang Wang, Kai Gao, and Shanshan Zhang. A survey on information diffusion in online social networks: Models and methods. *Information*, 8(4):118, 2017.

[41] Sanjay Kumar, Muskan Saini, Muskan Goel, and BS Panda. Modeling information diffusion in online social networks using a modified forest-fire model. *Journal of intelligent information systems*, pages 1–23, 2020.

[42] Frank M Bass. A new product growth for model consumer durables. *Management science*, 15(5):215–227, 1969.

[43] Haifeng Zhang and Yevgeniy Vorobeychik. Empirically grounded agent-based models of innovation diffusion: a critical review. *Artificial Intelligence Review*, pages 1–35, 2019.

[44] Vahideh Sadat Abedi. Compartmental diffusion modeling: Describing customer heterogeneity & communication network to support decisions for new product introductions. *Physica A: Statistical Mechanics and its Applications*, 536:120964, 2019.

[45] Trichy V Krishnan and Dipak C Jain. Optimal dynamic advertising policy for new products. *Management Science*, 52(12):1957–1969, 2006.

[46] Gila E Fruchter and Christophe Van den Bulte. Why the generalized bass model leads to odd optimal advertising policies. *International Journal of Research in Marketing*, 28(3):218–230, 2011.

[47] Shlomo Kalish. A new product adoption model with price, advertising, and uncertainty. *Management science*, 31(12):1569–1585, 1985.

[48] Christophe Van den Bulte. New product diffusion acceleration: Measurement and analysis. *Marketing Science*, 19(4):366–380, 2000.

[49] Rabik Ar Chatterjee and Jehoshua Eliashberg. The innovation diffusion process in a heterogeneous population: A micromodeling approach. *Management science*, 36(9):1057–1079, 1990.

[50] DJ Bartholomew. Stochastic models for social processes. new york: John wiley. 1982.

[51] Karmeshu and RK Pathria. Stochastic evolution of a nonlinear model of diffusion of information. *Journal of Mathematical Sociology*, 7(1):59–71, 1980.

[52] Luigi Luca Cavalli-Sforza and Marcus W Feldman. *Cultural transmission and evolution: A quantitative approach*. Princeton University Press, 1981.

[53] Beth Allen. A stochastic interactive model for the diffusion of information. *Journal of Mathematical Sociology*, 8(2):265–281, 1982.

[54] Fang Jin, Edward Dougherty, Parang Saraf, Yang Cao, and Naren Ramakrishnan. Epidemiological modeling of news and rumors on twitter. In *Proceedings of the 7th workshop on social network mining and analysis*, pages 1–9, 2013.

[55] Ece Çiğdem Mutlu, Amirarsalan Rajabi, and Ivan Garibay. Cd-seiz: Cognition-driven seiz compartmental model for the prediction of information cascades on twitter. *arXiv preprint arXiv:2008.12723*, 2020.

[56] Luís MA Bettencourt, Ariel Cintrón-Arias, David I Kaiser, and Carlos Castillo-Chávez. The power of a good idea: Quantitative modeling of the spread of ideas from epidemiological models. *Physica A: Statistical Mechanics and its Applications*, 364:513–536, 2006.

[57] Raul Isea and Karl E Lonngren. A new variant of the seiz model to describe the spreading of a rumor. *International Journal of Data Science and Analysis*, 3(4):28–33, 2017.

[58] Fang Jin, Wei Wang, Liang Zhao, Edward Dougherty, Yang Cao, Chang-Tien Lu, and Naren Ramakrishnan. Misinformation propagation in the age of twitter. *Computer*, (12):90–94, 2014.

[59] Chao Wang, Xu-ying Yang, Ke Xu, and JF Ma. Seir-based model for the information spreading over sns. *Acta Electronica Sinica*, 11:031, 2014.

[60] Ru-Zhi Xu, He-Li Li, and Chang-Ming Xing. Research on information dissemination model for social networking services. *International Journal of Computer Science and Application*, 2(1):1–6, 2013.

[61] Ding Xuejun. Research on propagation model of public opinion topics based on scir in microblogging [j]. *Computer Engineering and Applications*, 8:20–26, 2015.

[62] John Cannarella and Joshua A Spechler. Epidemiological modeling of online social network dynamics. *arXiv preprint arXiv:1401.4208*, 2014.

[63] Ling Feng, Yanqing Hu, Baowen Li, H Eugene Stanley, Shlomo Havlin, and Lidia A Braunstein. Competing for attention in social media under information overload conditions. *PloS one*, 10(7):e0126090, 2015.

[64] Quan-Hui Liu, Feng-Mao Lü, Qian Zhang, Ming Tang, and Tao Zhou. Impacts of opinion leaders on social contagions. *Chaos: An Interdisciplinary Journal of Nonlinear Science*, 28(5):053103, 2018.

[65] Daniel A Sprague and Thomas House. Evidence for complex contagion models of social contagion from observational data. *PloS one*, 12(7):e0180802, 2017.

[66] Pramesh Singh, Sameet Sreenivasan, Boleslaw K Szymanski, and Gyorgy Korniss. Threshold-limited spreading in social networks with multiple initiators. *Scientific reports*, 3:2330, 2013.

[67] Huiyuan Zhang, Subhankar Mishra, My T Thai, J Wu, and Y Wang. Recent advances in information diffusion and influence maximization in complex social networks. *Opportunistic Mobile Social Networks*, 37(1.1):37, 2014.

[68] David Peleg. Local majority voting, small coalitions and controlling monopolies in graphs: A review. In *Proc. of 3rd Colloquium on Structural Information and Communication Complexity*, pages 152–169, 1997.

[69] Ning Chen. On the approximability of influence in social networks. *SIAM Journal on Discrete Mathematics*, 23(3):1400–1415, 2009.

[70] Everett M Rogers. *Diffusion of innovations*. Simon and Schuster, 2010.

[71] David Kempe, Jon Kleinberg, and Éva Tardos. Influential nodes in a diffusion model for social networks. In *International Colloquium on Automata, Languages, and Programming*, pages 1127–1138. Springer, 2005.

[72] N. Barbieri, F. Bonchi, and G. Manco. Topic-aware social influence propagation models. *Knowledge and Information Systems*, 37:555–584, 2012.

[73] Thi Kim Thoa Ho, Q. V. Bui, and M. Bui. Homophily independent cascade diffusion model based on textual information. In *ICCCI*, 2018.

[74] Zhipeng A. Wang, Jichang Zhao, and K. Xu. Emotion-based independent cascade model for information propagation in online social media. *2016 13th International Conference on Service Systems and Service Management (ICSSSM)*, pages 1–6, 2016.

[75] Terrence Leung and K. Chung. Persuasion driven influence propagation in social networks. *2014 IEEE/ACM International Conference on Advances in Social Networks Analysis and Mining (ASONAM 2014)*, pages 548–554, 2014.

[76] Seth A Myers, Chenguang Zhu, and Jure Leskovec. Information diffusion and external influence in networks. In *Proceedings of the 18th ACM SIGKDD international conference on Knowledge discovery and data mining*, pages 33–41, 2012.

[77] Zhuo Chen. An agent-based model for information diffusion over online social networks. *Papers in Applied Geography*, 5(1-2):77–97, 2019.

[78] Daniel Gruhl, Ramanathan Guha, David Liben-Nowell, and Andrew Tomkins. Information diffusion through blogspace. In *Proceedings of the 13th international conference on World Wide Web*, pages 491–501, 2004.

[79] Fang Jin, E. Dougherty, P. Saraf, Yang Cao, and Naren Ramakrishnan. Epidemiological modeling of news and rumors on twitter. In *SNAKDD '13*, 2013.

[80] Pengyi Fan, Pei Li, Zhihong Jiang, Wei Li, and Hui Wang. Measurement and analysis of topology and information propagation on sina-microblog. In *Proceedings of 2011 IEEE International Conference on Intelligence and Security Informatics*, pages 396–401. IEEE, 2011.

[81] Lilian Weng, Jacob Ratkiewicz, Nicola Perra, Bruno Gonçalves, Carlos Castillo, Francesco Bonchi, Rossano Schifanella, Filippo Menczer, and Alessandro Flammini. The role of information diffusion in the evolution of social networks. In *Proceedings of the 19th ACM SIGKDD international conference on Knowledge discovery and data mining*, pages 356–364, 2013.

[82] Ece C Mutlu and Ivan Garibay. The degree-dependent threshold model: Towards a better understanding of opinion dynamics on online social networks. *arXiv preprint arXiv:2003.11671*, 2020.

[83] Kazumi Saito, Ryohei Nakano, and Masahiro Kimura. Prediction of information diffusion probabilities for independent cascade model. In *International conference on knowledge-based and intelligent information and engineering systems*, pages 67–75. Springer, 2008.

[84] Devesh Varshney, Sandeep Kumar, and Vineet Gupta. Predicting information diffusion probabilities in social networks: A bayesian networks based approach. *Knowledge-Based Systems*, 133:66–76, 2017.

[85] Q. Wang, Y. Jin, Tan Yang, and S. Cheng. An emotion-based independent cascade model for sentiment spreading. *Knowl. Based Syst.*, 116:86–93, 2017.

[86] T. Wang, Min Hu, and Lan Kou. A information propagation model based on various emotions and heterogeneous mean field in social networks. 2019.

[87] Xi Xiong, Y. Li, Shaojie Qiao, Nan Han, Yue Wu, Jing Peng, and Binyong Li. An emotional contagion model for heterogeneous social media with multiple behaviors. *Physica A-statistical Mechanics and Its Applications*, 490:185–202, 2018.

[88] C. Wang, Wei Chen, and Yajun Wang. Scalable influence maximization for independent cascade model in large-scale social networks. *Data Mining and Knowledge Discovery*, 25:545–576, 2012.

[89] David Kempe, Jon Kleinberg, and Éva Tardos. Maximizing the spread of influence through a social network. In *Proceedings of the ninth ACM SIGKDD international conference on Knowledge discovery and data mining*, pages 137–146, 2003.

[90] Wei Chen, Yajun Wang, and Siyu Yang. Efficient influence maximization in social networks. In *Proceedings of the 15th ACM SIGKDD international conference on Knowledge discovery and data mining*, pages 199–208, 2009.

[91] W. Liu, Xin Chen, B. Jeon, Ling Chen, and Bolun Chen. Influence maximization on signed networks under independent cascade model. *Applied Intelligence*, 49:912–928, 2018.

[92] F. Erlandsson, Piotr Bródka, and A. Borg. Seed selection for information cascade in multilayer networks. *ArXiv*, abs/1710.04391, 2017.

[93] Yan Xia, T. Chen, and Mikko Kivelä. Spread of tweets in climate discussions. *ArXiv*, abs/2010.09801, 2020.

[94] K. Lei, Y. Liu, Shangru Zhong, K. Xu, Ying Shen, and M. Yang. Understanding user behavior in sina weibo online social network: A community approach. *IEEE Access*, 6:13302–13316, 2018.

[95] Raghuram Iyengar, Christophe Van den Bulte, and Thomas W Valente. Opinion leadership and social contagion in new product diffusion. *Marketing Science*, 30(2):195–212, 2011.

[96] Aron Culotta and Jennifer Cutler. Mining brand perceptions from twitter social networks. *Marketing science*, 35(3):343–362, 2016.

[97] Kevin Lewis and Jason Kaufman. The conversion of cultural tastes into social network ties. *American journal of sociology*, 123(6):1684–1742, 2018.

[98] Peter Hedström. Contagious collectivities: On the spatial diffusion of swedish trade unions, 1890-1940. *American Journal of Sociology*, 99(5):1157–1179, 1994.

[99] Feng Shi, Misha Teplitskiy, Eamon Duede, and James A Evans. The wisdom of polarized crowds. *Nature Human Behaviour*, page 1, 2019.

[100] Zhongyuan Ruan, Gerardo Iniguez, Márton Karsai, and János Kertész. Kinetics of social contagion. *Physical review letters*, 115(21):218702, 2015.

[101] Shraddha Mishra, Surya Prakash Singh, John Johansen, Yang Cheng, and Sami Farooq. Evaluating indicators for international manufacturing network under circular economy. *Management Decision*, 57(4):811–839, 2019.

[102] Ece C Mutlu and Toktam A Oghaz. Review on graph feature learning and feature extraction techniques for link prediction. *arXiv preprint arXiv:1901.03425*, 2019.

[103] Taibo Li, Rasmus Wernersson, Rasmus B Hansen, Heiko Horn, Johnathan Mercer, Greg Slodkowicz, Christopher T Workman, Olga Rigina, Kristoffer Rapacki, Hans H Stærfeldt, et al. A scored human protein–protein interaction network to catalyze genomic interpretation. *Nature methods*, 14(1):61, 2017.

[104] Duncan J Watts and Peter Sheridan Dodds. Influentials, networks, and public opinion formation. *Journal of consumer research*, 34(4):441–458, 2007.

[105] Soroush Vosoughi, Deb Roy, and Sinan Aral. The spread of true and false news online. *Science*, 359(6380):1146–1151, 2018.

[106] Johan Ugander, Lars Backstrom, Cameron Marlow, and Jon Kleinberg. Structural diversity in social contagion. *Proceedings of the National Academy of Sciences*, 109(16):5962–5966, 2012.

[107] Alexandre Bovet and Hernán A Makse. Influence of fake news in twitter during the 2016 us presidential election. *Nature communications*, 10(1):7, 2019.

[108] James P Gleeson. Binary-state dynamics on complex networks: Pair approximation and beyond. *Physical Review X*, 3(2):021004, 2013.

[109] Eun Lee and Petter Holme. Social contagion with degree-dependent thresholds. *Physical Review E*, 96(1):012315, 2017.

[110] Mark Newman. *Networks: an introduction*. Oxford university press, 2010.

[111] Alfonso Allen-Perkins, Juan Manuel Pastor, and Ernesto Estrada. Two-walks degree assortativity in graphs and networks. *Applied Mathematics and Computation*, 311:262–271, 2017.

[112] Mark EJ Newman. Assortative mixing in networks. *Physical review letters*, 89(20):208701, 2002.

[113] Mark EJ Newman. Mixing patterns in networks. *Physical Review E*, 67(2):026126, 2003.

[114] Insuk Lee, Eiru Kim, and Edward M Marcotte. Modes of interaction between individuals dominate the topologies of real world networks. *PloS one*, 10(3):e0121248, 2015.

[115] Kiho Im, Michael J Paldino, Annapurna Poduri, Olaf Sporns, and P Ellen Grant. Altered white matter connectivity and network organization in polymicrogyria revealed by individual gyral topology-based analysis. *Neuroimage*, 86:182–193, 2014.

[116] Johan Ugander, Brian Karrer, Lars Backstrom, and Cameron Marlow. The anatomy of the facebook social graph. *arXiv preprint arXiv:1111.4503*, 2011.

[117] Hai-Bo Hu and Xiao-Fan Wang. Disassortative mixing in online social networks. *EPL (Europhysics Letters)*, 86(1):18003, 2009.

[118] Gang Wang, Bolun Wang, Tianyi Wang, Ana Nika, Haitao Zheng, and Ben Y Zhao. Whispers in the dark: analysis of an anonymous social network. In *Proceedings of the 2014 Conference on Internet Measurement Conference*, pages 137–150. ACM, 2014.

[119] David N Fisher, Matthew J Silk, and Daniel W Franks. The perceived assortativity of social networks: methodological problems and solutions. In *Trends in Social Network Analysis*, pages 1–19. Springer, 2017.

[120] Ece Mutlu and Ozlem Ozmen Garibay. Effects of assortativity on consensus formation with heterogeneous agents. In *Conference of the Computational Social Science Society of the Americas*, pages 1–10. Springer, 2022.

[121] Matthew C VanDyke and Christopher D Hall. Decentralized coordinated attitude control within a formation of spacecraft. *Journal of Guidance, Control, and Dynamics*, 29(5):1101–1109, 2006.

[122] Ronald C Arkin and Tucker Balch. Cooperative multiagent robotic systems. 1997.

[123] Cheng Jin, Yifu Li, and Xiaogang Jin. Political opinion formation: Initial opinion distribution and individual heterogeneity of tolerance. *Physica A: Statistical Mechanics and its Applications*, 467:257–266, 2017.

[124] Javier Borge-Holthoefer and Yamir Moreno. Absence of influential spreaders in rumor dynamics. *Physical Review E*, 85(2):026116, 2012.

[125] Robin IM Dunbar. Neocortex size as a constraint on group size in primates. *Journal of human evolution*, 22(6):469–493, 1992.

[126] Ramón Xulvi-Brunet and Igor M Sokolov. Changing correlations in networks: assortativity and dissortativity. *Acta Physica Polonica B*, 36(5):1431, 2005.

[127] Ninareh Mehrabi, Fred Morstatter, Nripsuta Saxena, Kristina Lerman, and Aram Galstyan. A survey on bias and fairness in machine learning. *arXiv preprint arXiv:1908.09635*, 2019.

[128] Alexandra Chouldechova. Fair prediction with disparate impact: A study of bias in recidivism prediction instruments. *Big data*, 5(2):153–163, 2017.

[129] Dana Pessach and Erez Shmueli. Algorithmic fairness. *arXiv preprint arXiv:2001.09784*, 2020.

[130] Amit Datta, Michael Carl Tschantz, and Anupam Datta. Automated experiments on ad privacy settings: A tale of opacity, choice, and discrimination. *Proceedings on privacy enhancing technologies*, 2015(1):92–112, 2015.

[131] Michael Feldman, Sorelle A Friedler, John Moeller, Carlos Scheidegger, and Suresh Venkatasubramanian. Certifying and removing disparate impact. In *proceedings of the 21th ACM SIGKDD international conference on knowledge discovery and data mining*, pages 259–268, 2015.

[132] Cynthia Dwork, Moritz Hardt, Toniann Pitassi, Omer Reingold, and Richard Zemel. Fairness through awareness. In *Proceedings of the 3rd innovations in theoretical computer science conference*, pages 214–226, 2012.

[133] Moritz Hardt, Eric Price, and Nathan Srebro. Equality of opportunity in supervised learning. *arXiv preprint arXiv:1610.02413*, 2016.

[134] Chelsea Barabas, Madars Virza, Karthik Dinakar, Joichi Ito, and Jonathan Zittrain. Interventions over predictions: Reframing the ethical debate for actuarial risk assessment. In *Conference on Fairness, Accountability and Transparency*, pages 62–76. PMLR, 2018.

[135] Silvia Chiappa. Path-specific counterfactual fairness. In *Proceedings of the AAAI Conference on Artificial Intelligence*, volume 33, pages 7801–7808, 2019.

[136] Niki Kilbertus, Mateo Rojas-Carulla, Giambattista Parascandolo, Moritz Hardt, Dominik Janzing, and Bernhard Schölkopf. Avoiding discrimination through causal reasoning. *arXiv preprint arXiv:1706.02744*, 2017.

[137] Matt J Kusner, Joshua R Loftus, Chris Russell, and Ricardo Silva. Counterfactual fairness. *arXiv preprint arXiv:1703.06856*, 2017.

[138] Chris Russell, M Kusner, C Loftus, and Ricardo Silva. When worlds collide: integrating different counterfactual assumptions in fairness. In *Advances in neural information processing systems*, volume 30. NIPS Proceedings, 2017.

[139] Junzhe Zhang and Elias Bareinboim. Fairness in decision-making—the causal explanation formula. In *Thirty-Second AAAI Conference on Artificial Intelligence*, 2018.

[140] Joshua R Loftus, Chris Russell, Matt J Kusner, and Ricardo Silva. Causal reasoning for algorithmic fairness. *arXiv preprint arXiv:1805.05859*, 2018.

[141] Tapabrata Chakraborti, Arijit Patra, and J Alison Noble. Contrastive fairness in machine learning. *IEEE Letters of the Computer Society*, 3(2):38–41, 2020.

[142] Babak Salimi, Luke Rodriguez, Bill Howe, and Dan Suciu. Interventional fairness: Causal database repair for algorithmic fairness. In *Proceedings of the 2019 International Conference on Management of Data*, pages 793–810, 2019.

[143] Aria Khademi, Sanghack Lee, David Foley, and Vasant Honavar. Fairness in algorithmic decision making: An excursion through the lens of causality. In *The World Wide Web Conference*, pages 2907–2914, 2019.

[144] Peter D Bruza, Zheng Wang, and Jerome R Busemeyer. Quantum cognition: a new theoretical approach to psychology. *Trends in cognitive sciences*, 19(7):383–393, 2015.

[145] Andrei Khrennikov. Quantum-like modeling of cognition. *Frontiers in Physics*, 3:77, 2015.

[146] Ece C Mutlu and Ozlem Ozmen Garibay. Quantum contagion: A quantum-like approach for the analysis of social contagion dynamics with heterogeneous adoption thresholds. *Entropy*, 23(5):538, 2021.

[147] Christos Dimitrakakis, Yang Liu, David C Parkes, and Goran Radanovic. Bayesian fairness. In *Proceedings of the AAAI Conference on Artificial Intelligence*, volume 33, pages 509–516, 2019.

[148] I Northpointe. Practitioner's guide to compas core. 2015.

[149] Julia Angwin, Jeff Larson, Surya Mattu, and Lauren Kirchner. Machine bias. *ProPublica, May*, 23(2016):139–159, 2016.

[150] Jeff Larson, Surya Mattu, Lauren Kirchner, and Julia Angwin. How we analyzed the compas recidivism algorithm. *ProPublica (5 2016)*, 9(1), 2016.

[151] Clausius Rudolf. The mechanical theory of heat: With its applications to the steam-engine and to the physical properties of bodies. 1867.

[152] Alireza Namdari and Zhaojun Li. A review of entropy measures for uncertainty quantification of stochastic processes. *Advances in Mechanical Engineering*, 11(6):1687814019857350, 2019.

[153] Claude Elwood Shannon. A mathematical theory of communication. *ACM SIGMOBILE mobile computing and communications review*, 5(1):3–55, 2001.

[154] Claude Elwood Shannon. A mathematical theory of communication. *The Bell system technical journal*, 27(3):379–423, 1948.

[155] Alfréd Rényi. On measures of entropy and information. In *Proceedings of the Fourth Berkeley Symposium on Mathematical Statistics and Probability, Volume 1: Contributions to the Theory of Statistics*, volume 4, pages 547–562. University of California Press, 1961.

[156] Constantino Tsallis. Possible generalization of boltzmann-gibbs statistics. *Journal of statistical physics*, 52(1):479–487, 1988.

[157] Yong Deng. Deng entropy. *Chaos, Solitons & Fractals*, 91:549–553, 2016.

[158] Petr Jizba and Toshihico Arimitsu. The world according to rényi: thermodynamics of multifractal systems. *Annals of Physics*, 312(1):17–59, 2004.

[159] Constantino Tsallis. Entropic nonextensivity: a possible measure of complexity. *Chaos, Solitons & Fractals*, 13(3):371–391, 2002.

[160] Zhiming Huang, Lin Yang, and Wen Jiang. Uncertainty measurement with belief entropy on the interference effect in the quantum-like bayesian networks. *Applied Mathematics and Computation*, 347:417–428, 2019.

[161] Catarina Moreira and Andreas Wichert. Quantum-like bayesian networks for modeling decision making. *Frontiers in psychology*, page 11, 2016.

[162] Quan-Hui Liu, Lin-Feng Zhong, Wei Wang, Tao Zhou, and H Eugene Stanley. Interactive social contagions and co-infections on complex networks. *Chaos: An Interdisciplinary Journal of Nonlinear Science*, 28(1):013120, 2018.

[163] Wei Wang, Ming Tang, H Eugene Stanley, and Lidia A Braunstein. Unification of theoretical approaches for epidemic spreading on complex networks. *Reports on Progress in Physics*, 80(3):036603, 2017.